Cytoplasmic and nuclear Sw-5b NLR act both independently and synergistically to dictate full host defense against tospovirus infection

Hongyu Chen[1,¶], Xin Qian[1,¶], Xiaojiao Chen[1,¶], Tongqing Yang[1], Mingfeng Feng[1], Jing Chen[1], Ruixiang Cheng[1], Hao Hong[1], Ying Zheng[1], Yuzhen Mei[4], Danyu Shen[1], Yi Xu[1], Min Zhu[1], Xin Shun Ding[1] and Xiaorong Tao[1,*]

[1] Key Laboratory of Plant Immunity, Department of Plant Pathology, College of Plant Protection, Nanjing Agricultural University, Nanjing 210095, P. R. China.

[2] Huaiyin Institute of Agricultural Sciences of Xuhuai Region in Jiangsu，Huaian 223001, Jiangsu, P. R. China.

[3] College of Plant Protection, Yunnan Agricultural University, Kunming 650201, Yunnan, P. R. China.

[4] State Key Laboratory of Rice Biology, Institute of Biotechnology, Zhejiang University, Hanghzou 310029, P. R. China.

[¶] These authors contributed equally to this work.

Author for correspondence:

Xiaorong Tao

Tel: (+86)-25-84399027

Email: taoxiaorong@njau.edu.cn

RUNNING HEAD

Independent role of cytoplasmic and nuclear Sw-5b in immunity

Word Count: Main body of the text, 8136

Title 18, Summary 249, Keywords 8, Introduction 1286, Materials and Methods 1562, Results 3030, Discussion 1884, Acknowledgments 35, References 3687, Figure Legends 1103, Supporting Information Legends 786

9 Figures (Colors); Supporting information: 8 Supplemental Figures, 6 Supplemental Tables

Summary

- Plant intracellular nucleotide binding-leucine-rich repeat (NLR) receptors play critical roles in mediating host immunity to pathogen attack. We use tomato Sw-5b::tospovirus as a model system to study the specific role of the compartmentalized plant NLR in dictating host defense against virus at different infection steps.
- We demonstrated here that tomato NLR Sw-5b translocates to cytoplasm and nucleus, respectively, to play different roles in inducing host resistances against *Tomato spotted wilt tospovirus* (TSWV) infection. The cytoplasmic Sw-5b functions to induce a strong cell death response to inhibit TSWV replication. This host response is, however, insufficient to block viral intercellular and long-distance movement. The nucleus-localized Sw-5b triggers a host defense that weakly inhibits viral replication but strongly impedes virus intercellular and systemic movement. Furthermore, the cytoplasmic and nuclear Sw-5b act synergistically to dictate full host defense to TSWV infection.
- We further demonstrated that the extended N-terminal *Solanaceae* domain (SD) of Sw-5b plays critical roles in cytoplasm/nucleus partitioning. Sw-5b nucleotide-binding leucine-rich repeat (NB-LRR) controls its cytoplasm localization. Strikingly, the SD but not coil-coil (CC) domain is crucial for Sw-5b receptor to translocate from cytoplasm to nucleus to trigger the immunity. The SD was found to interact with importins. Silencing both importin α and β expression disrupted Sw-5b nucleus translocation and host immunity

against TSWV systemic infection.

- Collectively, our findings suggest that Sw-5b bifurcates disease resistances by cytoplasm/nucleus partitioning to block different infection steps of TSWV. The findings also identified a new regulatory role of extra domain of a plant NLR in mediating host innate immunity.

Keywords:

NLRs, Cytoplasm, Nuclear, Plant innate immunity, Tomato spotted wilt virus, Replication, Cell-to-cell movement and Long distance movement

93

94 # Introduction

95 Plant innate immunity plays critical roles in host defense against pathogen invasions,
96 and is triggered by cell-surface receptors or intracellular nucleotide-binding
97 leucine-rich repeat (NLR) receptors (Soosaar *et al.*, 2005; Dodds & Rathjen, 2010;
98 Cui *et al.*, 2015; Li *et al.*, 2015; Jones *et al.*, 2016; Kourelis & van der Hoorn, 2018;
99 Kapos *et al.*, 2019; van Wersch, 2020). Plant intracellular NLRs are the largest
100 classes of resistance proteins that function to detect pathogen effectors, and to activate
101 host immunity upon pathogen attack (Caplan, J *et al.*, 2008; Takken & Goverse, 2012;
102 Li *et al.*, 2015; Jones *et al.*, 2016; Kourelis & van der Hoorn, 2018; Kapos *et al.*,
103 2019). Plant NLRs typically contain an N-terminal domain, a central
104 nucleotide-binding domain (NB), a nucleotide-binding adaptor (ARC domain shared
105 by Apaf-1, certain resistance proteins, and CED-4), and a C-terminal leucine-rich
106 repeat (LRR) domain (Ea & Jones, 1998; Jones *et al.*, 2016; Ma *et al.*, 2018; Wang *et*
107 *al.*, 2019a; Wang *et al.*, 2019b; Ma *et al.*, 2020). Based on the differences among the
108 N-terminal domains, plant NLRs can be further divided into two main categories,
109 known as the coiled-coil NLR (refers to as CNL) category and the Toll/interleukin-1
110 receptor NLR (TNL) category (Meyers *et al.*, 2003; Collier & Moffett, 2009; Qi &
111 Innes, 2013). The CC- or the TIR-domain-bearing NLRs have distinct genetic
112 requirements and can regulate different functions in the downstream of defense
113 signaling (Collier & Moffett, 2009; Qi & Innes, 2013; Horsefield *et al.*, 2019; Jubic *et*

114 *al.*, 2019; van Wersch & Li, 2019; Wan *et al.*, 2019).

115 In addition to classical domains, non-canonical domains were frequently found to
116 integrate into certain NLRs. The additional domain, called BED, was first found in 32
117 poplar NLR proteins (Germain & Seguin, 2011). This extra BED domain was also
118 found in nine rice NLRs (Das *et al.*, 2014). The RATX1/HMA domain in the rice
119 NLRs RGA5 and Pik‐1 was found to act as integrated decoys to detect the cognate
120 pathogen effectors (Kanzaki *et al.*, 2012; Cesari *et al.*, 2013; Cesari *et al.*, 2014). The
121 WRKY domain on Arabidopsis thaliana NLR RRS1 was further found to function as
122 an integrated decoy that recognizes the effectors AvrRps4 and PopP2 (Le Roux *et al.*,
123 2015; Sarris *et al.*, 2015). Genome-wide analyses of plant NLR receptors revealed
124 that about 3.5 % of the NLRs carried specific non-canonical domains (Cesari *et al.*,
125 2014; Kroj *et al.*, 2016; Sarris *et al.*, 2016), and some of these non-canonical domains
126 were shown to be targeted by pathogen effectors during pathogen infections (Sarris *et*
127 *al.*, 2016). However, molecular functions of most non-canonical domains in plant
128 NLRs remain largely unexplored.

129 Translocations of plant NLRs into proper subcellular compartments are critical for
130 the induction of innate immunity (Cui *et al.*, 2015; van Wersch, 2020). Multiple plant
131 NLRs and immune regulators, including tobacco N, Arabidopsis snc1, RRS1/RPS4,
132 barley MLA10, and Arabidopsis EDS1, NPR1, have been shown to accumulate in
133 both cytoplasm and nucleus, and for several nucleocytoplasmic NLRs accumulation
134 in nucleus is required for triggering host resistance to pathogen infections (Deslandes
135 *et al.*, 2003; Burch-Smith *et al.*, 2007; Shen *et al.*, 2007; Wirthmueller *et al.*, 2007;

136 Tasset *et al.*, 2010; Bai *et al.*, 2012; Inoue *et al.*, 2013; Padmanabhan *et al.*, 2013).
137 Wheat Sr33, a homolog of barley MLA10, however, was reported to accumulate in
138 cytoplasm to induce host resistance against stem rust pathogen (Cesari *et al.*, 2016).
139 For potato Rx, a balanced cytoplasm and nucleus accumulation of Rx is needed to
140 induce the host immunity (Slootweg *et al.*, 2010; Tameling *et al.*, 2010). Other studies
141 have shown that *Arabidopsis* Rpm1 (Gao *et al.*, 2011), RPS2 (Axtell & Staskawicz,
142 2003), RPS5 (Qi *et al.*, 2012), rice Pit (Takemoto *et al.*, 2012), and tomato Tm-2^2
143 (Chen *et al.*, 2017; Wang *et al.*, 2020) need to associate with plasma membrane in
144 order to trigger cell death and host immunity. Latest studies have shown that the
145 activated *Arabidopsis* ZAR1 can bind to cellular membrane, leading to a membrane
146 leakage followed by cell death and host immunity (Wang *et al.*, 2019a; Wang *et al.*,
147 2019b). Flax L6 and M have been shown to accumulate in both Golgi apparatus and
148 tonoplast, and these compartmentalized localizations are necessary for the induction
149 of host resistance (Kawano *et al.*, 2014). The re-distribution of potato R3a from
150 cytosol to endosomal compartments is crucial for the induction of host resistance to
151 *Phytophthora infestans* infection (Engelhardt *et al.*, 2012). Different plant NLRs have
152 diverse subcellular localizations for their proper functions. However, how the
153 compartmentalized plant NLRs specifically dictate defense signaling remains largely
154 unknown.

155 Tomato spotted wilt tospovirus (TSWV) is one of most destructive plant NSVs,
156 infecting more than 1000 plant species, and causes crop losses more than one billion
157 US dollars annually worldwide (Kormelink *et al.*, 2011; Scholthof *et al.*, 2011; Oliver

158 & Whitfield, 2016). Tomato NLR Sw-5b confers strong resistance to TSWV infection
159 and has been widely used in tomato breeding projects to produce tospovirus resistant
160 tomato cultivars (Brommonschenkel *et al.*, 2000; Spassova M I, 2001; Turina *et al.*,
161 2016; Zhu *et al.*, 2019). Upon recognition of TSWV movement protein, NSm, Sw-5b
162 can trigger a hypersensitive response (HR), which typically associated with localized
163 cell death (Lopez *et al.*, 2011; Hallwass *et al.*, 2014; Peiro *et al.*, 2014; De Oliveira *et*
164 *al.*, 2016; Zhao *et al.*, 2016; Leastro *et al.*, 2017). Tospoviruses are divided into
165 American and Euro-Asia type based on their geographic distribution and amino acid
166 sequence identity of viral nucleocapsid protein. We have previously shown that
167 Sw-5b can confer a broad-spectrum resistance to American type tospoviruses,
168 including TSWV, through recognition of a conserved 21 amino acid PAMP-like
169 region in the viral movement protein NSm (Zhu *et al.*, 2017). Sw-5b carries an
170 extended N-terminal *Solanaceae* domain (SD), a CC domain, a NB-ARC domain, and
171 a LRR domain (Brommonschenkel *et al.*, 2000; Spassova M I, 2001;
172 Lukasik-Shreepaathy *et al.*, 2012). Similar SDs have also been found in the Mi-1.2,
173 R8, Rpi-blb2, and Hero (Milligan *et al.*, 1998; Vos *et al.*, 1998; Ernst *et al.*, 2002; van
174 der Vossen *et al.*, 2005; Lukasik-Shreepaathy *et al.*, 2012; Vossen *et al.*, 2016). More
175 recently, Seong and others reported that the extended CNL has been evolved initially
176 in the ancestor of *Asterids* and *Amaranthaceae*, predated the *Solanaceae* family
177 (Seong *et al.*, 2020). In the presence of the extended N-terminal SD, Sw-5b is in an
178 autoinhibited state through multilayered interactions between SD, CC, NB-ARC, and
179 LRR domains (Chen *et al.*, 2016). For activation, the extra SD also recognizes NSm.

180 Sw-5b adopts a two-step NSm recognition strategy through SD and then LRR domain
181 (Li *et al.*, 2019). This two-step recognition mechanism significantly enhances the
182 sensitivity of the detection on TSWV NSm (Li *et al.*, 2019). Although Sw-5b is
183 known to localize in both cytoplasm and nucleus (De Oliveira *et al.*, 2016), the
184 biological roles of the cytoplasm- and the nucleus-accumulated Sw-5b in host
185 immunity signaling are unknown.

186 In this study, we investigated the subcellular distribution pattern of Sw-5b and the
187 functions of the compartmentalized Sw-5b in the induction of host immunity to
188 TSWV infection. We determined here that cytoplasm- and nucleus-accumulated
189 Sw-5b functions differently in inducing host defense response to inhibit multiple
190 tospovirus infection steps. The cytoplasmic Sw-5b can induce a strong cell death
191 response to suppress TSWV replication, whereas the nucleus-accumulated Sw-5b can
192 induce a strong defense against viral intercellular movement and systemic infection.
193 The combination of cytoplasmic and nuclear Sw-5b induces a synergistic and strong
194 plant immunity against tospovirus infection. We also found that the extended SD
195 functions as the key regulator for this critical intracellular translocation. The SD was
196 also found to interact with importins α and β to mediate Sw-5b nucleus translocation,
197 and to confer the full host immunity against tospovirus infection.

198

199 **Materials and Methods**

200 **Plasmid construction**

201 p2300S-YFP-Sw-5b was from a previously described source (Chen *et al.*, 2016).

202 Different domains of Sw-5b were PCR-amplified from p2300S-Sw-5b (Chen *et al.*,
203 2016) and cloned individually behind the *YFP* gene in the p2300S vector using a
204 two-step overlap PCR procedure as described (Li *et al.*, 2019). All the primers used in
205 this study are listed in Table S1.

206 To visualize the subcellular localization patterns of various fusion proteins, a SV40
207 T-Ag-derived nuclear localization signal (NLS, QPKKKRKVGG) (Lanford & Butel,
208 1984) or a PK1 nuclear export signal (NES, NELALKLAGLDINK) (Wen *et al.*, 1995)
209 was fused to the N-terminus of YFP-Sw-5b or the C-terminus of NSm-YFP, as
210 described (Kong *et al.*, 2017), to produce pNES-YFP-Sw-5b, pNLS-YFP-Sw-5b,
211 pNSm-YFP-NES, and pNSm-YFP-NLS, respectively. In addition, YFP-Sw-5b and
212 NSm-YFP were fused individually with a mutant NLS (nls, QPKKTRKVGG) or a
213 mutant NES (nes, NELALKAAGADANK) to produce pnes-YFP-Sw-5b,
214 pnls-YFP-Sw-5b, pNSm-YFP-nes, and pNSm-YFP-nls. The constructs were then
215 transformed individually into *Agrobacterium tumefaciens* strain GV3101 cells.

216

217 **Transient gene expression, stable plant transformation, and virus inoculation**

218 *Nicotiana benthamiana* were grown in soil in pots inside a greenhouse maintained at
219 25°C and a 16 h light/8 h dark photoperiod. Six-to-eight week-old *N. benthamiana*
220 plants were used for various assays. Transient gene expression assays were performed
221 in *N. benthamiana* leaves through agro-infiltration using Agrobacterium cultures
222 carrying specific expressing constructs as described previously (Feng *et al.*, 2016; Ma
223 *et al.*, 2017). Transgenic *N. benthamiana* lines expressing YFP-Sw-5b or its

224 derivatives were made using constructs with a 35S promoter or a Sw-5b native
225 promoter via a standard leaf-disc transformation method (Chen *et al.*, 2016). The
226 resulting transgenic *N. benthamiana* lines were named as NES-YFP-Sw-5b,
227 NLS-YFP-Sw-5b, nes-YFP-Sw-5b, nls-YFP-Sw-5b, YFP-Sw-5b, and EV
228 (transformed with an empty vector), respectively. Inoculation of transgenic *N.*
229 *benthamiana* plants with TSWV was done by rubbing plant leaves with TSWV-YN
230 isolate-infected crude saps as described (Zhu *et al.*, 2017). TRV-mediated VIGS in *N.*
231 *benthamiana* plants was done as described (Ma *et al.*, 2015). The agro-infiltrated or
232 the virus-inoculated plants were growning inside a growth chamber maintained at
233 25/23 °C (day/night) with a 16/8 h light and dark photoperiod.
234
235 **Particle bombardment**
236 The particle bombardment is described (Feng et al., 2016). Briefly, 60 mg Tungsten
237 M-10 microcarrier (Bio-RAD) was placed into a 1.5 ml Eppendorf tube with 1 mL
238 70% ethanol. The tube was vortexes for 3 minutes, and then stood at room
239 temperature for 15 minutes. After centrifuge at low speed for 5 seconds, the
240 supernatant was removed and the pellet was rinsed with 70% ethanol for 3 times. One
241 mL 50% sterile glycerol solution was added and divided Tungsten M-10 microcarrier
242 into 50 µl. Five µg pRTL2-YFP, pRTL2-YFP-Sw-5b or pRTL2-YFP-Sw-5bD857V
243 plasmid DNA, 50 µl of 2.5 M CaCl2, and 20 µl of 0.1 M spermidine, respectively
244 were added and mixed with microcarrier. After centrifuge at low speed for 5 seconds
245 and the supernatant removed. The pellet was resuspended in 200 µl 70% ethanol and

246 centrifugation as described above. Use 48 µl of 100% ethanol to resuspend the
247 tungsten particle::plasmid DNA complexes, and load 15 48 µl mixture onto the center
248 of carrier (Bio-RAD), air dry, and use He/1000 particle transport system (BIO-RAD)
249 to bombard tomato leaves harvested from 3- or 4-week-old of Money Marker. The
250 bombarded leaves were incubated in Petri dishes for 24 hours at 25°C followed with
251 Confocal Microscope analysis.

252

253 **Trypan blue staining**

254 *N. benthamiana* leaves were harvested at 3 days post agro-infiltration (dpai) and
255 boiled for 5 min in a 1.15:1 (v/v) mixed ethanol and trypan blue staining solution (10
256 g phenol, 10 mL glycerol, 10 mL lactic acid, and 20 mg trypan blue in 10 mL distilled
257 water). The stained leaves were then de-stained in a chloral hydrate solution (2.5 g per
258 mL distilled water) as described (Bai *et al.*, 2012).

259

260 **Electrolyte leakage assay**

261 Electrolyte leakage assay was performed as previously described (Mittler *et al.*, 1999;
262 Zhu *et al.*, 2017) with slight modifications. Briefly, five leaf discs (9 mm in diameter
263 each) were taken from the agro-infiltrated leaves per treatment and at various dpai.
264 The harvested leaf discs from a specific treatment were floated on a 10 mL distilled
265 water for 3 h at room temperature (RT), and the conductivity of each bathing water
266 was measured (referred to as value A) using a Multiparameter Meter as instructed
267 (Mettler Toledo, Zurich, Switzerland). After the first measurement, the leaf discs were

268 returned to the bathing water and incubated at 95°C for 25 min. After cooling down to
269 RT, the conductivity of each bathing sample was measured again (referred to as value
270 B). The ion leakage was expressed as the ratio determined by value A/value B × 100.
271 The mean value and standard error of each treatment were calculated using the data
272 from three biological replicates per treatment at each sampling time point.
273

274 **Confocal laser scanning microscopy**

275 Tissue samples were collected from the leaves of transiently expressing YFP-Sw-5b
276 or one of the fusion proteins at 24–36 hours post agro-infiltration (hpai). The collected
277 tissue samples were mounted in water between a glass slide and a coverslip. Images
278 of individual samples were captured under a Carl Zeiss LSM 710 confocal laser
279 scanning microscope. YFP fusions were excited at 488 nm and the emission was
280 captured at 497–520 nm. The resulting images were further processed using the Zeiss
281 710 CLSM software followed by the Adobe Photoshop software (San Jose, CA,
282 USA).
283

284 **Nucleus and cytoplasm fractionations**

285 *N. benthamiana* leaf tissues (1 g per sample), representing a specific treatment, were
286 collected at 24 hpai, frozen in liquid nitrogen, ground to fine powders, and then
287 homogenized in 2 mL (per sample) extraction buffer 1 (20 mM Tris-HCl, pH 7.5, 20
288 mM KCl, 2.5 mM $MgCl_2$, 2 mM EDTA, 25% glycerol, 250 mM sucrose, 1×Protease
289 Inhibitor Cocktail, and 5 mM DTT). The resulting lysate was filtered through 30 μm

290 filters to remove debris, and the filtrate was centrifuged at 2,000 × *g* for 5 minutes
291 to pellet nuclei. The supernatant from a sample was transferred into a new tube and
292 centrifuged at 10,000 × *g* for 10 min. The resulting supernatant was used as the
293 cytoplasm fraction. The nuclei containing pellet was resuspended in 5 mL extraction
294 buffer 2 (20 mM Tris-HCl, pH 7.4, 25% glycerol, 2.5 mM MgCl2, and 0.2% Triton
295 X-100), centrifuged for 10 min at 2,000 × *g* followed by 4-6 cycles of resuspension
296 and centrifugation as described above. The resulting pellet was resuspended again in
297 500 μl extraction buffer 3 (20 mM Tris-HCl, pH 7.5, 0.25 M sucrose, 10 mM MgCl2,
298 0.5% Triton X-100, and 5 mM β-mercaptoethanol). The nuclei fraction was carefully
299 layered on the top of 500 mL extraction buffer 4 (20 mM Tris-HCl, pH 7.5, 1.7 M
300 sucrose, 10 mM MgCl2, 0.5% Triton X-100, 1×Protease Inhibitor Cocktail, and 5
301 mM β-mercaptoethanol), and then centrifuged at 16,000 × *g* for 1 h. The resulting
302 pellet was resuspended in 500 μL extraction buffer 1 and stored at −80°C until use or
303 used immediately for SDS-PAGE assays. All the processes were performed on ice or
304 at 4°C. In this study, actin and histone H3 were used as the cytoplasmic and the
305 nuclear markers, respectively.
306
307 **Western blot, co-immunoprecipitation and mass spectrometry analysis**
308 Western blot and co-immunoprecipitation assays were performed as described (Zhu *et*
309 *al.*, 2017). Briefly, agro-infiltrated leaf samples (1 g per sample) were harvested and
310 homogenized individually in pre-chilled mortars with pestles in 2 mL extraction
311 buffer [10% (v/v) glycerol, 25 mM Tris, pH 7.5, 1 mM EDTA, 150 mM NaCl, 10 mM

312 DTT, 2% (w/v) polyvinylpolypyrrolidone, and 1 × protease inhibitor cocktail (Sigma,
313 Shanghai, China)]. Each crude slurry was transferred into a 2 mL Eppendorf tube, and
314 spun for 2 min at full speed in a refrigerated microcentrifuge. The supernatant was
315 transferred into a clean 1.5 mL Eppendorf tube and spun for 10 min at 4°C. For
316 Western blot assays, 50 μL supernatant from a sample was mixed with 150 μL
317 Laemmli buffer, boiled for 5 min, and analyzed in SDS-PAGE gels through
318 electrophoresis. For immunoprecipitation assays, 1 mL supernatant was mixed with
319 25 μL GFP-trap agarose beads (ChromoTek, Planegg-Martinsried, Germany),
320 incubated for 2 h at 4°C on an orbital shaker, and then pelleted through low speed
321 centrifugation. The blots were probed with a 1:2,500 (v/v) diluted anti-YFP antibody
322 or other specific antibodies followed a 1:10,000 (v/v) diluted horseradish peroxidase
323 (HRP)-conjugated goat anti-rabbit or a goat anti-mouse antibody (Sigma-Aldrich, St.
324 Louis, MO, USA). The detection signal was developed using the ECL substrate kit as
325 instructed (Thermo Scientific, Hudson, NH, USA).

326 For mass spectrometry analysis, the immunoprecipitation samples of YFP-SD
327 and SD without tag were processed by The Beijing Genomics Institute (BGI) for mass
328 spectrometry analysis. The immunoprecipitation samples of YFP-Sw-5b and Sw-5b
329 without tag were processed by Applied Protein Technology in Shanghai. Database
330 searches were performed using the Mascot search engine against *N. benthamiana*.
331 (https://solgenomics.net/organism/Nicotiana_benthamiana/genome).

332

333 **RT-PCR detection of TSWV infection**

334 Total RNA was extracted from TSWV-inoculated *N. benthamiana* plant leaves using
335 an RNA Purification Kit (Tiangen Biotech, Beijing, China), and then treated with
336 RNase-free DNase I (TaKaRa, Dalian, China). First-strand cDNA was synthesized
337 using a TSWV-specific primer (S3 Table). PCR reactions were as follows: initial
338 denaturation at 94°C for 2 min followed by 35 cycles of 94°C for 30 s, 52°C for 30 s,
339 and 72°C for 1 min. The final extension was 72°C for 10 min. The resulting PCR
340 products were visualized in 1.0% (w/v) agarose gels through electrophoresis.
341

342 # Results

343 **Determination of Sw-5b subcellular localization pattern**

344 Expression of YFP-Sw-5b in *N. benthamiana* leaves resulted in a strong HR cell death
345 as well as Sw-5b (Chen *et al.*, 2016; Zhu *et al.*, 2017). To investigate the subcellular
346 localization pattern of Sw-5b, we transiently expressed YFP and YFP-Sw-5b in *N.*
347 *benthamiana* leaves, respectively, through agro-infiltration. Confocal Microscopy
348 results showed that the YFP-Sw-5b fusion accumulated in both cytoplasm and nucleus
349 in *N. benthamiana* leaf cells (Fig. 1b, middle image). This subcellular localization
350 pattern was similar to that of YFP (Fig. 1b, left image). When a D857V mutation,
351 which keeps Sw-5b in an autoactivated state (Chen *et al.*, 2016), was introduced into
352 Sw-5b to produce pYFP-Sw-5b^{D857V} and expressed in *N. benthamiana* leaves, the
353 mutant YFP-Sw-5b^{D857V} fusion also accumulated in both cell cytoplasm and nucleus
354 (Fig. 1b, right image). We also making a construct pNativePro::YFP-Sw-5b

355 expressing YFP-Sw-5b under native Sw-5b promoter. However, the expression of
356 YFP-Sw-5b by native Sw-5b promoter is too low to detect green fluorescence signal.
357 To investigate the subcellular localization pattern of Sw-5b in tomato leaf cells,
358 we transiently expressed YFP, YFP-Sw-5b, and YFP-Sw-5b^{D857V}, respectively,
359 through particle bombardment. Confocal Microscopy results showed that these three
360 proteins exhibited the same subcellular localization pattern as that in the *N.*
361 *benthamiana* leaf cells (Fig. 1c).
362 To further confirm the above results, we harvested *N. benthamiana* leaves
363 expressing YFP-Sw-5b or YFP-Sw-5b^{D857V} and analyzed by cytoplasm and nucleus
364 fractionation assay. Leaf samples agro-infiltrated with the empty vector (p2300S)
365 were also harvested and used as controls. Analyses of total protein, cytoplasm
366 fractions, and nucleus fractions from these harvested leaves using Western blot assays
367 showed that both YFP-Sw-5b and YFP-Sw-5b^{D857V} were accumulated in the
368 cytoplasm and nucleus (Fig. 1d).
369
370 **Sw-5b recognizes TSWV NSm in the cytoplasm**
371 TSWV NSm is known to reside in cytoplasm and plasmodesmata, but not in nucleus
372 (Kormelink *et al.*, 1994; Feng *et al.*, 2016). To determine where Sw-5b can recognize
373 TSWV NSm, we fused a NES, a nes, a NLS or a nls signal peptide to the C-terminus
374 of NSm-YFP to produce NSm-YFP-NES, NSm-YFP-nes, NSm-YFP-NLS, and
375 NSm-YFP-nls, respectively. Transient expressions of these fusions in *N. benthamiana*
376 leaves showed that NSm-YFP-NES accumulated exclusively in the cytoplasm, while

377 NSm-YFP-NLS accumulated in the nucleus (Fig. S1a). As expected, NSm-YFP-nes
378 and NSm-YFP-nls showed the same accumulation pattern as that of NSm-YFP (Fig.
379 S1a). When Sw-5b was co-expressed with one of the above four fusions in *N.*
380 *benthamiana* leaves through agro-infiltration, the leaf tissues co-expressing Sw-5b
381 and NSm-YFP-NES (Sw-5b + NSm-YFP-NES), Sw-5b and NSm-YFP-nes (Sw-5b +
382 NSm-YFP-nes), or Sw-5b and NSm-YFP-nls (Sw-5b + NSm-YFP-nls) developed a
383 strong HR cell death (Fig. S1b). In contrast, the leaf tissues co-expressing Sw-5b and
384 NSm-YFP-NLS (Sw-5b + NSm-YFP-NLS) did not. Western blot assays using a YFP
385 specific antibody confirmed that all the assayed proteins were expressed in the
386 infiltrated tissues (Fig. S1c), indicating that Sw-5b recognizes NSm in the cytoplasm.
387

388 **Sw-5b activity in cell death induction is enhanced in the cytoplasm but**
389 **suppressed in the nucleus**

390 To investigate the roles of the cytoplasmic and nuclear Sw-5b in the induction of cell
391 death and host immunity, we produced constructs to express YFP-Sw-5b,
392 NLS-YFP-Sw-5b, nls-YFP-Sw-5b, NES-YFP-Sw-5b, and nes-YFP-Sw-5b,
393 respectively, and then tested their abilities to elicit cell death and host immunity to
394 tospovirus infection. Transient expressions of these fusions in *N. benthamiana* leaves
395 showed that NES-YFP-Sw-5b accumulated exclusively in the cytoplasm, while
396 NLS-YFP-Sw-5b accumulated only in the nucleus (Fig. 2a). In addition,
397 nes-YFP-Sw-5b and nls-YFP-Sw-5b showed the same accumulation pattern as that
398 shown by YFP-Sw-5b. We then tested cell death induction through co-expressions of

399 NSm and YFP-Sw-5b (NSm + YFP-Sw-5b), NSm and NES-YFP-Sw-5b (NSm +
400 NES-YFP-Sw-5b), NSm and nes-YFP-Sw-5b (NSm + nes-YFP-Sw-5b), NSm and
401 NLS-YFP-Sw-5b (NSm + NLS-YFP-Sw-5b), or NSm and nls-YFP-Sw-5b (NSm +
402 nls-YFP-Sw-5b) in *N. benthamiana* leaves through agro-infiltration. Results of this
403 study showed that the NSm + NES-YFP-Sw-5b-induced cell death was stronger than
404 that induced by NSm + nes-YFP-Sw-5b or NSm + nls-YFP-Sw-5b co-expression (Fig.
405 2b). In addition, the cell death induced by NSm + NLS-YFP-Sw-5b co-expression
406 was suppressed (Fig. 2b). Western blot results showed that the stronger cell death
407 caused by NSm + NES-YFP-Sw-5b co-expression was not due to a greater
408 accumulation of NES-YFP-Sw-5b in the leaves (Fig. 2c). The ion leakage assay
409 results (Fig. 2d) agreed with the phenotype observation results, and indicated that
410 co-expression of NSm + NES-YFP-Sw-5b in leaves lead to a greater ion leakage
411 compared with that induced by the co-expression of NSm + nes-YFP-Sw-5b at 24 and
412 48 hours post agro-infiltration (hpai). The ion leakage caused by the co-expression of
413 NSm + NLS-YFP-Sw-5b was significantly weaker than that caused by the
414 co-expression of NSm + nls-YFP-Sw-5b (Fig. 2d).
415

416 **Cytoplasmic Sw-5b induces a strong host defense against tospovirus replication**

417 Virus infection in plant starts with virus replication in the initially infected cells
418 followed by spreading into adjacent cells for further infection. To monitor tospovirus
419 replication in plant cells, we recently developed a TSWV mini-replicon-based reverse
420 genetic system (Feng et al., 2020). In this study, co-expression of TSWV

421 mini-replicon $SR_{(+)eGFP}$, $L_{(+)opt}$ (with a codon usage optimized RdRp), VSRs and NSm
422 resulted in a cell-to-cell movement of $SR_{(+)eGFP}$. In contrast, co-expression of $SR_{(+)eGFP}$,
423 $L_{(+)opt}$, VSRs, and $NSm^{H93A\&H94A}$ mutant, a defective movement protein but can be
424 recognized by Sw-5b to cause a strong HR (Li *et al.*, 2009; Zhao *et al.*, 2016), in cells
425 resulted in the expression of $SR_{(+)eGFP}$ in only single cells (Fig. S2), thus dissecting the
426 viral replication from viral cell-to-cell movement. We then co-expressed $SR_{(+)eGFP}$,
427 $L_{(+)opt}$, VSRs, $NSm^{H93A\&H94A}$ mutant and one of the five proteins (i.e., Sw-5b,
428 NES-Sw-5b, nes-Sw-5b, NLS-Sw-5b, nls-Sw-5b) in *N. benthamiana* leaves. Leaves
429 co-expressing $SR_{(+)eGFP}$, $L_{(+)opt}$, VSRs, $NSm^{H93A\&H94A}$ mutant and p2300 (empty vector,
430 EV) were used as controls. The results showed that in the presence of Sw-5b or one of
431 its derivatives, the expression of $SR_{(+)eGFP}$ was strongly suppressed compared with
432 that expressed in the presence of EV (Fig. 3a). It is noteworthy that the expression of
433 $SR_{(+)eGFP}$ was less inhibited in the presence of NLS-Sw-5b (Fig. 3a). Western blot
434 result indicated that the GFP accumulation of $SR_{(+)eGFP}$ was strongly inhibited in the
435 presence of Sw-5b, NES-Sw-5b, nes-Sw-5b or nls-Sw-5b compared with that
436 expressed in the presence of NLS-Sw-5b or EV (Fig. 3b). This finding indicates that
437 the cytoplasmic Sw-5b can inhibit $SR_{(+)eGFP}$ expression, possibly through induction of
438 a host defense against TSWV replication.
439
440 **Sw-5b induces a host defense against viral NSm intercellular movement**
441 In our previous study, we used pmCherry-HDEL//NSm-GFP vector (Fig. 4a) to
442 investigate TSWV NSm cell-to-cell movement (Feng *et al.*, 2016). The expressed

443 mCherry-HDEL binds ER membrane in the initial cells but NSm-eGFP traffics
444 between cells. To investigate whether the Sw-5b-induced host defense can affect
445 TSWV NSm cell-to-cell movement, we co-expressed mCherry-HDEL, NSm-GFP,
446 and Sw-5b or mCherry-HDEL, NSm-GFP, and EV in *N. benthamiana* leaves through
447 agro-infiltration. Under the fluorescence microscope, both NSm-GFP and
448 mCherry-HDEL were found in single cells in the presence of Sw-5b. In the presence
449 of EV, however, NSm-GFP moved into multiple cells, while mCherry-HDEL
450 accumulated in the initial cells (Fig. 4b, upper two panels). The result suggested that
451 Sw-5b elicited a defense that strongly inhibited cell-to-cell movement of viral NSm.
452 To make sure this inhibition to viral NSm cell-to-cell movement is not caused by
453 overexpression of Sw-5b, we also used the NSm^{T120N} mutant, from the resistance -
454 breaking (RB) TSWV isolates, which cannot be recognized by Sw-5b (Zhao et al.,
455 2016). The assays showed that in the presence of either Sw-5b or EV, NSm^{T120N}-GFP
456 moved into multiple cells, while mCherry-HDEL retained in the initial cells (Fig S3a).
457

458 **Sw-5b in the nucleus but not in the cytoplasm triggers a defense against NSm**
459 **cell-to-cell movement**

460 To determine the effects of the cytoplasmic and nuclear Sw-5b on host defense against
461 TSWV NSm intercellular movement, we co-expressed mCherry-HDEL and
462 NSm-GFP with NES-Sw-5b, nes-Sw-5b, NLS-Sw-5b, or nls-Sw-5b in *N.*
463 *benthamiana* leaves via agro-infiltration. The results showed that in the presence of
464 NLS-Sw-5b, the cell-to-cell movement of NSm-GFP was inhibited (Fig. 4b). Similar

465 results were also obtained in the leaves co-expressing mCherry-HDEL and NSm-GFP
466 with nls-YFP-Sw-5b or nes-YFP-Sw-5b (Fig S3b). In the presence of
467 NES-YFP-Sw-5b, however, NSm-GFP did move into surrounding cells. (Fig. 4b).
468 This finding indicates that the Sw-5b in the nucleus but not in the cytoplasm induced
469 a host defense that inhibited TSWV NSm cell-to-cell movement.
470

471 **Nuclear Sw-5b confers host immunity to TSWV systemic infection**

472 To dissect the host immunity induced by the cytoplasmic and the nuclear Sw-5b, we
473 generated transgenic *N. benthamiana* lines expressing YFP-Sw-5b, NES-YFP-Sw-5b,
474 nes-YFP-Sw-5b, NLS-YFP-Sw-5b, and nls-YFP-Sw-5b, respectively (Tables S1 and
475 S2). After inoculation of these transgenic lines with TSWV-YN isolate, the EV
476 (control) transgenic plants developed typical viral symptoms including stunt, leaf curl
477 and mosaic at 7 to 15 days post inoculation (dpi). The NES-YFP-Sw-5b transgenic
478 plants developed a strong HR trailing in the systemic leaves by 7 to 15 days post
479 inoculation (dpi) (Fig. 5a and Fig. S4a), suggesting that NES-YFP-Sw-5b transgenic
480 plant did not block TSWV systemic infection and caused virus infection-related
481 systemic HR. In contrast, no systemic virus infection symptoms were observed in the
482 YFP-Sw-5b and the nes-YFP-Sw-5b transgenic plants. The RT-PCR agreed with the
483 symptom observation results and showed that TSWV-YN genomic RNA was
484 accumulated in the systemic leaves of the TSWV-YN-inoculated NES-YFP-Sw-5b or
485 the EV transgenic plants, but not in the systemic leaves of the TSWV-YN-inoculated
486 YFP-Sw-5b or nes-YFP-Sw-5b transgenic plants (Fig. 5c and Fig. S4b). Also in this

487 study, the TSWV-YN-inoculated NLS-YFP-Sw-5b or nls-YFP-Sw-5b transgenic
488 plants did not show virus like symptoms in their systemic leaves by 7-15 dpi (Fig. 5a,
489 and Fig. S4a). The RT-PCR result confirmed that TSWV-N genomic RNA had not
490 accumulated in the systemic leaves of the NLS-YFP-Sw-5b or the nls-YFP-Sw-5b
491 transgenic plants (Fig. 5c, and Fig. S4b), indicating that the nuclear Sw-5b is
492 responsible for the host immunity against TSWV systemic infection.
493

494 **The cytoplasmic and the nuclear Sw-5b act synergistically to confer a strong**
495 **immunity to TSWV infection in *N. benthamiana***

496 To investigate whether cytoplasm-targeted and nucleus-targeted Sw-5b have joint
497 effects on the defense against TSWV infection, we constructed a $M_{(-)opt}$-$pSR_{(+)eGFP}$
498 vector by inserting a cassette expressing optimized TSWV M genomic sequence
499 (Feng *et al.*, 2020) into the $pSR_{(+)eGFP}$ mini-replicon to express NSm, N, and eGFP
500 simultaneously in the same cells (Fig. 6a). The construct $M_{(-)opt}$-$pSR_{(+)eGFP}$ couples the
501 functions for both viral replication and viral cell-to-cell movement, mimicking the
502 virus infection in plant leaves. After co-expressing this vector, the $L_{(+)opt}$ and the EV in
503 *N. benthamiana* leaves through agro-infiltration, the eGFP fluorescence was observed
504 in many cells, due to the presence of the NSm movement protein and the $RdRp_{opt}$ (Fig.
505 6b, upper left image). When $M_{(-)opt}$-$SR_{(+)eGFP}$, $L_{(+)opt}$ and Sw-5b were co-expressed in
506 *N. benthamiana* leaves, the eGFP fluorescence was hardly detected and some were
507 observed only in single leaf cells (Fig. 6b upper right image, Fig. S5a and b). When
508 $M_{(-)opt}$-$SR_{(+)eGFP}$, $L_{(+)opt}$ and NES-Sw-5b were co-expressed in *N. benthamiana* leaves,

509 the eGFP fluorescence was observed in clusters of a few cells (Fig. 6b, Fig. S5a),
510 indicating that limited cell-to-cell movement had occurred in these leaves (Fig. S5b).
511 When $M_{(-)opt}$-$SR_{(+)eGFP}$, $L_{(+)opt}$ and NLS-Sw-5b were co-expressed in leaves, a few of
512 eGFP fluorescence were detected but they were in single cells only. When leaves
513 co-expressing $M_{(-)opt}$-$SR_{(+)eGFP}$, $L_{(+)opt}$ and NES-Sw-5b + NLS-Sw-5b, the eGFP
514 fluorescence was also hardly detected and some were observed only in single leaf
515 cells. Western blot results showed that more eGFP had accumulated in the leaves
516 co-expressing $M_{(-)opt}$-$SR_{(+)eGFP}$, $L_{(+)opt}$, and EV, followed by the leaves co-expressing
517 $M_{(-)opt}$-$SR_{(+)eGFP}$, $L_{(+)opt}$, and NLS-Sw-5b, and then the leaves co-expressing
518 $M_{(-)opt}$-$SR_{(+)eGFP}$, $L_{(+)opt}$, and NES-Sw-5b. Much less eGFP had accumulated in the
519 leaves co-expressing $M_{(-)opt}$-$SR_{(+)eGFP}$, $L_{(+)opt}$, and NLS-Sw-5b + NES-Sw-5b, and in
520 the leaves co-expressing $M_{(-)opt}$-$SR_{(+)eGFP}$, $L_{(+)opt}$, and Sw-5b (Fig. 6c and d). The
521 accumulation of eGFP was lower in the leaves co-expressing NES-Sw-5b +
522 NLS-Sw-5b than that in the leaves co-expressing NES-Sw-5b or NLS-Sw-5b (Fig. 6c
523 and d), indicating that NES-Sw-5b and NLS-Sw-5b have additive role in mediating
524 host immunity against different TSWV infection steps.
525

526 **The Sw-5b NB-ARC-LRR control its cytoplasm localization whereas the**
527 **extended N-terminal SD domain is crucial for targeting Sw-5b into nucleus, and**
528 **for inducing host systemic immunity**

529 Sw-5b has an extended N-terminal SD domain, a CC domain, a NB-ARC domain, and
530 a C-terminal LRR domain (Chen *et al.*, 2016). To determine which domain(s) of

531 Sw-5b is/are responsible for nucleoplasm/nucleolus targeting and for plant immunity,
532 we tested these domains using various deletion mutants and YFP fusion proteins (Fig.
533 7a). We reported previously that the Sw-5b NB-ARC-LRR region was able to induce
534 HR cell death in plant in the presence of NSm (Chen *et al.*, 2016). In this study, we
535 fused YFP to the N-terminus of NB-ARC-LRR (Fig. 7a). Transient expression of
536 YFP-NB-ARC-LRR (112 kDa) in *N. benthamiana* leaf cells resulted in a localization
537 of the fusion protein in cytoplasm exclusively (Fig. 7b).

538 A previous study had shown that the CC domain of potato NLR receptor Rx was
539 required for targeting this protein to nucleus (Slootweg *et al.*, 2010). To determine the
540 function of Sw-5b CC domain in intracellular trafficking, we inserted the CC domain
541 between the YFP and NB-ARC-LRR to generate an YFP-CC-NB-ARC-LRR
542 construct or fused the CC domain to YFP to produce an YFP-CC construct. Transient
543 expression of these two fusion proteins individually in *N. benthamiana* leaves, and
544 examined the leaves under a confocal microscope, we determined that the YFP-CC
545 fusion protein accumulated in both cytoplasm and nucleus of the cells while the
546 YFP-CC-NB-ARC-LRR fusion protein was in the cytoplasm only (Fig. 7b). This
547 result indicated that addition of the CC domain to YFP-NB-ARC-LRR was not
548 sufficient to traffic the fusion protein into the nucleus.

549 An extended N-terminal SD domain is known to be present at the upstream of the
550 Sw-5b CC domain. In this study, we first generated an YFP-SD and an YFP-SD-CC
551 constructs, and transiently expressed them individually in *N. benthamiana* leaf cells.
552 Confocal Microscopy showed that both YFP-SD and YFP-SD-CC fusion proteins

553 accumulated in the cytoplasm and nucleus (Fig. 7b). We then inserted a SD between
554 the YFP and CC-NB-ARC-LRR to produce an YFP-SD-CC-NB-ARC-LRR
555 construction. Transient expression of this construct in *N. benthamiana* leaf cells
556 showed that this fusion protein accumulated in the cytoplasm and nucleus (Fig. 7b).

557 We next generated stable transgenic *N. benthamiana* plants expressing
558 YFP-NB-ARC-LRR, YFP-CC-NB-ARC-LRR and YFP-SD-CC-NB-ARC-LRR.
559 Upon inoculation transgenic *N. benthamiana* plants expressing YFP-NB-ARC-LRR
560 with TSWV, large HR foci were observed in the TSWV-inoculated leaves and later,
561 HR trailing was seen in the systemic leaves of most assayed plants (Fig. 7c; Table S2
562 and S3). RT-PCR results confirmed the presence of TSWV genomic RNA in these
563 systemic leaves (Fig. S6b). We also inoculate *N. benthamiana* plants expressing
564 YFP-CC-NB-ARC-LRR with TSWV. By 7 dpi, no systemic resistance to TSWV
565 infection was observed in these plants (Fig. 6a and B, Table S4). RT-PCR results
566 showed that systemic infection of TSWV did occur in the TSWV-inoculated
567 YFP-CC-NB-ARC-LRR transgenic plants (Fig. S6b). In contrast, transgenic plants
568 expressing YFP-SD-CC-NB-ARC-LRR fusion exhibited a systemic immunity to
569 TSWV infection (Fig. 7c, Fig. S6b).

570 These data indicated that Sw-5b NB-ARC-LRR control its cytoplasm localization,
571 CC domain of Sw-5b alone was not sufficient to transport the NB-ARC-LRR into
572 nucleus and the extended SD domain is required for targeting Sw-5b to the nucleus,
573 and for inducing host immunity.

574

575 **The extended SD domain interacted with *importin α1*, *α2* and *β***

576 To identify the cellular machinery needed for transporting Sw-5b into nucleus, we
577 co-expressed YFP-SD and YFP-Sw-5b in *N. benthamiana* leaves followed by a
578 co-immunoprecipitation (co-IP) and Mass Spectrometry. The results identified *N.*
579 *benthamiana* importin α as one of candidate proteins interacted with YFP-SD and
580 YFP-Sw-5b (Table S5 and S6). The co-IP and Mass Spectrometry also identified
581 nuclear pore complex protein TPRb and nuclear pore complex protein Nup160a
582 interacted with YFP-Sw-5b (Table S6). *Importins* play important roles in
583 translocating proteins from cytoplasm into nucleus (Kanneganti *et al.*, 2007). We used
584 BiFC analysis to confirm the interaction between YFP-SD with *N. benthamiana*
585 importin homologs α1, α2 and *β*. The result showed that co-expression of cYFP-SD
586 with nYFP-IMP α1, nYFP-IMP α2 or nYFP-IMP *β* produced a strong YFP
587 fluorescence signal in nucleus. Co-expression of cYFP-Sw-5b with nYFP-IMP α1,
588 nYFP-IMP α2 or nYFP-IMP *β* also detected a strong YFP fluorescence signal in
589 nucleus (Fig. S7). In contrast, co-expression of controls cYFP-SD and nYFP,
590 cYFP-Sw-5b and nYFP, cYFP and nYFP-IMP α1, cYFP and nYFP-IMP α2 or cYFP
591 and nYFP-IMP *β* did not show fluorescence signal in *N. benthamiana* leaf cells (Fig.
592 S7).

593

594 **Silencing *importin α1*, *α2* and *β* expression abolished Sw-5b nucleus**
595 **accumulation and host resistance to TSWV systemic infection**

596 To determine the functions of importin α1, α2 and β in Sw-5b nucleus localization, we

597 silenced *importin α1, α2, β, α1* and *α2,* and *α1* and *α2* and *β* expressions, respectively,
598 in *N. benthamiana* leaves using a tobacco rattle virus (TRV)-based virus-induced gene
599 silencing (VIGS) vector, and then transiently expressed YFP-Sw-5b in these plants.
600 Analyses of these plants through RT-PCR using gene specific primers showed that
601 silencing of these *importin* genes in *N. benthamiana* leaves were successful (Fig.
602 S8a). However, silencing individual *importin* gene or both *importin α1* and *α2* was
603 not enough to block the nucleus accumulation of YFP-Sw-5b (Fig. 8a). In contrast,
604 after *importin α1*, *α2* and *β* were all silenced through VIGS, the nucleus accumulation
605 of YFP-Sw-5b was inhibited (Fig. 8a, the middle image in the bottom panel).

606 To investigate the effects of nuclear import defected Sw-5b on host immunity to
607 TSWV systemic infection, we silenced these *importin* genes in the Sw-5b transgenic
608 *N. benthamiana* plants as described above, and then inoculated them with TSWV. The
609 results showed that the plants silenced for *importin α1*, *α2*, and *β* gene, individually,
610 did not show TSWV systemic infection (Fig. 8b and Fig. S8b). In addition, the
611 transgenic plants silenced for both *importin α1* and *α2* genes also did not show
612 TSWV systemic infection (Fig. 8b and Fig. S8b). In contrast, after silencing *importin*
613 *α1*, *α2* and *β* together, the plants developed clear TSWV symptoms in systemic
614 leaves followed by HR (Fig. 8b, white arrow and Fig. S8b), indicating that the nucleus
615 accumulation of Sw-5b is indispensable for the induction of host immunity against
616 TSWV systemic infection.

617

618 **Discussion**

619 In this report, we provide evidence to show that the cytoplasm-accumulated and the
620 nucleus-accumulated Sw-5b, a tomato immune receptor, play different roles in
621 inducing host defense against TSWV infection in plant. The cytoplasmic Sw-5b
622 functions to induce a strong cell death response to inhibit TSWV replication. This
623 host response is, however, insufficient to block virus intercellular and long-distance
624 movement. The nuclear-localized Sw-5b triggers a host defense that weakly inhibit
625 viral replication but strongly inhibit tospovirus intercellular and systemic movement.
626 These findings suggest that tomato Sw-5b NLR induces different types of defense
627 responses by cytoplasm and nucleus partitioning to combat virus at different infection
628 steps. Furthermore, the cytoplasmic and the nuclear Sw-5b act synergistically to
629 confer a strong host immunity to TSWV infection in plant. We also demonstrated that
630 the extra SD domain functioned as a critical intracellular translocation modulator,
631 allowing Sw-5b receptor to translocate from cytoplasm to nucleus to trigger the
632 immunity. The Sw-5b NB-LRR controls its cytoplasm localization. Unlike Rx CC
633 domain, Sw-5b CC domain is not sufficient to translocate NB-LRR into nucleus.
634 Strikingly, the SD is crucial for Sw-5b to translocate from cytoplasm for nucleus. This
635 SD-mediated receptor translocation is dependent on importins α and β.

636 Successful virus infection in plant requires several steps including viral replication
637 in the initially infected cells followed by cell-to-cell and long-distance movement
638 (Heinlein, 2015; Wang, 2015). After entering into plant cells, virus first encode
639 multiple proteins needed for its replication. Once the initial replication is established,
640 virus will encode specific protein(s), known as movement proteins (MPs), to traffic

641 viral genome or virions into adjacent cells through plasmodesmata in cell walls, and
642 then long-distantly into other parts of the plant to cause a systemic infection (Rao,
643 2002; Lucas, 2006; Taliansky *et al.*, 2008). To date, multiple plant NLRs, conferring
644 host resistance against plant viruses have been identified (Soosaar *et al.*, 2005; Meier
645 *et al.*, 2019), but how these plant NLRs induce host resistance against virus infection
646 remain largely unknown.

647 In this study, we have determined that the forced cytoplasm accumulation of
648 Sw-5b can induce a stronger cell death than that caused by the accumulation of Sw-5b
649 in both cytoplasm and nucleus. While, the cell death induced by the forced nucleus
650 accumulation of Sw-5b was significantly weakened. We then analyzed
651 Sw-5b-mediated immunity against TSWV replication using a TSWV mini-replicon
652 system and a movement defective NSm mutant. Our results showed that the forced
653 cytoplasm accumulation of Sw-5b can induce a strong host defense against virus
654 replication in cells. This finding implies that cytoplasm is one of the main source of
655 defense signaling against TSWV replication. The defense signaling generated in
656 nucleus can only induce a weak defense against TSWV replication. Therefore, the
657 nuclear localized Sw-5b is only partially responsible for the induction of host defense
658 against TSWV replication. It is also possible that this nuclear localized
659 Sw-5b-induced weak host response is caused by a trace of NLS-YFP-Sw-5b
660 maintained in the cytoplasm that maybe below the detection limit of Confocal
661 Microscope. It has been shown to accumulate in both cytoplasm and nucleus, and the
662 forced cytoplasm accumulation of Barley MLA10 enhance cell death signaling (Bai *et*

663 *al.*, 2012). We speculate that, for both MLA10 and Sw-5b, the cytoplasm
664 accumulation is crucial for the initiation and/or amplification of the cell death
665 signaling. The CC and the TIR domain of several plant NLRs have been shown to
666 trigger cell death (Swiderski *et al.*, 2009; Krasileva *et al.*, 2010; Bernoux *et al.*, 2011;
667 Collier *et al.*, 2011; Maekawa *et al.*, 2011; Bai *et al.*, 2012; Chen *et al.*, 2017; Wang
668 *et al.*, 2020). Analyses of the three dimensional structures of Arabidopsis ZAR1
669 resistosome have also shown that its CC domain can form pentamer structures that
670 was able to target into host cell membranes, leading to ion leakage and cell death
671 (Wang *et al.*, 2019a; Wang *et al.*, 2019b). We speculate that cell death likely cause the
672 toxicity on viral replicase or other proteins associated with virus replication in cells.

673 Plant virus encodes specific movement protein(s) to traffic viral genome between
674 cells and then leaves to cause systemic infection (Rao, 2002; Lucas, 2006; Taliansky
675 *et al.*, 2008). We reported previously that TSWV NSm alone can move between plant
676 cells (Feng *et al.*, 2016). In this study, we investigated the effect of the
677 Sw-5b-mediated host defense on TSWV intercellular movement. Through this study,
678 we have determined that after the recognition of NSm, Sw-5b receptor induced a
679 strong reaction to block NSm intercellular trafficking. Previous reports have some
680 indications on the role of plant NLRs in viral movement. Nevertheless it has no direct
681 evidence showing that plant NLRs induce resistance against viral movement. Deom
682 and colleagues had shown that the 9.4-kDa fluorescein isothiocyanate-labeled dextran
683 was unable to move between cells in the transgenic tobacco *N* leaves expressing
684 tobacco mosaic virus (TMV) movement protein at 24°C, an HR-permissive

685 temperature (Deom *et al.*, 1991). However, that study did not involve a TMV Avr
686 protein. In a different report, TMV-GFP showed a limited cell-to-cell movement in
687 leaves of tobacco cv. Sumsan NN at 33°C, an HR-nonpermissive temperature (Canto
688 & Palukaitis, 2002). Li and colleagues found that after treatment of SMV-inoculated
689 Jidou 7 resistant plants with a callose synthase inhibitor, the plants showed enlarged
690 HR lesions (Li *et al.*, 2012). The soybean *Rsv3* induced extreme resistance. However,
691 after this extremely resistant soybean line was treated with a callose synthase inhibitor,
692 the plants developed HR lesions upon SMV-G5H inoculation (Seo *et al.*, 2014). These
693 reports indicate that plant NLRs likely involves the defense against viral movement.
694 Here we provide the direct evidence that Sw-5b NLR can induce a strong defense
695 response to impede NSm intercellular trafficking. More importantly, we have
696 determined that the induction of host immunity to TSWV intercellular movement
697 requires the accumulation of Sw-5b in nucleus. Although the cytoplasmic Sw-5b can
698 induce a strong cell death response, it cannot prevent TSWV NSm cell-to-cell
699 movement. Consequently, we propose that nucleus is a key compartment to generate
700 defense signaling to block TSWV cell-to-cell movement.

701 In this study, although the NES-YFP-Sw-5b transgenic *N. benthamiana* plants
702 showed an HR, they were unable to stop TSWV systemic infection. We also showed
703 that Sw-5b YFP-NB-ARC-LRR (112 kDa) accumulates in cytoplasm exclusively (Fig.
704 7b), however, transgenic *N. benthamiana* plants expressing YFP-NB-ARC-LRR show
705 strong systemic HR trailing caused by TSWV infection. Based on these findings, we
706 conclude that HR cell death alone is not sufficient to block TSWV long-distance

707 movement. In our study, the NLS-YFP-Sw-5b transgenic plants were resistant to
708 TSWV systemic infection. After silencing the expressions of *importin α1*, *α2* and *β*
709 simultaneously to inhibit the nucleus accumulation of Sw-5b, however, the resistance
710 to TSWV systemic infection was abolished. These findings indicate that the
711 Sw-5b-mediated resistance signaling against viral systemic infection is generated in
712 nucleus. Some plant NLRs are known to interact with specific transcription factors in
713 nucleus upon recognition of pathogen effectors (Cui *et al.*, 2015; Kapos *et al.*, 2019).
714 The immune regulator EDS1 has also been shown to accumulate in nucleus to
715 reprogram RNA transcription (Garcia *et al.*, 2010; Heidrich *et al.*, 2011; Cui *et al.*,
716 2015; Lapin *et al.*, 2020). How Sw-5b regulates host immunity in nucleus requires
717 further investigations.

718 Several plant immune receptors and immune regulators, including, e.g. potato Rx
719 (Slootweg *et al.*, 2010; Tameling *et al.*, 2010), tobacco N (Burch-Smith *et al.*, 2007;
720 Caplan, JL *et al.*, 2008), barley MLA10 (Shen *et al.*, 2007), Arabidopsis
721 RRS1-R/RPS4, and snc1 (Deslandes *et al.*, 2003; Wirthmueller *et al.*, 2007; Cheng *et*
722 *al.*, 2009), as well as Arabidopsis NPR1 (Katagiri & Tsuda, 2010), and EDS1 (Lapin
723 *et al.*, 2020) have been found to be nucleocytoplasmic. For some of them, nuclear
724 accumulation of NLRs are required for the induction of plant immunity to pathogen
725 attacks. Moreover, the MLA10-YFP-NES fusion was found to induce a strong cell
726 death response, but not a strong host resistance to powdery mildew fungus infection.
727 In contrast, the MLA10-YFP-NLS fusion inhibited its activity to induce a cell death
728 response, but caused a host immunity to this pathogen (Bai *et al.*, 2012). In many

729 plant-pathogen interactions, cell death responses can be uncoupled from disease
730 resistance (Bendahmane *et al.*, 1999; Gassmann, 2005; Coll *et al.*, 2010; Heidrich *et*
731 *al.*, 2011). This separation raises questions about how host resistance prevents
732 pathogen invasion and what are the roles of cell death during pathogen infection. It is
733 unclear whether the MLA10-YFP-NES-induced cell death has some inhibitory effects
734 on powdery mildew fungus infection. In this study, we determined that cytoplasm-
735 and nuclear-accumulation of Sw-5b have different functions. The
736 cytoplasm-accumulated Sw-5b induces a strong defense against virus replication,
737 whereas the nuclear-accumulated Sw-5b induced an inhibition of virus cell-to-cell and
738 long distance movement. Both cytoplasmic and nuclear Sw-5b are needed to confer a
739 synergistic and full defense against tospovirus infection.

740 We have also determined that Sw-5b NB-ARC-LRR and SD domains are
741 important to regulate the proper subcellular localization of Sw-5b and the proper
742 nucleoplasmic distribution of Sw-5b is needed to elicit full immune responses to
743 inhibit different TSWV infection steps. Sw-5b NB-ARC-LRR controls its cytoplasm
744 localization. The CC domain of the Sw-5b is not sufficient to target the receptor into
745 nuclear. Importantly, the extended SD of Sw-5b is absolutely required for the nucleus
746 translocation. Because non-canonical domains are frequently found in other NLRs
747 and are quite diversified, our findings have broad implications to investigate the
748 potential new functions of non-canonical domains that integrated in the plant NLRs to
749 regulate the plant immunity against pathogen invasions.

750 Through co-IP, Mass Spectrometry and BiFC analysis, we found that the extended

751 SD domain and Sw-5b interacted with host importin machineries to translocate the
752 Sw-5b receptor from cytoplasm into nucleus to mediate local and systemic resistance
753 to tospovirus. Recent studies have shown that nuclearporin MOS3, MOS6 and nuclear
754 pore complex component MOS7/Nup88 proteins played important roles in regulating
755 Arabidopsis innate immunity (Palma *et al.*, 2005; Zhang & Li, 2005; Cheng *et al.*,
756 2009). We found that when *importin α1*, *importin α2* and *importin β* gene were all
757 silenced through VIGS, the nucleus targeting of Sw-5b were completely blocked, and
758 consequently, the Sw-5b-mediated systemic immunity to tospovirus infection was
759 compromised. Importin α and β are known to form a nucleus import complex.
760 Binding with importin β could activate importin α to form a binding surface for NLS
761 proteins (Stewart, 2007). Hence, disruption of either importin α or importin β would
762 block the nucleus import of NLS proteins. Because silencing *importin α* or
763 *importin β* gene expression through VIGS did not disrupt the nuclear targeting of
764 Sw-5b, we speculate that a non-canonical nuclear import pathway may take part in
765 importing Sw-5b into nucleus.

766 Based on the above results, we have created a working model for the Sw-5b
767 NLR-induced host resistance against TSWV replication, and intercellular and
768 long-distance movement in plant (Fig. 9). Upon recognition of NSm in cytoplasm,
769 Sw-5b switched from an autoinhibited state to an activated state. The activated Sw-5b
770 accumulated in cytoplasm and also translocate into nucleus via importins α and β .
771 The cytoplasm-accumulated and the nucleus-accumulated Sw-5b play different roles
772 in inducing host immunity against TSWV infection. The cytoplasmic Sw-5b functions

773 to induce a cell death response to inhibit TSWV replication, while the nuclear Sw-5b
774 functions to induce a weak host defense against TSWV replication, but a strong
775 defense against TSWV cell-to-cell and long-distance movement. The concerted
776 defense signaling generated in the cytoplasm and nucleus resulted in a strong host
777 resistance to tospovirus infection.
778
779
780 **Acknowledgments**
781 This work was supported by the National Natural Science Foundation of China
782 (31630062, 31925032 and 31870143), the Fundamental Research Funds for the
783 Central Universities (JCQY201904 and KYXK202012), Youth Science and
784 Technology Innovation Program to XT.
785
786 **Author contributions**
787 HC XQ, XC and XT, designed the research; HC, XQ and XC, TY, MF, JC, RC, HH,
788 YZ, YM, DS, YX, MZ performed the experiments; HC, XSD and XT interpreted the
789 result and wrote the paper.
790
791 **ORCID**
792 Hongyu Chen, 0000-0001-8142-0653
793 Yi Xu, 0000-0002-1913-4530
794 Min Zhu, 0000-0002-9354-4300

Xiaorong Tao, 0000-0003-1259-366X

Competing interests

The authors declare that nocompeting interests exist.

Data availability

All data produced in this study are presented in this manuscript or as the supporting files

References

Axtell MJ, Staskawicz BJ. 2003. Initiation of RPS2-specified disease resistance in Arabidopsis is coupled to the AvrRpt2-directed elimination of RIN4. *Cell* **112**(3): 369-377.

Bai S, Liu J, Chang C, Zhang L, Maekawa T, Wang Q, Xiao W, Liu Y, Chai J, Takken FL, Schulze-Lefert P, Shen QH. 2012. Structure-function analysis of barley NLR immune receptor MLA10 reveals its cell compartment specific activity in cell death and disease resistance. *PLoS Pathog* **8**(6): e1002752.

Bendahmane A, Kanyuka K, Baulcombe DC. 1999. The Rx gene from potato controls separate virus resistance and cell death responses. *Plant Cell* **11**(5): 781-792.

Bernoux M, Ve T, Williams S, Warren C, Hatters D, Valkov E, Zhang X, Ellis JG, Kobe B, Dodds PN. 2011. Structural and functional analysis of a plant resistance protein TIR domain reveals interfaces for self-association, signaling, and autoregulation. *Cell Host Microbe* **9**(3): 200-211.

Brommonschenkel SH, Frary A, Frary A, Tanksley SD. 2000. The broad-spectrum tospovirus resistance gene Sw-5 of tomato is a homolog of the root-knot nematode resistance gene Mi. *Mol Plant Microbe Interact* **13**(10): 1130-1138.

Burch-Smith TM, Schiff M, Caplan JL, Tsao J, Czymmek K, Dinesh-Kumar SP. 2007. A novel role for the TIR domain in association with pathogen-derived elicitors. *PLoS Biol* **5**(3): e68.

Canto T, Palukaitis P. 2002. Novel N gene-associated, temperature-independent resistance to the movement of tobacco mosaic virus vectors neutralized by a cucumber mosaic virus RNA1 transgene. *J Virol* **76**(24): 12908-12916.

Caplan J, Padmanabhan M, Dinesh-Kumar SP. 2008. Plant NB-LRR Immune Receptors: From Recognition to Transcriptional Reprogramming. *Cell Host Microbe* **3**(3): 126-135.

827 **Caplan JL, Mamillapalli P, Burch-Smith TM, Czymmek K, Dinesh-Kumar SP. 2008.**
828 Chloroplastic protein NRIP1 mediates innate immune receptor recognition of a viral effector.
829 *Cell* **132**(3): 449-462.
830 **Cesari S, Bernoux M, Moncuquet P, Kroj T, Dodds PN. 2014.** A novel conserved mechanism for
831 plant NLR protein pairs: the "integrated decoy" hypothesis. *Front Plant Sci* **5**: 606.
832 **Cesari S, Moore J, Chen C, Webb D, Periyannan S, Mago R, Bernoux M, Lagudah ES, Dodds**
833 **PN. 2016.** Cytosolic activation of cell death and stem rust resistance by cereal MLA-family
834 CC-NLR proteins. *Proc Natl Acad Sci U S A* **113**(36): 10204-10209.
835 **Cesari S, Thilliez G, Ribot C, Chalvon V, Michel C, Jauneau A, Rivas S, Alaux L, Kanzaki H,**
836 **Okuyama Y, Morel JB, Fournier E, Tharreau D, Terauchi R, Kroj T. 2013.** The rice
837 resistance protein pair RGA4/RGA5 recognizes the Magnaporthe oryzae effectors AVR-Pia
838 and AVR1-CO39 by direct binding. *Plant Cell* **25**(4): 1463-1481.
839 **Chen T, Liu D, Niu X, Wang J, Qian L, Han L, Liu N, Zhao J, Hong Y, Liu Y. 2017.** Antiviral
840 Resistance Protein Tm-2(2) Functions on the Plasma Membrane. *Plant Physiol* **173**(4):
841 2399-2410.
842 **Chen X, Zhu M, Jiang L, Zhao W, Li J, Wu J, Li C, Bai B, Lu G, Chen H, Moffett P, Tao X. 2016.**
843 A multilayered regulatory mechanism for the autoinhibition and activation of a plant
844 CC-NB-LRR resistance protein with an extra N-terminal domain. *New Phytol* **212**(1):
845 161-175.
846 **Cheng YT, Germain H, Wiermer M, Bi D, Xu F, Garcia AV, Wirthmueller L, Despres C, Parker**
847 **JE, Zhang Y, Li X. 2009.** Nuclear pore complex component MOS7/Nup88 is required for
848 innate immunity and nuclear accumulation of defense regulators in Arabidopsis. *Plant Cell*
849 **21**(8): 2503-2516.
850 **Coll NS, Vercammen D, Smidler A, Clover C, Van Breusegem F, Dangl JL, Epple P. 2010.**
851 Arabidopsis type I metacaspases control cell death. *Science* **330**(6009): 1393-1397.
852 **Collier SM, Hamel LP, Moffett P. 2011.** Cell death mediated by the N-terminal domains of a unique
853 and highly conserved class of NB-LRR protein. *Mol Plant Microbe Interact* **24**(8): 918-931.
854 **Collier SM, Moffett P. 2009.** NB-LRRs work a "bait and switch" on pathogens. *Trends Plant Sci*
855 **14**(10): 521-529.
856 **Cui H, Tsuda K, Parker JE. 2015.** Effector-triggered immunity: from pathogen perception to robust
857 defense. *Annu Rev Plant Biol* **66**: 487-511.
858 **Das B, Sengupta S, Prasad M, Ghose TK. 2014.** Genetic diversity of the conserved motifs of six
859 bacterial leaf blight resistance genes in a set of rice landraces. *BMC Genet* **15**: 82.
860 **De Oliveira AS, Koolhaas I, Boiteux LS, Caldararu OF, Petrescu AJ, Oliveira Resende R,**
861 **Kormelink R. 2016.** Cell death triggering and effector recognition by Sw-5 SD-CNL proteins
862 from resistant and susceptible tomato isolines to Tomato spotted wilt virus. *Mol Plant Pathol*
863 **17**(9): 1442-1454.
864 **Deom CM, Wolf S, Holt CA, Lucas WJ, Beachy RN. 1991.** Altered function of the tobacco mosaic
865 virus movement protein in a hypersensitive host. *Virology* **180**(1): 251-256.
866 **Deslandes L, Olivier J, Peeters N, Feng DX, Khounlotham M, Boucher C, Somssich I, Genin S,**
867 **Marco Y. 2003.** Physical interaction between RRS1-R, a protein conferring resistance to
868 bacterial wilt, and PopP2, a type III effector targeted to the plant nucleus. *Proc Natl Acad Sci*
869 *U S A* **100**(13): 8024-8029.
870 **Dodds PN, Rathjen JP. 2010.** Plant immunity: towards an integrated view of plant-pathogen

871 interactions. *Nat Rev Genet* **11**(8): 539-548.
872 **Ea VDB, Jones JD. 1998.** Plant disease-resistance proteins and the gene-for-gene concept. *Trends in*
873 *Biochemical Sciences* **23**(12): 454-456(453).
874 **Engelhardt S, Boevink PC, Armstrong MR, Ramos MB, Hein I, Birch PR. 2012.** Relocalization of
875 late blight resistance protein R3a to endosomal compartments is associated with effector
876 recognition and required for the immune response. *Plant Cell* **24**(12): 5142-5158.
877 **Ernst K, Kumar A, Kriseleit D, Kloos DU, Phillips MS, Ganal MW. 2002.** The broad-spectrum
878 potato cyst nematode resistance gene (Hero) from tomato is the only member of a large gene
879 family of NBS-LRR genes with an unusual amino acid repeat in the LRR region. *Plant J* **31**(2):
880 127-136.
881 **Feng M, Cheng R, Chen M, Guo R, Li L, Feng Z, Wu J, Xie L, Hong J, Zhang Z, Kormelink R,**
882 **Tao X. 2020.** Rescue of tomato spotted wilt virus entirely from complementary DNA clones.
883 *Proc Natl Acad Sci U S A* **117**(2): 1181-1190.
884 **Feng Z, Xue F, Xu M, Chen X, Zhao W, Garcia-Murria MJ, Mingarro I, Liu Y, Huang Y, Jiang**
885 **L, Zhu M, Tao X. 2016.** The ER-Membrane Transport System Is Critical for Intercellular
886 Trafficking of the NSm Movement Protein and Tomato Spotted Wilt Tospovirus. *PLoS*
887 *Pathog* **12**(2): e1005443.
888 **Gao Z, Chung EH, Eitas TK, Dangl JL. 2011.** Plant intracellular innate immune receptor Resistance
889 to Pseudomonas syringae pv. maculicola 1 (RPM1) is activated at, and functions on, the
890 plasma membrane. *Proc Natl Acad Sci U S A* **108**(18): 7619-7624.
891 **Garcia AV, Blanvillain-Baufume S, Huibers RP, Wiermer M, Li G, Gobbato E, Rietz S, Parker**
892 **JE. 2010.** Balanced nuclear and cytoplasmic activities of EDS1 are required for a complete
893 plant innate immune response. *PLoS Pathog* **6**: e1000970.
894 **Gassmann W. 2005.** Natural variation in the Arabidopsis response to the avirulence gene hopPsyA
895 uncouples the hypersensitive response from disease resistance. *Mol Plant Microbe Interact*
896 **18**(10): 1054-1060.
897 **Germain H, Seguin A. 2011.** Innate immunity: has poplar made its BED? *New Phytol* **189**(3):
898 678-687.
899 **Hallwass M, de Oliveira AS, de Campos Dianese E, Lohuis D, Boiteux LS, Inoue-Nagata AK,**
900 **Resende RO, Kormelink R. 2014.** The Tomato spotted wilt virus cell-to-cell movement
901 protein (NSM) triggers a hypersensitive response in Sw-5-containing resistant tomato lines
902 and in Nicotiana benthamiana transformed with the functional Sw-5b resistance gene copy.
903 *Mol Plant Pathol* **15**(9): 871-880.
904 **Heidrich K, Wirthmueller L, Tasset C, Pouzet C, Deslandes L, Parker JE. 2011.** Arabidopsis
905 EDS1 connects pathogen effector recognition to cell compartment-specific immune responses.
906 *Science* **334**(6061): 1401-1404.
907 **Heinlein M. 2015.** Plant virus replication and movement. *Virology* **479-480**: 657-671.
908 **Horsefield S, Burdett H, Zhang X, Manik MK, Shi Y, Chen J, Qi T, Gilley J, Lai JS, Rank MX,**
909 **Casey LW, Gu W, Ericsson DJ, Foley G, Hughes RO, Bosanac T, von Itzstein M,**
910 **Rathjen JP, Nanson JD, Boden M, Dry IB, Williams SJ, Staskawicz BJ, Coleman MP,**
911 **Ve T, Dodds PN, Kobe B. 2019.** NAD(+) cleavage activity by animal and plant TIR domains
912 in cell death pathways. *Science* **365**(6455): 793-799.
913 **Inoue H, Hayashi N, Matsushita A, Xinqiong L, Nakayama A, Sugano S, Jiang CJ, Takatsuji H.**
914 **2013.** Blast resistance of CC-NB-LRR protein Pb1 is mediated by WRKY45 through

915 protein-protein interaction. *Proc Natl Acad Sci U S A* **110**(23): 9577-9582.
916 **Jones JD, Vance RE, Dangl JL. 2016.** Intracellular innate immune surveillance devices in plants and
917 animals. *Science* **354**(6316).
918 **Jubic LM, Saile S, Furzer OJ, El Kasmi F, Dangl JL. 2019.** Help wanted: helper NLRs and plant
919 immune responses. *Curr Opin Plant Biol* **50**: 82-94.
920 **Kanneganti TD, Bai X, Tsai CW, Win J, Meulia T, Goodin M, Kamoun S, Hogenhout SA. 2007.**
921 A functional genetic assay for nuclear trafficking in plants. *Plant J* **50**(1): 149-158.
922 **Kanzaki H, Yoshida K, Saitoh H, Fujisaki K, Hirabuchi A, Alaux L, Fournier E, Tharreau D,**
923 **Terauchi R. 2012.** Arms race co-evolution of Magnaporthe oryzae AVR-Pik and rice Pik
924 genes driven by their physical interactions. *Plant J* **72**(6): 894-907.
925 **Kapos P, Devendrakumar KT, Li X. 2019.** Plant NLRs: From discovery to application. *Plant Sci* **279**:
926 3-18.
927 **Katagiri F, Tsuda K. 2010.** Understanding the plant immune system. *Mol Plant Microbe Interact*
928 **23**(12): 1531-1536.
929 **Kawano Y, Fujiwara T, Yao A, Housen Y, Hayashi K, Shimamoto K. 2014.**
930 Palmitoylation-dependent membrane localization of the rice resistance protein pit is critical
931 for the activation of the small GTPase OsRac1. *J Biol Chem* **289**(27): 19079-19088.
932 **Kong L, Qiu X, Kang J, Wang Y, Chen H, Huang J, Qiu M, Zhao Y, Kong G, Ma Z, Wang Y, Ye**
933 **W, Dong S, Ma W, Wang Y. 2017.** A Phytophthora Effector Manipulates Host Histone
934 Acetylation and Reprograms Defense Gene Expression to Promote Infection. *Curr Biol* **27**(7):
935 981-991.
936 **Kormelink R, Garcia ML, Goodin M, Sasaya T, Haenni AL. 2011.** Negative-strand RNA viruses:
937 the plant-infecting counterparts. *Virus Res* **162**(1-2): 184-202.
938 **Kormelink R, Storms M, Van Lent J, Peters D, Goldbach R. 1994.** Expression and subcellular
939 location of the NSM protein of tomato spotted wilt virus (TSWV), a putative viral movement
940 protein. *Virology* **200**(1): 56-65.
941 **Kourelis J, van der Hoorn RAL. 2018.** Defended to the Nines: 25 Years of Resistance Gene Cloning
942 Identifies Nine Mechanisms for R Protein Function. *Plant Cell* **30**(2): 285-299.
943 **Krasileva KV, Dahlbeck D, Staskawicz BJ. 2010.** Activation of an Arabidopsis resistance protein is
944 specified by the in planta association of its leucine-rich repeat domain with the cognate
945 oomycete effector. *Plant Cell* **22**(7): 2444-2458.
946 **Kroj T, Chanclud E, Michel-Romiti C, Grand X, Morel JB. 2016.** Integration of decoy domains
947 derived from protein targets of pathogen effectors into plant immune receptors is widespread.
948 *New Phytol* **210**(2): 618-626.
949 **Lanford RE, Butel JS. 1984.** Construction and characterization of an SV40 mutant defective in
950 nuclear transport of T antigen. *Cell* **37**(3): 801-813.
951 **Lapin D, Bhandari DD, Parker JE. 2020.** Origins and Immunity Networking Functions of EDS1
952 Family Proteins. *Annu Rev Phytopathol* **58**: 253-276.
953 **Le Roux C, Huet G, Jauneau A, Camborde L, Tremousaygue D, Kraut A, Zhou B, Levaillant M,**
954 **Adachi H, Yoshioka H, Raffaele S, Berthome R, Coute Y, Parker JE, Deslandes L. 2015.**
955 A receptor pair with an integrated decoy converts pathogen disabling of transcription factors
956 to immunity. *Cell* **161**(5): 1074-1088.
957 **Leastro MO, Pallas V, Resende RO, Sanchez-Navarro JA. 2017.** The functional analysis of distinct
958 tospovirus movement proteins (NSM) reveals different capabilities in tubule formation,

959 cell-to-cell and systemic virus movement among the tospovirus species. *Virus Res* **227**: 57-68.
960 **Li J, Huang H, Zhu M, Huang S, Zhang W, Dinesh-Kumar SP, Tao X. 2019.** A Plant Immune
961 Receptor Adopts a Two-Step Recognition Mechanism to Enhance Viral Effector Perception.
962 *Mol Plant* **12**(2): 248-262.
963 **Li W, Lewandowski DJ, Hilf ME, Adkins S. 2009.** Identification of domains of the Tomato spotted
964 wilt virus NSm protein involved in tubule formation, movement and symptomatology.
965 *Virology* **390**(1): 110-121.
966 **Li W, Zhao Y, Liu C, Yao G, Wu S, Hou C, Zhang M, Wang D. 2012.** Callose deposition at
967 plasmodesmata is a critical factor in restricting the cell-to-cell movement of Soybean mosaic
968 virus. *Plant Cell Rep* **31**(5): 905-916.
969 **Li X, Kapos P, Zhang Y. 2015.** NLRs in plants. *Curr Opin Immunol* **32**: 114-121.
970 **Lopez C, Aramburu J, Galipienso L, Soler S, Nuez F, Rubio L. 2011.** Evolutionary analysis of
971 tomato Sw-5 resistance-breaking isolates of Tomato spotted wilt virus. *J Gen Virol* **92**(Pt 1):
972 210-215.
973 **Lucas WJ. 2006.** Plant viral movement proteins: agents for cell-to-cell trafficking of viral genomes.
974 *Virology* **344**(1): 169-184.
975 **Lukasik-Shreepaathy E, Slootweg E, Richter H, Goverse A, Cornelissen BJ, Takken FL. 2012.**
976 Dual regulatory roles of the extended N terminus for activation of the tomato MI-1.2
977 resistance protein. *Mol Plant Microbe Interact* **25**(8): 1045-1057.
978 **Ma S, Lapin D, Liu L, Sun Y, Song W, Zhang X, Logemann E, Yu D, Wang J, Jirschitzka J, Han**
979 **Z, Schulze-Lefert P, Parker JE, Chai J. 2020.** Direct pathogen-induced assembly of an
980 NLR immune receptor complex to form a holoenzyme. *Science* **370**(6521).
981 **Ma Y, Guo H, Hu L, Martinez PP, Moschou PN, Cevik V, Ding P, Duxbury Z, Sarris PF, Jones**
982 **JDG. 2018.** Distinct modes of derepression of an Arabidopsis immune receptor complex by
983 two different bacterial effectors. *Proc Natl Acad Sci U S A* **115**(41): 10218-10227.
984 **Ma Z, Song T, Zhu L, Ye W, Wang Y, Shao Y, Dong S, Zhang Z, Dou D, Zheng X, Tyler BM,**
985 **Wang Y. 2015.** A Phytophthora sojae Glycoside Hydrolase 12 Protein Is a Major Virulence
986 Factor during Soybean Infection and Is Recognized as a PAMP. *Plant Cell* **27**(7): 2057-2072.
987 **Ma Z, Zhu L, Song T, Wang Y, Zhang Q, Xia Y, Qiu M, Lin Y, Li H, Kong L, Fang Y, Ye W,**
988 **Wang Y, Dong S, Zheng X, Tyler BM, Wang Y. 2017.** A paralogous decoy protects
989 Phytophthora sojae apoplastic effector PsXEG1 from a host inhibitor. *Science* **355**(6326):
990 710-714.
991 **Maekawa T, Cheng W, Spiridon LN, Toller A, Lukasik E, Saijo Y, Liu P, Shen QH, Micluta MA,**
992 **Somssich IE, Takken FLW, Petrescu AJ, Chai J, Schulze-Lefert P. 2011.** Coiled-coil
993 domain-dependent homodimerization of intracellular barley immune receptors defines a
994 minimal functional module for triggering cell death. *Cell Host Microbe* **9**(3): 187-199.
995 **Meier N, Hatch C, Nagalakshmi U, Dinesh-Kumar SP. 2019.** Perspectives on intracellular
996 perception of plant viruses. *Mol Plant Pathol* **20**(9): 1185-1190.
997 **Meyers BC, Kozik A, Griego A, Kuang H, Michelmore RW. 2003.** Genome-wide analysis of
998 NBS-LRR-encoding genes in Arabidopsis. *Plant Cell* **15**(4): 809-834.
999 **Milligan SB, Bodeau J, Yaghoobi J, Kaloshian I, Zabel P, Williamson VM. 1998.** The root knot
1000 nematode resistance gene Mi from tomato is a member of the leucine zipper, nucleotide
1001 binding, leucine-rich repeat family of plant genes. *Plant Cell* **10**(8): 1307-1319.
1002 **Mittler R, Herr EH, Orvar BL, van Camp W, Willekens H, Inze D, Ellis BE. 1999.** Transgenic

1003 tobacco plants with reduced capability to detoxify reactive oxygen intermediates are
1004 hyperresponsive to pathogen infection. *Proc Natl Acad Sci U S A* **96**(24): 14165-14170.
1005 **Oliver JE, Whitfield AE. 2016.** The Genus Tospovirus: Emerging Bunyaviruses that Threaten Food
1006 Security. *Annu Rev Virol* **3**(1): 101-124.
1007 **Padmanabhan MS, Ma S, Burch-Smith TM, Czymmek K, Huijser P, Dinesh-Kumar SP. 2013.**
1008 Novel positive regulatory role for the SPL6 transcription factor in the N TIR-NB-LRR
1009 receptor-mediated plant innate immunity. *PLoS Pathog* **9**(3): e1003235.
1010 **Palma K, Zhang Y, Li X. 2005.** An importin alpha homolog, MOS6, plays an important role in plant
1011 innate immunity. *Curr Biol* **15**(12): 1129-1135.
1012 **Peiro A, Canizares MC, Rubio L, Lopez C, Moriones E, Aramburu J, Sanchez-Navarro J. 2014.**
1013 The movement protein (NSm) of Tomato spotted wilt virus is the avirulence determinant in
1014 the tomato Sw-5 gene-based resistance. *Mol Plant Pathol* **15**(8): 802-813.
1015 **Qi D, DeYoung BJ, Innes RW. 2012.** Structure-function analysis of the coiled-coil and leucine-rich
1016 repeat domains of the RPS5 disease resistance protein. *Plant Physiol* **158**(4): 1819-1832.
1017 **Qi D, Innes RW. 2013.** Recent Advances in Plant NLR Structure, Function, Localization, and
1018 Signaling. *Front Immunol* **4**: 348.
1019 **Rao ALNC, Y. G，Khan, J. A，Dijkstra, J. 2002.** Molecular biology of plant virus movement.
1020 *Plant Viruses As Molecular Pathogens*.
1021 **Sarris PF, Cevik V, Dagdas G, Jones JD, Krasileva KV. 2016.** Comparative analysis of plant
1022 immune receptor architectures uncovers host proteins likely targeted by pathogens. *BMC Biol*
1023 **14**: 8.
1024 **Sarris PF, Duxbury Z, Huh SU, Ma Y, Segonzac C, Sklenar J, Derbyshire P, Cevik V, Rallapalli**
1025 **G, Saucet SB, Wirthmueller L, Menke FL, Sohn KH, Jones JD. 2015.** A Plant Immune
1026 Receptor Detects Pathogen Effectors that Target WRKY Transcription Factors. *Cell* **161**(5):
1027 1089-1100.
1028 **Scholthof KB, Adkins S, Czosnek H, Palukaitis P, Jacquot E, Hohn T, Hohn B, Saunders K,**
1029 **Candresse T, Ahlquist P, Hemenway C, Foster GD. 2011.** Top 10 plant viruses in
1030 molecular plant pathology. *Mol Plant Pathol* **12**(9): 938-954.
1031 **Seo JK, Kwon SJ, Cho WK, Choi HS, Kim KH. 2014.** Type 2C protein phosphatase is a key
1032 regulator of antiviral extreme resistance limiting virus spread. *Sci Rep* **4**: 5905.
1033 **Seong K, Seo E, Witek K, Li M, Staskawicz B. 2020.** Evolution of NLR resistance genes with
1034 noncanonical N-terminal domains in wild tomato species. *New Phytol* **227**(5): 1530-1543.
1035 **Shen QH, Saijo Y, Mauch S, Biskup C, Bieri S, Keller B, Seki H, Ulker B, Somssich IE,**
1036 **Schulze-Lefert P. 2007.** Nuclear activity of MLA immune receptors links isolate-specific and
1037 basal disease-resistance responses. *Science* **315**(5815): 1098-1103.
1038 **Slootweg E, Roosien J, Spiridon LN, Petrescu AJ, Tameling W, Joosten M, Pomp R, van Schaik**
1039 **C, Dees R, Borst JW, Smant G, Schots A, Bakker J, Goverse A. 2010.** Nucleocytoplasmic
1040 distribution is required for activation of resistance by the potato NB-LRR receptor Rx1 and is
1041 balanced by its functional domains. *Plant Cell* **22**(12): 4195-4215.
1042 **Soosaar JL, Burch-Smith TM, Dinesh-Kumar SP. 2005.** Mechanisms of plant resistance to viruses.
1043 *Nat Rev Microbiol* **3**(10): 789-798.
1044 **Spassova M I PTW, Folkertsma R T, et al. 2001.** The tomato gene Sw-5 is a member of the coiled
1045 coil, nucleotide binding, leucine-rich repeat class of plant resistance genes and confers
1046 resistance to TSWV in tobacco. *Molecular Breeding.* **7(2)**: 151.

1047 **Stewart M. 2007.** Molecular mechanism of the nuclear protein import cycle. *Nat Rev Mol Cell Biol*
1048 **8**(3): 195-208.
1049 **Swiderski MR, Birker D, Jones JD. 2009.** The TIR domain of TIR-NB-LRR resistance proteins is a
1050 signaling domain involved in cell death induction. *Mol Plant Microbe Interact* **22**(2):
1051 157-165.
1052 **Takemoto D, Rafiqi M, Hurley U, Lawrence GJ, Bernoux M, Hardham AR, Ellis JG, Dodds PN,**
1053 **Jones DA. 2012.** N-terminal motifs in some plant disease resistance proteins function in
1054 membrane attachment and contribute to disease resistance. *Mol Plant Microbe Interact* **25**(3):
1055 379-392.
1056 **Takken FLW, Goverse A. 2012.** How to build a pathogen detector: structural basis of NB-LRR
1057 function. *Current Opinion in Plant Biology* **15**(4): 375-384.
1058 **Taliansky M, Torrance L, Kalinina NO. 2008.** Role of plant virus movement proteins. *Methods Mol*
1059 *Biol* **451**: 33-54.
1060 **Tameling WI, Nooijen C, Ludwig N, Boter M, Slootweg E, Goverse A, Shirasu K, Joosten MH.**
1061 **2010.** RanGAP2 mediates nucleocytoplasmic partitioning of the NB-LRR immune receptor
1062 Rx in the Solanaceae, thereby dictating Rx function. *Plant Cell* **22**(12): 4176-4194.
1063 **Tasset C, Bernoux M, Jauneau A, Pouzet C, Briere C, Kieffer-Jacquinod S, Rivas S, Marco Y,**
1064 **Deslandes L. 2010.** Autoacetylation of the Ralstonia solanacearum effector PopP2 targets a
1065 lysine residue essential for RRS1-R-mediated immunity in Arabidopsis. *PLoS Pathog* **6**(11):
1066 e1001202.
1067 **Turina M, Kormelink R, Resende RO. 2016.** Resistance to Tospoviruses in Vegetable Crops:
1068 Epidemiological and Molecular Aspects. *Annu Rev Phytopathol* **54**: 347-371.
1069 **van der Vossen EA, Gros J, Sikkema A, Muskens M, Wouters D, Wolters P, Pereira A, Allefs S.**
1070 **2005.** The Rpi-blb2 gene from Solanum bulbocastanum is an Mi-1 gene homolog conferring
1071 broad-spectrum late blight resistance in potato. *Plant J* **44**(2): 208-222.
1072 **van Wersch S, Li X. 2019.** Stronger When Together: Clustering of Plant NLR Disease resistance
1073 Genes. *Trends Plant Sci* **24**(8): 688-699.
1074 **van Wersch S, Tian, L., Hoy, R., Li, X. . 2020.** Plant NLRs: The whistleblowers of
1075 plant immunity. *Plant Commun*: doi: https://doi.org/10.1016/j.xplc.2019.100016.
1076 **Vos P, Simons G, Jesse T, Wijbrandi J, Heinen L, Hogers R, Frijters A, Groenendijk J,**
1077 **Diergaarde P, Reijans M, Fierens-Onstenk J, de Both M, Peleman J, Liharska T,**
1078 **Hontelez J, Zabeau M. 1998.** The tomato Mi-1 gene confers resistance to both root-knot
1079 nematodes and potato aphids. *Nat Biotechnol* **16**(13): 1365-1369.
1080 **Vossen JH, van Arkel G, Bergervoet M, Jo KR, Jacobsen E, Visser RG. 2016.** The Solanum
1081 demissum R8 late blight resistance gene is an Sw-5 homologue that has been deployed
1082 worldwide in late blight resistant varieties. *Theor Appl Genet* **129**(9): 1785-1796.
1083 **Wan L, Essuman K, Anderson RG, Sasaki Y, Monteiro F, Chung EH, Osborne Nishimura E,**
1084 **DiAntonio A, Milbrandt J, Dangl JL, Nishimura MT. 2019.** TIR domains of plant immune
1085 receptors are NAD(+)-cleaving enzymes that promote cell death. *Science* **365**(6455): 799-803.
1086 **Wang A. 2015.** Dissecting the molecular network of virus-plant interactions: the complex roles of host
1087 factors. *Annu Rev Phytopathol* **53**: 45-66.
1088 **Wang J, Chen T, Han M, Qian L, Li J, Wu M, Han T, Cao J, Nagalakshmi U, Rathjen JP, Hong**
1089 **Y, Liu Y. 2020.** Plant NLR immune receptor Tm-22 activation requires NB-ARC
1090 domain-mediated self-association of CC domain. *PLoS Pathog* **16**(4): e1008475.

1091 **Wang J, Hu M, Wang J, Qi J, Han Z, Wang G, Qi Y, Wang HW, Zhou JM, Chai J. 2019a.**
1092 Reconstitution and structure of a plant NLR resistosome conferring immunity. *Science*
1093 **364**(6435).
1094 **Wang J, Wang J, Hu M, Wu S, Qi J, Wang G, Han Z, Qi Y, Gao N, Wang HW, Zhou JM, Chai J.**
1095 **2019b.** Ligand-triggered allosteric ADP release primes a plant NLR complex. *Science*
1096 **364**(6435).
1097 **Wen W, Meinkoth JL, Tsien RY, Taylor SS. 1995.** Identification of a signal for rapid export of
1098 proteins from the nucleus. *Cell* **82**(3): 463-473.
1099 **Wirthmueller L, Zhang Y, Jones JD, Parker JE. 2007.** Nuclear accumulation of the Arabidopsis
1100 immune receptor RPS4 is necessary for triggering EDS1-dependent defense. *Curr Biol* **17**(23):
1101 2023-2029.
1102 **Zhang Y, Li X. 2005.** A putative nucleoporin 96 Is required for both basal defense and constitutive
1103 resistance responses mediated by suppressor of npr1-1,constitutive 1. *Plant Cell* **17**(4):
1104 1306-1316.
1105 **Zhao W, Jiang L, Feng Z, Chen X, Huang Y, Xue F, Huang C, Liu Y, Li F, Liu Y, Tao X. 2016.**
1106 Plasmodesmata targeting and intercellular trafficking of Tomato spotted wilt tospovirus
1107 movement protein NSm is independent of its function in HR induction. *J Gen Virol* **97**(8):
1108 1990-1997.
1109 **Zhu M, Jiang L, Bai B, Zhao W, Chen X, Li J, Liu Y, Chen Z, Wang B, Wang C, Wu Q, Shen Q,**
1110 **Dinesh-Kumar SP, Tao X. 2017.** The Intracellular Immune Receptor Sw-5b Confers
1111 Broad-Spectrum Resistance to Tospoviruses through Recognition of a Conserved 21-Amino
1112 Acid Viral Effector Epitope. *Plant Cell* **29**(9): 2214-2232.
1113 **Zhu M, van Grinsven IL, Kormelink R, Tao X. 2019.** Paving the Way to Tospovirus Infection:
1114 Multilined Interplays with Plant Innate Immunity. *Annu Rev Phytopathol* **57**: 41-62.

1115

1116

1117

1118

1119 **FIGURE LEGENDS**

1120 **Fig. 1.** Subcellular localization of Sw-5b in *Nicotiana benthamiana* and tomato leaf
1121 cells. (a) Schematic diagrams of Sw-5b. (b) Subcellular localizations of free YFP
1122 (left), YFP-Sw-5b (middle) and autoactive YFP-Sw-5b^{D857V} mutant (right) in *N.*
1123 *benthamiana* leaf cells at 24 hours post agro-infiltration (hpi). (c) Subcellular
1124 localization of free YFP (left), YFP-Sw-5b (middle) and autoactive YFP-Sw-5b^{D857V}
1125 mutant (right) in tomato leaf cells at 24 hpi. N nucleus, and C cytoplasm inside the
1126 cell are indicated. Bar = 10 μm. (d) Nucleocytoplasmic partitioning analysis of
1127 YFP-Sw-5b and autoactive YFP-Sw-5b^{D857V}. Total lysate (T) from p2300S empty
1128 vector (EV), YFP-Sw-5b or YFP-Sw-5b^{D857V} expressing leaves were fractionated into
1129 cytoplasm and nucleus, and analyzed by immunoblots using antibodies against YFP.
1130 The actin and histone were used as a cytoplasm marker and nucleus marker,
1131 respectively, in the fractionation analysis. Ponceau S staining was also used as
1132 cytoplasm marker.

1133

1134 **Fig. 2.** Effect of Sw-5b subcellular localization pattern on HR induction. (a) Confocal
1135 images of *N. benthamiana* leaf cells transiently expressing NES-YFP-Sw-5b,
1136 nes-YFP-Sw-5b, NLS-YFP-Sw-5b or nls-YFP-Sw-5b fusion. The images were taken
1137 at 24–36 hpi. N nucleus and C cytoplasm (c). Bar = 10 μm. (b) Induction of HR in *N.*
1138 *benthamiana* leaf tissues co-expressing NSm and one of the five Sw-5b fusion
1139 proteins. The infiltrated *N. benthamiana* leaf was photographed at 3 dpi (left image).
1140 Induction of HR in the infiltrated tissues were visualized using a trypan blue staining

1141 method (right image). (c) Immunoblot analysis of NES-YFP-Sw-5b, nes-YFP-Sw-5b,
1142 NLS-YFP-Sw-5b, and nls-YFP-Sw-5b expressions in the infiltrated *N. benthamiana*
1143 leaf tissues. These fusion proteins were enriched using the GFP-Trap beads prior to
1144 SDS-PAGE, and the blot was probed using an YFP specific antibody. Ponceau-S
1145 staining was used to estimate sample loadings. (d) Time course analysis of ion
1146 leakage in Nicotiana benthamiana leaves co-expressing NSm with one of the five
1147 Sw-5b fusion proteins. Measurements were performed at 4 h intervals starting from
1148 24 to 48 hpi. Error bars (SEs) were calculated using the results from three biological
1149 replicates per treatment collected at each time point.
1150
1151 **Fig. 3.** The effect of cytoplasm- and nucleus-targeted Sw-5b on viral replication. (a)
1152 Schematic representation of binary constructs to express TSWV $SR_{(-)eGFP}$
1153 mini-genome replicon, TSWV L RNA segment containing an optimized RdRp and
1154 $NSm^{H93A\&H94A}$ mutant that defected in viral movement. Minus sign (-) and 5′ to 3′
1155 designation represent the negative (genomic)-strand of tospovirus RNA. 35S: a
1156 double 35S promoter; HH: hammerhead ribozyme; RZ: hepatitis delta virus (HDV)
1157 ribozyme; NOS: nopaline synthase terminator; 35S Ter: a 35S transcription terminator.
1158 (b) Accumulation of eGFP fluorescence in *N. benthamiana* leaves co-expressing
1159 p2300S empty vector (EV), Sw-5b, NES-Sw-5b, nes-Sw-5b, NLS-Sw-5b, or
1160 nls-Sw-5b with TSWV $SR_{(-)eGFP}$, L, and $NSm^{H93A\&H94A}$ at 4 days post infiltration (dpi)
1161 viewed with a fluorescence microscope. Bar represents 400 μm. (c) Immunoblot
1162 analysis of expression of eGFP proteins in leaves shown in panel (b) using specific

1163 antibodies against YFP. Ponceau S staining of rubisco large subunit is shown for
1164 protein loading control.
1165
1166 **Fig. 4.** Effect of subcellular localization of Sw-5b on cell-to-cell movement of NSm
1167 in leaf epidermis of *N. benthamiana.* (a) Schematic diagram of the binary construct to
1168 co-express mCherry-HDEL and NSm-GFP. (b) Cell-to-cell movement analysis of
1169 NSm-GFP in *N. benthamiana* leaves co-expressing p2300S empty vector (EV), Sw-5b,
1170 NES-Sw-5b, NLS-Sw-5b, or nls-Sw-5b with the construct harboring both
1171 mCherry-HDEL and NSm-GFP. *Agrobacterium* containing the construct to co-express
1172 mCherry-HDEL and NSm-GFP was diluted 500 times for expression in a single
1173 epidermal cell. All other *Agrobacterium* were infiltrated at the concentration of OD_{600}
1174 = 0.2. Bar, 50 μm.
1175
1176 **Fig. 5.** Analysis of cytoplasm- and nucleus-targeted Sw-5b-mediated host immunity
1177 to TSWV systemic infection. (a) TSWV systemic infection in transgenic *N.*
1178 *benthamiana* plants expressing NES-YFP-Sw-5b, nes-YFP-Sw-5b, NLS-YFP-Sw-5b,
1179 nls-YFP-Sw-5b, YFP-Sw-5b or p2300S empty vector (EV) driven by 35S promoter.
1180 TSWV-inoculated plants were photographed at 15 dpi. White arrow indicates the
1181 systemic leaves showing HR trailing. White arrowhead indicates the systemic leaves
1182 showing mosaic. (b) Immunoblot analysis of NES-YFP-Sw-5b, nes-YFP-Sw-5b,
1183 NLS-YFP-Sw-5b, nls-YFP-Sw-5b and YFP-Sw-5b expressions in different transgenic
1184 *N. benthamiana* plants. EV plants transformed with an empty vector and were used as

1185 a negative control. (c) RT-PCR analysis of TSWV accumulation in the systemic
1186 leaves of different transgenic *N. benthamiana* plants at 15 dpi.
1187
1188 **Fig. 6.** Joint effects of cytoplasm- and nucleus-targeted Sw-5b on defenses against
1189 tospovirus infection in *Nicotiana benthamiana* leaves. (a) Schematic representation of
1190 binary constructs to express TSWV $SR_{(+)eGFP}$-$M_{(-)op}$ and TSWV L RNA segment
1191 containing an optimized RdRp. 35S: a double 35S promoter; HH: hammerhead
1192 ribozyme; RZ: hepatitis delta virus (HDV) ribozyme; NOS: nopaline synthase
1193 terminator. (b) Accumulation of eGFP fluorescence in *N. benthamiana* leaves
1194 co-expressing p2300S empty vector (EV), Sw-5b, NES-Sw-5b, NLS-Sw-5b, or
1195 NES-Sw-5b+NLS-Sw-5b with TSWV $SR_{(+)eGFP}$-$M_{(-)op}$ at 4 days post infiltration (dpi)
1196 viewed with a fluorescence microscope. Bar represents 400 μm. (c) Immunoblot
1197 analysis of expression of eGFP proteins in leaves shown in panel (b) using specific
1198 antibodies against YFP. Ponceau S staining of rubisco large subunit is shown for
1199 protein loading control. (d) Quantification of eGFP proteins in leaves shown in panel
1200 (c).
1201
1202 **Fig. 7.** Functional analysis and subcellular localization patterns of individual or
1203 combined Sw-5b domains. (a) Schematic diagrams showing a full length Sw-5b or
1204 Sw-5b domains fused with YFP. (b) Confocal images of *N. benthamiana* leaf
1205 epidermal cells expressing various YFP fusions. Images of the cells were taken at 24
1206 hpi. N nucleus, Nu nucleolus, and C cytoplasm. Bar = 10 μm. (c) TSWV-inoculated

1207 transgenic *N. benthamiana* plants expressing these various YFP fusions and
1208 photographed at 15 dpi.
1209
1210 **Fig. 8.** Roles of *importins* α and β in YFP-Sw-5b nucleus targeting and
1211 Sw-5b-mediated immunity to TSWV systemic infection. (a) Transient expression of
1212 YFP-Sw-5b in *N. benthamiana* leaf epidermal cells silenced for *importin*
1213 $\alpha 1$ (IMP α1 KD), *importin* $\alpha 2$ (IMP α2 KD), *importin* $\alpha 1$ and $\alpha 2$ (IMP α1 & α2 KD),
1214 *importin* β (IMP β KD) or *importin* $\alpha 1$ and $\alpha 2$ and β (IMP α1 & α2 & β KD) through
1215 VIGS. Images of the cells were captured using a confocal microscope at 26 hpi. N
1216 nucleus, C cytoplasm. Bar = 10 μm. (b) YFP-Sw-5b transgenic *N. benthamiana* plants
1217 were silenced for *importin* $\alpha 1$, *importin* $\alpha 2$, *importin* $\alpha 1$ and $\alpha 2$, *importin* β or
1218 *importin* $\alpha 1$ and $\alpha 2$ and β expression through VIGS followed by inoculation with
1219 TSWV. TSWV-inoculated YFP-Sw-5b transgenic *N. benthamiana* plants were
1220 photographed at 15 dpi. White arrowhead indicates HR trailing in systemic leaves.
1221
1222 **Fig. 9.** A working model for Sw-5b. Sw-5b furcates disease resistances by proper
1223 nucleocytoplasmic partition to block different infection steps of tomato spotted wilt
1224 tospovirus. Sw-5b switched from the autoinhibited state to an activated state upon
1225 recognition of NSm in the cytoplasm. Cytoplasm portion of Sw-5b induce cell death
1226 and defense that inhibit viral replication. The activated Sw-5b also translocated into
1227 nucleus via *importins* α and β. Nucleus-localized Sw-5b induces a defense that block
1228 viral cell-to-cell and long-distance movement. Cytoplasm- and nucleus-localized

1229 Sw-5b have additively effects on defense to inhibit viral replication, intercellular and

1230 long-distance movement during tospovirus infection.

1231

1232 **Supporting Information**

1233 **Short legends**

1234 **Fig. S1** Sw-5b recognizes TSWV NSm in cytoplasm.

1235 **Fig. S2** Analysis of virus replication monitoring system using a TSWV-based
1236 mini-genome replicon and a movement defective NSm mutant.

1237 **Fig. S3** Effects of nes-Sw-5b and nls-Sw-5b on NSm-GFP cell-to-cell movement and
1238 effects of Sw-5b and EV on NSm^{T120N}-GFP cell-to-cell movement.

1239 **Fig. S4** Effects of cytoplasmic and nuclear Sw-5b on host immunity to TSWV
1240 systemic infection.

1241 **Fig. S5** Cytoplasmic and nuclear Sw-5b activity on TSWV-GFP cell-to-cell
1242 movement in *N. benthamiana* leaves.

1243 **Fig. S6** An immunoblot showing the accumulations of various YFP-tagged proteins
1244 expressed in different transgenic *N. benthamiana* plants and RT-PCR analysis of
1245 TSWV accumulation in the systemic leaves.

1246 **Fig. S7** Bimolecular fluorescence complementation (BiFC) assay of cYFP-SD,
1247 cYFP-Sw-5b and nYFP-Importin α1 (nYFP-IMP α1), nYFP-Importin α2 (nYFP-IMP
1248 α2), nYFP-Importin β (nYFP-IMP β) interaction in *N. benthamiana* leaf epidermal
1249 cells.

1250 **Fig. S8** RT-PCR analyses of *importin a1*, *a2* and *b* expressions in the assayed plants
1251 and their effects on TSWV systemic infection.

1252 **Table S1.** List of primers used in this study.

1253 **Table S2.** Response of six different types of transgenic *Nicotiana benthamina* plants

1254 driven by 35S promoter to TSWV infection.

1255 **Table S3.** Response of six different types of transgenic *Nicotiana benthamina* plants

1256 driven by Sw-5b native promoter to TSWV infection.

1257 **Table S4.** Response of six different types of transgenic *Nicotiana benthamina* plants

1258 to TSWV infection.

1259 **Table S5.** Mass spectrum data of YFP-SD

1260 **Table S6.** Mass spectrum data of YFP-Sw-5b

1261

Cytoplasmic and nuclear Sw-5b NLR act both independently and synergistically to dictate full host defense against tospovirus infection

Hongyu Chen[1,¶], Xin Qian[1,¶], Xiaojiao Chen[1,¶], Tongqing Yang[1], Mingfeng Feng[1], Jing Chen[1], Ruixiang Cheng[1], Hao Hong[1], Ying Zheng[1], Yuzhen Mei[4], Danyu Shen[1], Yi Xu[1], Min Zhu[1], Xin Shun Ding[1] and Xiaorong Tao[1,*]

[1] Key Laboratory of Plant Immunity, Department of Plant Pathology, College of Plant Protection, Nanjing Agricultural University, Nanjing 210095, P. R. China.

[2] Huaiyin Institute of Agricultural Sciences of Xuhuai Region in Jiangsu，Huaian 223001, Jiangsu, P. R. China.

[3] College of Plant Protection, Yunnan Agricultural University, Kunming 650201, Yunnan, P. R. China.

[4] State Key Laboratory of Rice Biology, Institute of Biotechnology, Zhejiang University, Hanghzou 310029, P. R. China.

[¶] These authors contributed equally to this work.

Author for correspondence:

Xiaorong Tao

Tel: (+86)-25-84399027

Email: taoxiaorong@njau.edu.cn

RUNNING HEAD

Independent role of cytoplasmic and nuclear Sw-5b in immunity

Word Count: Main body of the text, 8136

Title 18, Summary 249, Keywords 8, Introduction 1286, Materials and Methods 1562, Results 3030, Discussion 1884, Acknowledgments 35, References 3687, Figure Legends 1103, Supporting Information Legends 786

9 Figures (Colors); Supporting information: 8 Supplemental Figures, 6 Supplemental Tables

Summary

- Plant intracellular nucleotide binding-leucine-rich repeat (NLR) receptors play critical roles in mediating host immunity to pathogen attack. We use tomato Sw-5b::tospovirus as a model system to study the specific role of the compartmentalized plant NLR in dictating host defense against virus at different infection steps.
- We demonstrated here that tomato NLR Sw-5b translocates to cytoplasm and nucleus, respectively, to play different roles in inducing host resistances against *Tomato spotted wilt tospovirus* (TSWV) infection. The cytoplasmic Sw-5b functions to induce a strong cell death response to inhibit TSWV replication. This host response is, however, insufficient to block viral intercellular and long-distance movement. The nucleus-localized Sw-5b triggers a host defense that weakly inhibits viral replication but strongly impedes virus intercellular and systemic movement. Furthermore, the cytoplasmic and nuclear Sw-5b act synergistically to dictate full host defense to TSWV infection.
- We further demonstrated that the extended N-terminal *Solanaceae* domain (SD) of Sw-5b plays critical roles in cytoplasm/nucleus partitioning. Sw-5b nucleotide-binding leucine-rich repeat (NB-LRR) controls its cytoplasm localization. Strikingly, the SD but not coil-coil (CC) domain is crucial for Sw-5b receptor to translocate from cytoplasm to nucleus to trigger the immunity. The SD was found to interact with importins. Silencing both importin α and β expression disrupted Sw-5b nucleus translocation and host immunity

against TSWV systemic infection.

- Collectively, our findings suggest that Sw-5b bifurcates disease resistances by cytoplasm/nucleus partitioning to block different infection steps of TSWV. The findings also identified a new regulatory role of extra domain of a plant NLR in mediating host innate immunity.

Keywords:

NLRs, Cytoplasm, Nuclear, Plant innate immunity, Tomato spotted wilt virus, Replication, Cell-to-cell movement and Long distance movement

93

94 # Introduction

95 Plant innate immunity plays critical roles in host defense against pathogen invasions,
96 and is triggered by cell-surface receptors or intracellular nucleotide-binding
97 leucine-rich repeat (NLR) receptors (Soosaar *et al.*, 2005; Dodds & Rathjen, 2010;
98 Cui *et al.*, 2015; Li *et al.*, 2015; Jones *et al.*, 2016; Kourelis & van der Hoorn, 2018;
99 Kapos *et al.*, 2019; van Wersch, 2020). Plant intracellular NLRs are the largest
100 classes of resistance proteins that function to detect pathogen effectors, and to activate
101 host immunity upon pathogen attack (Caplan, J *et al.*, 2008; Takken & Goverse, 2012;
102 Li *et al.*, 2015; Jones *et al.*, 2016; Kourelis & van der Hoorn, 2018; Kapos *et al.*,
103 2019). Plant NLRs typically contain an N-terminal domain, a central
104 nucleotide-binding domain (NB), a nucleotide-binding adaptor (ARC domain shared
105 by Apaf-1, certain resistance proteins, and CED-4), and a C-terminal leucine-rich
106 repeat (LRR) domain (Ea & Jones, 1998; Jones *et al.*, 2016; Ma *et al.*, 2018; Wang *et*
107 *al.*, 2019a; Wang *et al.*, 2019b; Ma *et al.*, 2020). Based on the differences among the
108 N-terminal domains, plant NLRs can be further divided into two main categories,
109 known as the coiled-coil NLR (refers to as CNL) category and the Toll/interleukin-1
110 receptor NLR (TNL) category (Meyers *et al.*, 2003; Collier & Moffett, 2009; Qi &
111 Innes, 2013). The CC- or the TIR-domain-bearing NLRs have distinct genetic
112 requirements and can regulate different functions in the downstream of defense
113 signaling (Collier & Moffett, 2009; Qi & Innes, 2013; Horsefield *et al.*, 2019; Jubic *et*

114 *al.*, 2019; van Wersch & Li, 2019; Wan *et al.*, 2019).

115 In addition to classical domains, non-canonical domains were frequently found to
116 integrate into certain NLRs. The additional domain, called BED, was first found in 32
117 poplar NLR proteins (Germain & Seguin, 2011). This extra BED domain was also
118 found in nine rice NLRs (Das *et al.*, 2014). The RATX1/HMA domain in the rice
119 NLRs RGA5 and Pik‐1 was found to act as integrated decoys to detect the cognate
120 pathogen effectors (Kanzaki *et al.*, 2012; Cesari *et al.*, 2013; Cesari *et al.*, 2014). The
121 WRKY domain on Arabidopsis thaliana NLR RRS1 was further found to function as
122 an integrated decoy that recognizes the effectors AvrRps4 and PopP2 (Le Roux *et al.*,
123 2015; Sarris *et al.*, 2015). Genome-wide analyses of plant NLR receptors revealed
124 that about 3.5 % of the NLRs carried specific non-canonical domains (Cesari *et al.*,
125 2014; Kroj *et al.*, 2016; Sarris *et al.*, 2016), and some of these non-canonical domains
126 were shown to be targeted by pathogen effectors during pathogen infections (Sarris *et*
127 *al.*, 2016). However, molecular functions of most non-canonical domains in plant
128 NLRs remain largely unexplored.

129 Translocations of plant NLRs into proper subcellular compartments are critical for
130 the induction of innate immunity (Cui *et al.*, 2015; van Wersch, 2020). Multiple plant
131 NLRs and immune regulators, including tobacco N, Arabidopsis snc1, RRS1/RPS4,
132 barley MLA10, and Arabidopsis EDS1, NPR1, have been shown to accumulate in
133 both cytoplasm and nucleus, and for several nucleocytoplasmic NLRs accumulation
134 in nucleus is required for triggering host resistance to pathogen infections (Deslandes
135 *et al.*, 2003; Burch-Smith *et al.*, 2007; Shen *et al.*, 2007; Wirthmueller *et al.*, 2007;

136 Tasset *et al.*, 2010; Bai *et al.*, 2012; Inoue *et al.*, 2013; Padmanabhan *et al.*, 2013).
137 Wheat Sr33, a homolog of barley MLA10, however, was reported to accumulate in
138 cytoplasm to induce host resistance against stem rust pathogen (Cesari *et al.*, 2016).
139 For potato Rx, a balanced cytoplasm and nucleus accumulation of Rx is needed to
140 induce the host immunity (Slootweg *et al.*, 2010; Tameling *et al.*, 2010). Other studies
141 have shown that *Arabidopsis* Rpm1 (Gao *et al.*, 2011), RPS2 (Axtell & Staskawicz,
142 2003), RPS5 (Qi *et al.*, 2012), rice Pit (Takemoto *et al.*, 2012), and tomato Tm-2^2
143 (Chen *et al.*, 2017; Wang *et al.*, 2020) need to associate with plasma membrane in
144 order to trigger cell death and host immunity. Latest studies have shown that the
145 activated *Arabidopsis* ZAR1 can bind to cellular membrane, leading to a membrane
146 leakage followed by cell death and host immunity (Wang *et al.*, 2019a; Wang *et al.*,
147 2019b). Flax L6 and M have been shown to accumulate in both Golgi apparatus and
148 tonoplast, and these compartmentalized localizations are necessary for the induction
149 of host resistance (Kawano *et al.*, 2014). The re-distribution of potato R3a from
150 cytosol to endosomal compartments is crucial for the induction of host resistance to
151 *Phytophthora infestans* infection (Engelhardt *et al.*, 2012). Different plant NLRs have
152 diverse subcellular localizations for their proper functions. However, how the
153 compartmentalized plant NLRs specifically dictate defense signaling remains largely
154 unknown.

155 Tomato spotted wilt tospovirus (TSWV) is one of most destructive plant NSVs,
156 infecting more than 1000 plant species, and causes crop losses more than one billion
157 US dollars annually worldwide (Kormelink *et al.*, 2011; Scholthof *et al.*, 2011; Oliver

158 & Whitfield, 2016). Tomato NLR Sw-5b confers strong resistance to TSWV infection
159 and has been widely used in tomato breeding projects to produce tospovirus resistant
160 tomato cultivars (Brommonschenkel *et al.*, 2000; Spassova M I, 2001; Turina *et al.*,
161 2016; Zhu *et al.*, 2019). Upon recognition of TSWV movement protein, NSm, Sw-5b
162 can trigger a hypersensitive response (HR), which typically associated with localized
163 cell death (Lopez *et al.*, 2011; Hallwass *et al.*, 2014; Peiro *et al.*, 2014; De Oliveira *et*
164 *al.*, 2016; Zhao *et al.*, 2016; Leastro *et al.*, 2017). Tospoviruses are divided into
165 American and Euro-Asia type based on their geographic distribution and amino acid
166 sequence identity of viral nucleocapsid protein. We have previously shown that
167 Sw-5b can confer a broad-spectrum resistance to American type tospoviruses,
168 including TSWV, through recognition of a conserved 21 amino acid PAMP-like
169 region in the viral movement protein NSm (Zhu *et al.*, 2017). Sw-5b carries an
170 extended N-terminal *Solanaceae* domain (SD), a CC domain, a NB-ARC domain, and
171 a LRR domain (Brommonschenkel *et al.*, 2000; Spassova M I, 2001;
172 Lukasik-Shreepaathy *et al.*, 2012). Similar SDs have also been found in the Mi-1.2,
173 R8, Rpi-blb2, and Hero (Milligan *et al.*, 1998; Vos *et al.*, 1998; Ernst *et al.*, 2002; van
174 der Vossen *et al.*, 2005; Lukasik-Shreepaathy *et al.*, 2012; Vossen *et al.*, 2016). More
175 recently, Seong and others reported that the extended CNL has been evolved initially
176 in the ancestor of *Asterids* and *Amaranthaceae*, predated the *Solanaceae* family
177 (Seong *et al.*, 2020). In the presence of the extended N-terminal SD, Sw-5b is in an
178 autoinhibited state through multilayered interactions between SD, CC, NB-ARC, and
179 LRR domains (Chen *et al.*, 2016). For activation, the extra SD also recognizes NSm.

180 Sw-5b adopts a two-step NSm recognition strategy through SD and then LRR domain
181 (Li *et al.*, 2019). This two-step recognition mechanism significantly enhances the
182 sensitivity of the detection on TSWV NSm (Li *et al.*, 2019). Although Sw-5b is
183 known to localize in both cytoplasm and nucleus (De Oliveira *et al.*, 2016), the
184 biological roles of the cytoplasm- and the nucleus-accumulated Sw-5b in host
185 immunity signaling are unknown.

186 In this study, we investigated the subcellular distribution pattern of Sw-5b and the
187 functions of the compartmentalized Sw-5b in the induction of host immunity to
188 TSWV infection. We determined here that cytoplasm- and nucleus-accumulated
189 Sw-5b functions differently in inducing host defense response to inhibit multiple
190 tospovirus infection steps. The cytoplasmic Sw-5b can induce a strong cell death
191 response to suppress TSWV replication, whereas the nucleus-accumulated Sw-5b can
192 induce a strong defense against viral intercellular movement and systemic infection.
193 The combination of cytoplasmic and nuclear Sw-5b induces a synergistic and strong
194 plant immunity against tospovirus infection. We also found that the extended SD
195 functions as the key regulator for this critical intracellular translocation. The SD was
196 also found to interact with importins α and β to mediate Sw-5b nucleus translocation,
197 and to confer the full host immunity against tospovirus infection.

198

199 **Materials and Methods**

200 **Plasmid construction**

201 p2300S-YFP-Sw-5b was from a previously described source (Chen *et al.*, 2016).

202 Different domains of Sw-5b were PCR-amplified from p2300S-Sw-5b (Chen *et al.*,
203 2016) and cloned individually behind the *YFP* gene in the p2300S vector using a
204 two-step overlap PCR procedure as described (Li *et al.*, 2019). All the primers used in
205 this study are listed in Table S1.

206 To visualize the subcellular localization patterns of various fusion proteins, a SV40
207 T-Ag-derived nuclear localization signal (NLS, QPKKKRKVGG) (Lanford & Butel,
208 1984) or a PK1 nuclear export signal (NES, NELALKLAGLDINK) (Wen *et al.*, 1995)
209 was fused to the N-terminus of YFP-Sw-5b or the C-terminus of NSm-YFP, as
210 described (Kong *et al.*, 2017), to produce pNES-YFP-Sw-5b, pNLS-YFP-Sw-5b,
211 pNSm-YFP-NES, and pNSm-YFP-NLS, respectively. In addition, YFP-Sw-5b and
212 NSm-YFP were fused individually with a mutant NLS (nls, QPKKTRKVGG) or a
213 mutant NES (nes, NELALKAAGADANK) to produce pnes-YFP-Sw-5b,
214 pnls-YFP-Sw-5b, pNSm-YFP-nes, and pNSm-YFP-nls. The constructs were then
215 transformed individually into *Agrobacterium tumefaciens* strain GV3101 cells.

216

217 **Transient gene expression, stable plant transformation, and virus inoculation**

218 *Nicotiana benthamiana* were grown in soil in pots inside a greenhouse maintained at
219 25°C and a 16 h light/8 h dark photoperiod. Six-to-eight week-old *N. benthamiana*
220 plants were used for various assays. Transient gene expression assays were performed
221 in *N. benthamiana* leaves through agro-infiltration using Agrobacterium cultures
222 carrying specific expressing constructs as described previously (Feng *et al.*, 2016; Ma
223 *et al.*, 2017). Transgenic *N. benthamiana* lines expressing YFP-Sw-5b or its

224 derivatives were made using constructs with a 35S promoter or a Sw-5b native
225 promoter via a standard leaf-disc transformation method (Chen *et al.*, 2016). The
226 resulting transgenic *N. benthamiana* lines were named as NES-YFP-Sw-5b,
227 NLS-YFP-Sw-5b, nes-YFP-Sw-5b, nls-YFP-Sw-5b, YFP-Sw-5b, and EV
228 (transformed with an empty vector), respectively. Inoculation of transgenic *N.*
229 *benthamiana* plants with TSWV was done by rubbing plant leaves with TSWV-YN
230 isolate-infected crude saps as described (Zhu *et al.*, 2017). TRV-mediated VIGS in *N.*
231 *benthamiana* plants was done as described (Ma *et al.*, 2015). The agro-infiltrated or
232 the virus-inoculated plants were growning inside a growth chamber maintained at
233 25/23 °C (day/night) with a 16/8 h light and dark photoperiod.
234
235 **Particle bombardment**
236 The particle bombardment is described (Feng et al., 2016). Briefly, 60 mg Tungsten
237 M-10 microcarrier (Bio-RAD) was placed into a 1.5 ml Eppendorf tube with 1 mL
238 70% ethanol. The tube was vortexes for 3 minutes, and then stood at room
239 temperature for 15 minutes. After centrifuge at low speed for 5 seconds, the
240 supernatant was removed and the pellet was rinsed with 70% ethanol for 3 times. One
241 mL 50% sterile glycerol solution was added and divided Tungsten M-10 microcarrier
242 into 50 µl. Five µg pRTL2-YFP, pRTL2-YFP-Sw-5b or pRTL2-YFP-Sw-5bD857V
243 plasmid DNA, 50 µl of 2.5 M CaCl2, and 20 µl of 0.1 M spermidine, respectively
244 were added and mixed with microcarrier. After centrifuge at low speed for 5 seconds
245 and the supernatant removed. The pellet was resuspended in 200 µl 70% ethanol and

246 centrifugation as described above. Use 48 µl of 100% ethanol to resuspend the
247 tungsten particle::plasmid DNA complexes, and load 15 48 µl mixture onto the center
248 of carrier (Bio-RAD), air dry, and use He/1000 particle transport system (BIO-RAD)
249 to bombard tomato leaves harvested from 3- or 4-week-old of Money Marker. The
250 bombarded leaves were incubated in Petri dishes for 24 hours at 25°C followed with
251 Confocal Microscope analysis.

252

253 **Trypan blue staining**

254 *N. benthamiana* leaves were harvested at 3 days post agro-infiltration (dpai) and
255 boiled for 5 min in a 1.15:1 (v/v) mixed ethanol and trypan blue staining solution (10
256 g phenol, 10 mL glycerol, 10 mL lactic acid, and 20 mg trypan blue in 10 mL distilled
257 water). The stained leaves were then de-stained in a chloral hydrate solution (2.5 g per
258 mL distilled water) as described (Bai *et al.*, 2012).

259

260 **Electrolyte leakage assay**

261 Electrolyte leakage assay was performed as previously described (Mittler *et al.*, 1999;
262 Zhu *et al.*, 2017) with slight modifications. Briefly, five leaf discs (9 mm in diameter
263 each) were taken from the agro-infiltrated leaves per treatment and at various dpai.
264 The harvested leaf discs from a specific treatment were floated on a 10 mL distilled
265 water for 3 h at room temperature (RT), and the conductivity of each bathing water
266 was measured (referred to as value A) using a Multiparameter Meter as instructed
267 (Mettler Toledo, Zurich, Switzerland). After the first measurement, the leaf discs were

268 returned to the bathing water and incubated at 95°C for 25 min. After cooling down to
269 RT, the conductivity of each bathing sample was measured again (referred to as value
270 B). The ion leakage was expressed as the ratio determined by value A/value B × 100.
271 The mean value and standard error of each treatment were calculated using the data
272 from three biological replicates per treatment at each sampling time point.
273

274 **Confocal laser scanning microscopy**

275 Tissue samples were collected from the leaves of transiently expressing YFP-Sw-5b
276 or one of the fusion proteins at 24–36 hours post agro-infiltration (hpai). The collected
277 tissue samples were mounted in water between a glass slide and a coverslip. Images
278 of individual samples were captured under a Carl Zeiss LSM 710 confocal laser
279 scanning microscope. YFP fusions were excited at 488 nm and the emission was
280 captured at 497–520 nm. The resulting images were further processed using the Zeiss
281 710 CLSM software followed by the Adobe Photoshop software (San Jose, CA,
282 USA).
283

284 **Nucleus and cytoplasm fractionations**

285 *N. benthamiana* leaf tissues (1 g per sample), representing a specific treatment, were
286 collected at 24 hpai, frozen in liquid nitrogen, ground to fine powders, and then
287 homogenized in 2 mL (per sample) extraction buffer 1 (20 mM Tris-HCl, pH 7.5, 20
288 mM KCl, 2.5 mM $MgCl_2$, 2 mM EDTA, 25% glycerol, 250 mM sucrose, 1×Protease
289 Inhibitor Cocktail, and 5 mM DTT). The resulting lysate was filtered through 30 μm

290 filters to remove debris, and the filtrate was centrifuged at 2,000 × *g* for 5 minutes
291 to pellet nuclei. The supernatant from a sample was transferred into a new tube and
292 centrifuged at 10,000 × *g* for 10 min. The resulting supernatant was used as the
293 cytoplasm fraction. The nuclei containing pellet was resuspended in 5 mL extraction
294 buffer 2 (20 mM Tris-HCl, pH 7.4, 25% glycerol, 2.5 mM MgCl2, and 0.2% Triton
295 X-100), centrifuged for 10 min at 2,000 × *g* followed by 4-6 cycles of resuspension
296 and centrifugation as described above. The resulting pellet was resuspended again in
297 500 μl extraction buffer 3 (20 mM Tris-HCl, pH 7.5, 0.25 M sucrose, 10 mM MgCl2,
298 0.5% Triton X-100, and 5 mM β-mercaptoethanol). The nuclei fraction was carefully
299 layered on the top of 500 mL extraction buffer 4 (20 mM Tris-HCl, pH 7.5, 1.7 M
300 sucrose, 10 mM MgCl2, 0.5% Triton X-100, 1×Protease Inhibitor Cocktail, and 5
301 mM β-mercaptoethanol), and then centrifuged at 16,000 × *g* for 1 h. The resulting
302 pellet was resuspended in 500 μL extraction buffer 1 and stored at −80°C until use or
303 used immediately for SDS-PAGE assays. All the processes were performed on ice or
304 at 4°C. In this study, actin and histone H3 were used as the cytoplasmic and the
305 nuclear markers, respectively.
306
307 **Western blot, co-immunoprecipitation and mass spectrometry analysis**
308 Western blot and co-immunoprecipitation assays were performed as described (Zhu *et*
309 *al.*, 2017). Briefly, agro-infiltrated leaf samples (1 g per sample) were harvested and
310 homogenized individually in pre-chilled mortars with pestles in 2 mL extraction
311 buffer [10% (v/v) glycerol, 25 mM Tris, pH 7.5, 1 mM EDTA, 150 mM NaCl, 10 mM

312 DTT, 2% (w/v) polyvinylpolypyrrolidone, and 1 × protease inhibitor cocktail (Sigma,
313 Shanghai, China)]. Each crude slurry was transferred into a 2 mL Eppendorf tube, and
314 spun for 2 min at full speed in a refrigerated microcentrifuge. The supernatant was
315 transferred into a clean 1.5 mL Eppendorf tube and spun for 10 min at 4°C. For
316 Western blot assays, 50 μL supernatant from a sample was mixed with 150 μL
317 Laemmli buffer, boiled for 5 min, and analyzed in SDS-PAGE gels through
318 electrophoresis. For immunoprecipitation assays, 1 mL supernatant was mixed with
319 25 μL GFP-trap agarose beads (ChromoTek, Planegg-Martinsried, Germany),
320 incubated for 2 h at 4°C on an orbital shaker, and then pelleted through low speed
321 centrifugation. The blots were probed with a 1:2,500 (v/v) diluted anti-YFP antibody
322 or other specific antibodies followed a 1:10,000 (v/v) diluted horseradish peroxidase
323 (HRP)-conjugated goat anti-rabbit or a goat anti-mouse antibody (Sigma-Aldrich, St.
324 Louis, MO, USA). The detection signal was developed using the ECL substrate kit as
325 instructed (Thermo Scientific, Hudson, NH, USA).

326 For mass spectrometry analysis, the immunoprecipitation samples of YFP-SD
327 and SD without tag were processed by The Beijing Genomics Institute (BGI) for mass
328 spectrometry analysis. The immunoprecipitation samples of YFP-Sw-5b and Sw-5b
329 without tag were processed by Applied Protein Technology in Shanghai. Database
330 searches were performed using the Mascot search engine against *N. benthamiana*.
331 (https://solgenomics.net/organism/Nicotiana_benthamiana/genome).

332

333 **RT-PCR detection of TSWV infection**

334 Total RNA was extracted from TSWV-inoculated *N. benthamiana* plant leaves using
335 an RNA Purification Kit (Tiangen Biotech, Beijing, China), and then treated with
336 RNase-free DNase I (TaKaRa, Dalian, China). First-strand cDNA was synthesized
337 using a TSWV-specific primer (S3 Table). PCR reactions were as follows: initial
338 denaturation at 94°C for 2 min followed by 35 cycles of 94°C for 30 s, 52°C for 30 s,
339 and 72°C for 1 min. The final extension was 72°C for 10 min. The resulting PCR
340 products were visualized in 1.0% (w/v) agarose gels through electrophoresis.
341

342 # Results

343 **Determination of Sw-5b subcellular localization pattern**

344 Expression of YFP-Sw-5b in *N. benthamiana* leaves resulted in a strong HR cell death
345 as well as Sw-5b (Chen *et al.*, 2016; Zhu *et al.*, 2017). To investigate the subcellular
346 localization pattern of Sw-5b, we transiently expressed YFP and YFP-Sw-5b in *N.*
347 *benthamiana* leaves, respectively, through agro-infiltration. Confocal Microscopy
348 results showed that the YFP-Sw-5b fusion accumulated in both cytoplasm and nucleus
349 in *N. benthamiana* leaf cells (Fig. 1b, middle image). This subcellular localization
350 pattern was similar to that of YFP (Fig. 1b, left image). When a D857V mutation,
351 which keeps Sw-5b in an autoactivated state (Chen *et al.*, 2016), was introduced into
352 Sw-5b to produce pYFP-Sw-5b^{D857V} and expressed in *N. benthamiana* leaves, the
353 mutant YFP-Sw-5b^{D857V} fusion also accumulated in both cell cytoplasm and nucleus
354 (Fig. 1b, right image). We also making a construct pNativePro::YFP-Sw-5b

355 expressing YFP-Sw-5b under native Sw-5b promoter. However, the expression of
356 YFP-Sw-5b by native Sw-5b promoter is too low to detect green fluorescence signal.
357 To investigate the subcellular localization pattern of Sw-5b in tomato leaf cells,
358 we transiently expressed YFP, YFP-Sw-5b, and YFP-Sw-5b^{D857V}, respectively,
359 through particle bombardment. Confocal Microscopy results showed that these three
360 proteins exhibited the same subcellular localization pattern as that in the *N.*
361 *benthamiana* leaf cells (Fig. 1c).
362 To further confirm the above results, we harvested *N. benthamiana* leaves
363 expressing YFP-Sw-5b or YFP-Sw-5b^{D857V} and analyzed by cytoplasm and nucleus
364 fractionation assay. Leaf samples agro-infiltrated with the empty vector (p2300S)
365 were also harvested and used as controls. Analyses of total protein, cytoplasm
366 fractions, and nucleus fractions from these harvested leaves using Western blot assays
367 showed that both YFP-Sw-5b and YFP-Sw-5b^{D857V} were accumulated in the
368 cytoplasm and nucleus (Fig. 1d).
369
370 **Sw-5b recognizes TSWV NSm in the cytoplasm**
371 TSWV NSm is known to reside in cytoplasm and plasmodesmata, but not in nucleus
372 (Kormelink *et al.*, 1994; Feng *et al.*, 2016). To determine where Sw-5b can recognize
373 TSWV NSm, we fused a NES, a nes, a NLS or a nls signal peptide to the C-terminus
374 of NSm-YFP to produce NSm-YFP-NES, NSm-YFP-nes, NSm-YFP-NLS, and
375 NSm-YFP-nls, respectively. Transient expressions of these fusions in *N. benthamiana*
376 leaves showed that NSm-YFP-NES accumulated exclusively in the cytoplasm, while

377 NSm-YFP-NLS accumulated in the nucleus (Fig. S1a). As expected, NSm-YFP-nes
378 and NSm-YFP-nls showed the same accumulation pattern as that of NSm-YFP (Fig.
379 S1a). When Sw-5b was co-expressed with one of the above four fusions in *N.*
380 *benthamiana* leaves through agro-infiltration, the leaf tissues co-expressing Sw-5b
381 and NSm-YFP-NES (Sw-5b + NSm-YFP-NES), Sw-5b and NSm-YFP-nes (Sw-5b +
382 NSm-YFP-nes), or Sw-5b and NSm-YFP-nls (Sw-5b + NSm-YFP-nls) developed a
383 strong HR cell death (Fig. S1b). In contrast, the leaf tissues co-expressing Sw-5b and
384 NSm-YFP-NLS (Sw-5b + NSm-YFP-NLS) did not. Western blot assays using a YFP
385 specific antibody confirmed that all the assayed proteins were expressed in the
386 infiltrated tissues (Fig. S1c), indicating that Sw-5b recognizes NSm in the cytoplasm.
387

388 **Sw-5b activity in cell death induction is enhanced in the cytoplasm but**
389 **suppressed in the nucleus**

390 To investigate the roles of the cytoplasmic and nuclear Sw-5b in the induction of cell
391 death and host immunity, we produced constructs to express YFP-Sw-5b,
392 NLS-YFP-Sw-5b, nls-YFP-Sw-5b, NES-YFP-Sw-5b, and nes-YFP-Sw-5b,
393 respectively, and then tested their abilities to elicit cell death and host immunity to
394 tospovirus infection. Transient expressions of these fusions in *N. benthamiana* leaves
395 showed that NES-YFP-Sw-5b accumulated exclusively in the cytoplasm, while
396 NLS-YFP-Sw-5b accumulated only in the nucleus (Fig. 2a). In addition,
397 nes-YFP-Sw-5b and nls-YFP-Sw-5b showed the same accumulation pattern as that
398 shown by YFP-Sw-5b. We then tested cell death induction through co-expressions of

399 NSm and YFP-Sw-5b (NSm + YFP-Sw-5b), NSm and NES-YFP-Sw-5b (NSm +
400 NES-YFP-Sw-5b), NSm and nes-YFP-Sw-5b (NSm + nes-YFP-Sw-5b), NSm and
401 NLS-YFP-Sw-5b (NSm + NLS-YFP-Sw-5b), or NSm and nls-YFP-Sw-5b (NSm +
402 nls-YFP-Sw-5b) in *N. benthamiana* leaves through agro-infiltration. Results of this
403 study showed that the NSm + NES-YFP-Sw-5b-induced cell death was stronger than
404 that induced by NSm + nes-YFP-Sw-5b or NSm + nls-YFP-Sw-5b co-expression (Fig.
405 2b). In addition, the cell death induced by NSm + NLS-YFP-Sw-5b co-expression
406 was suppressed (Fig. 2b). Western blot results showed that the stronger cell death
407 caused by NSm + NES-YFP-Sw-5b co-expression was not due to a greater
408 accumulation of NES-YFP-Sw-5b in the leaves (Fig. 2c). The ion leakage assay
409 results (Fig. 2d) agreed with the phenotype observation results, and indicated that
410 co-expression of NSm + NES-YFP-Sw-5b in leaves lead to a greater ion leakage
411 compared with that induced by the co-expression of NSm + nes-YFP-Sw-5b at 24 and
412 48 hours post agro-infiltration (hpai). The ion leakage caused by the co-expression of
413 NSm + NLS-YFP-Sw-5b was significantly weaker than that caused by the
414 co-expression of NSm + nls-YFP-Sw-5b (Fig. 2d).
415

416 **Cytoplasmic Sw-5b induces a strong host defense against tospovirus replication**

417 Virus infection in plant starts with virus replication in the initially infected cells
418 followed by spreading into adjacent cells for further infection. To monitor tospovirus
419 replication in plant cells, we recently developed a TSWV mini-replicon-based reverse
420 genetic system (Feng et al., 2020). In this study, co-expression of TSWV

421 mini-replicon $SR_{(+)eGFP}$, $L_{(+)opt}$ (with a codon usage optimized RdRp), VSRs and NSm
422 resulted in a cell-to-cell movement of $SR_{(+)eGFP}$. In contrast, co-expression of $SR_{(+)eGFP}$,
423 $L_{(+)opt}$, VSRs, and $NSm^{H93A\&H94A}$ mutant, a defective movement protein but can be
424 recognized by Sw-5b to cause a strong HR (Li *et al.*, 2009; Zhao *et al.*, 2016), in cells
425 resulted in the expression of $SR_{(+)eGFP}$ in only single cells (Fig. S2), thus dissecting the
426 viral replication from viral cell-to-cell movement. We then co-expressed $SR_{(+)eGFP}$,
427 $L_{(+)opt}$, VSRs, $NSm^{H93A\&H94A}$ mutant and one of the five proteins (i.e., Sw-5b,
428 NES-Sw-5b, nes-Sw-5b, NLS-Sw-5b, nls-Sw-5b) in *N. benthamiana* leaves. Leaves
429 co-expressing $SR_{(+)eGFP}$, $L_{(+)opt}$, VSRs, $NSm^{H93A\&H94A}$ mutant and p2300 (empty vector,
430 EV) were used as controls. The results showed that in the presence of Sw-5b or one of
431 its derivatives, the expression of $SR_{(+)eGFP}$ was strongly suppressed compared with
432 that expressed in the presence of EV (Fig. 3a). It is noteworthy that the expression of
433 $SR_{(+)eGFP}$ was less inhibited in the presence of NLS-Sw-5b (Fig. 3a). Western blot
434 result indicated that the GFP accumulation of $SR_{(+)eGFP}$ was strongly inhibited in the
435 presence of Sw-5b, NES-Sw-5b, nes-Sw-5b or nls-Sw-5b compared with that
436 expressed in the presence of NLS-Sw-5b or EV (Fig. 3b). This finding indicates that
437 the cytoplasmic Sw-5b can inhibit $SR_{(+)eGFP}$ expression, possibly through induction of
438 a host defense against TSWV replication.
439
440 **Sw-5b induces a host defense against viral NSm intercellular movement**
441 In our previous study, we used pmCherry-HDEL//NSm-GFP vector (Fig. 4a) to
442 investigate TSWV NSm cell-to-cell movement (Feng *et al.*, 2016). The expressed

443 mCherry-HDEL binds ER membrane in the initial cells but NSm-eGFP traffics
444 between cells. To investigate whether the Sw-5b-induced host defense can affect
445 TSWV NSm cell-to-cell movement, we co-expressed mCherry-HDEL, NSm-GFP,
446 and Sw-5b or mCherry-HDEL, NSm-GFP, and EV in *N. benthamiana* leaves through
447 agro-infiltration. Under the fluorescence microscope, both NSm-GFP and
448 mCherry-HDEL were found in single cells in the presence of Sw-5b. In the presence
449 of EV, however, NSm-GFP moved into multiple cells, while mCherry-HDEL
450 accumulated in the initial cells (Fig. 4b, upper two panels). The result suggested that
451 Sw-5b elicited a defense that strongly inhibited cell-to-cell movement of viral NSm.
452 To make sure this inhibition to viral NSm cell-to-cell movement is not caused by
453 overexpression of Sw-5b, we also used the NSm^{T120N} mutant, from the resistance -
454 breaking (RB) TSWV isolates, which cannot be recognized by Sw-5b (Zhao et al.,
455 2016). The assays showed that in the presence of either Sw-5b or EV, NSm^{T120N}-GFP
456 moved into multiple cells, while mCherry-HDEL retained in the initial cells (Fig S3a).
457

458 **Sw-5b in the nucleus but not in the cytoplasm triggers a defense against NSm**
459 **cell-to-cell movement**

460 To determine the effects of the cytoplasmic and nuclear Sw-5b on host defense against
461 TSWV NSm intercellular movement, we co-expressed mCherry-HDEL and
462 NSm-GFP with NES-Sw-5b, nes-Sw-5b, NLS-Sw-5b, or nls-Sw-5b in *N.*
463 *benthamiana* leaves via agro-infiltration. The results showed that in the presence of
464 NLS-Sw-5b, the cell-to-cell movement of NSm-GFP was inhibited (Fig. 4b). Similar

465 results were also obtained in the leaves co-expressing mCherry-HDEL and NSm-GFP
466 with nls-YFP-Sw-5b or nes-YFP-Sw-5b (Fig S3b). In the presence of
467 NES-YFP-Sw-5b, however, NSm-GFP did move into surrounding cells. (Fig. 4b).
468 This finding indicates that the Sw-5b in the nucleus but not in the cytoplasm induced
469 a host defense that inhibited TSWV NSm cell-to-cell movement.
470

471 **Nuclear Sw-5b confers host immunity to TSWV systemic infection**

472 To dissect the host immunity induced by the cytoplasmic and the nuclear Sw-5b, we
473 generated transgenic *N. benthamiana* lines expressing YFP-Sw-5b, NES-YFP-Sw-5b,
474 nes-YFP-Sw-5b, NLS-YFP-Sw-5b, and nls-YFP-Sw-5b, respectively (Tables S1 and
475 S2). After inoculation of these transgenic lines with TSWV-YN isolate, the EV
476 (control) transgenic plants developed typical viral symptoms including stunt, leaf curl
477 and mosaic at 7 to 15 days post inoculation (dpi). The NES-YFP-Sw-5b transgenic
478 plants developed a strong HR trailing in the systemic leaves by 7 to 15 days post
479 inoculation (dpi) (Fig. 5a and Fig. S4a), suggesting that NES-YFP-Sw-5b transgenic
480 plant did not block TSWV systemic infection and caused virus infection-related
481 systemic HR. In contrast, no systemic virus infection symptoms were observed in the
482 YFP-Sw-5b and the nes-YFP-Sw-5b transgenic plants. The RT-PCR agreed with the
483 symptom observation results and showed that TSWV-YN genomic RNA was
484 accumulated in the systemic leaves of the TSWV-YN-inoculated NES-YFP-Sw-5b or
485 the EV transgenic plants, but not in the systemic leaves of the TSWV-YN-inoculated
486 YFP-Sw-5b or nes-YFP-Sw-5b transgenic plants (Fig. 5c and Fig. S4b). Also in this

487 study, the TSWV-YN-inoculated NLS-YFP-Sw-5b or nls-YFP-Sw-5b transgenic
488 plants did not show virus like symptoms in their systemic leaves by 7-15 dpi (Fig. 5a,
489 and Fig. S4a). The RT-PCR result confirmed that TSWV-N genomic RNA had not
490 accumulated in the systemic leaves of the NLS-YFP-Sw-5b or the nls-YFP-Sw-5b
491 transgenic plants (Fig. 5c, and Fig. S4b), indicating that the nuclear Sw-5b is
492 responsible for the host immunity against TSWV systemic infection.
493

494 **The cytoplasmic and the nuclear Sw-5b act synergistically to confer a strong**
495 **immunity to TSWV infection in *N. benthamiana***

496 To investigate whether cytoplasm-targeted and nucleus-targeted Sw-5b have joint
497 effects on the defense against TSWV infection, we constructed a $M_{(-)opt}$-$pSR_{(+)eGFP}$
498 vector by inserting a cassette expressing optimized TSWV M genomic sequence
499 (Feng *et al.*, 2020) into the $pSR_{(+)eGFP}$ mini-replicon to express NSm, N, and eGFP
500 simultaneously in the same cells (Fig. 6a). The construct $M_{(-)opt}$-$pSR_{(+)eGFP}$ couples the
501 functions for both viral replication and viral cell-to-cell movement, mimicking the
502 virus infection in plant leaves. After co-expressing this vector, the $L_{(+)opt}$ and the EV in
503 *N. benthamiana* leaves through agro-infiltration, the eGFP fluorescence was observed
504 in many cells, due to the presence of the NSm movement protein and the $RdRp_{opt}$ (Fig.
505 6b, upper left image). When $M_{(-)opt}$-$SR_{(+)eGFP}$, $L_{(+)opt}$ and Sw-5b were co-expressed in
506 *N. benthamiana* leaves, the eGFP fluorescence was hardly detected and some were
507 observed only in single leaf cells (Fig. 6b upper right image, Fig. S5a and b). When
508 $M_{(-)opt}$-$SR_{(+)eGFP}$, $L_{(+)opt}$ and NES-Sw-5b were co-expressed in *N. benthamiana* leaves,

509 the eGFP fluorescence was observed in clusters of a few cells (Fig. 6b, Fig. S5a),
510 indicating that limited cell-to-cell movement had occurred in these leaves (Fig. S5b).
511 When $M_{(-)opt}$-$SR_{(+)eGFP}$, $L_{(+)opt}$ and NLS-Sw-5b were co-expressed in leaves, a few of
512 eGFP fluorescence were detected but they were in single cells only. When leaves
513 co-expressing $M_{(-)opt}$-$SR_{(+)eGFP}$, $L_{(+)opt}$ and NES-Sw-5b + NLS-Sw-5b, the eGFP
514 fluorescence was also hardly detected and some were observed only in single leaf
515 cells. Western blot results showed that more eGFP had accumulated in the leaves
516 co-expressing $M_{(-)opt}$-$SR_{(+)eGFP}$, $L_{(+)opt}$, and EV, followed by the leaves co-expressing
517 $M_{(-)opt}$-$SR_{(+)eGFP}$, $L_{(+)opt}$, and NLS-Sw-5b, and then the leaves co-expressing
518 $M_{(-)opt}$-$SR_{(+)eGFP}$, $L_{(+)opt}$, and NES-Sw-5b. Much less eGFP had accumulated in the
519 leaves co-expressing $M_{(-)opt}$-$SR_{(+)eGFP}$, $L_{(+)opt}$, and NLS-Sw-5b + NES-Sw-5b, and in
520 the leaves co-expressing $M_{(-)opt}$-$SR_{(+)eGFP}$, $L_{(+)opt}$, and Sw-5b (Fig. 6c and d). The
521 accumulation of eGFP was lower in the leaves co-expressing NES-Sw-5b +
522 NLS-Sw-5b than that in the leaves co-expressing NES-Sw-5b or NLS-Sw-5b (Fig. 6c
523 and d), indicating that NES-Sw-5b and NLS-Sw-5b have additive role in mediating
524 host immunity against different TSWV infection steps.
525

526 **The Sw-5b NB-ARC-LRR control its cytoplasm localization whereas the**
527 **extended N-terminal SD domain is crucial for targeting Sw-5b into nucleus, and**
528 **for inducing host systemic immunity**

529 Sw-5b has an extended N-terminal SD domain, a CC domain, a NB-ARC domain, and
530 a C-terminal LRR domain (Chen *et al.*, 2016). To determine which domain(s) of

531 Sw-5b is/are responsible for nucleoplasm/nucleolus targeting and for plant immunity,
532 we tested these domains using various deletion mutants and YFP fusion proteins (Fig.
533 7a). We reported previously that the Sw-5b NB-ARC-LRR region was able to induce
534 HR cell death in plant in the presence of NSm (Chen *et al.*, 2016). In this study, we
535 fused YFP to the N-terminus of NB-ARC-LRR (Fig. 7a). Transient expression of
536 YFP-NB-ARC-LRR (112 kDa) in *N. benthamiana* leaf cells resulted in a localization
537 of the fusion protein in cytoplasm exclusively (Fig. 7b).

538 A previous study had shown that the CC domain of potato NLR receptor Rx was
539 required for targeting this protein to nucleus (Slootweg *et al.*, 2010). To determine the
540 function of Sw-5b CC domain in intracellular trafficking, we inserted the CC domain
541 between the YFP and NB-ARC-LRR to generate an YFP-CC-NB-ARC-LRR
542 construct or fused the CC domain to YFP to produce an YFP-CC construct. Transient
543 expression of these two fusion proteins individually in *N. benthamiana* leaves, and
544 examined the leaves under a confocal microscope, we determined that the YFP-CC
545 fusion protein accumulated in both cytoplasm and nucleus of the cells while the
546 YFP-CC-NB-ARC-LRR fusion protein was in the cytoplasm only (Fig. 7b). This
547 result indicated that addition of the CC domain to YFP-NB-ARC-LRR was not
548 sufficient to traffic the fusion protein into the nucleus.

549 An extended N-terminal SD domain is known to be present at the upstream of the
550 Sw-5b CC domain. In this study, we first generated an YFP-SD and an YFP-SD-CC
551 constructs, and transiently expressed them individually in *N. benthamiana* leaf cells.
552 Confocal Microscopy showed that both YFP-SD and YFP-SD-CC fusion proteins

553 accumulated in the cytoplasm and nucleus (Fig. 7b). We then inserted a SD between
554 the YFP and CC-NB-ARC-LRR to produce an YFP-SD-CC-NB-ARC-LRR
555 construction. Transient expression of this construct in *N. benthamiana* leaf cells
556 showed that this fusion protein accumulated in the cytoplasm and nucleus (Fig. 7b).

557 We next generated stable transgenic *N. benthamiana* plants expressing
558 YFP-NB-ARC-LRR, YFP-CC-NB-ARC-LRR and YFP-SD-CC-NB-ARC-LRR.
559 Upon inoculation transgenic *N. benthamiana* plants expressing YFP-NB-ARC-LRR
560 with TSWV, large HR foci were observed in the TSWV-inoculated leaves and later,
561 HR trailing was seen in the systemic leaves of most assayed plants (Fig. 7c; Table S2
562 and S3). RT-PCR results confirmed the presence of TSWV genomic RNA in these
563 systemic leaves (Fig. S6b). We also inoculate *N. benthamiana* plants expressing
564 YFP-CC-NB-ARC-LRR with TSWV. By 7 dpi, no systemic resistance to TSWV
565 infection was observed in these plants (Fig. 6a and B, Table S4). RT-PCR results
566 showed that systemic infection of TSWV did occur in the TSWV-inoculated
567 YFP-CC-NB-ARC-LRR transgenic plants (Fig. S6b). In contrast, transgenic plants
568 expressing YFP-SD-CC-NB-ARC-LRR fusion exhibited a systemic immunity to
569 TSWV infection (Fig. 7c, Fig. S6b).

570 These data indicated that Sw-5b NB-ARC-LRR control its cytoplasm localization,
571 CC domain of Sw-5b alone was not sufficient to transport the NB-ARC-LRR into
572 nucleus and the extended SD domain is required for targeting Sw-5b to the nucleus,
573 and for inducing host immunity.

574

575 **The extended SD domain interacted with *importin α1*, *α2* and *β***

576 To identify the cellular machinery needed for transporting Sw-5b into nucleus, we
577 co-expressed YFP-SD and YFP-Sw-5b in *N. benthamiana* leaves followed by a
578 co-immunoprecipitation (co-IP) and Mass Spectrometry. The results identified *N.*
579 *benthamiana* importin α as one of candidate proteins interacted with YFP-SD and
580 YFP-Sw-5b (Table S5 and S6). The co-IP and Mass Spectrometry also identified
581 nuclear pore complex protein TPRb and nuclear pore complex protein Nup160a
582 interacted with YFP-Sw-5b (Table S6). *Importins* play important roles in
583 translocating proteins from cytoplasm into nucleus (Kanneganti *et al.*, 2007). We used
584 BiFC analysis to confirm the interaction between YFP-SD with *N. benthamiana*
585 importin homologs α1, α2 and *β*. The result showed that co-expression of cYFP-SD
586 with nYFP-IMP α1, nYFP-IMP α2 or nYFP-IMP *β* produced a strong YFP
587 fluorescence signal in nucleus. Co-expression of cYFP-Sw-5b with nYFP-IMP α1,
588 nYFP-IMP α2 or nYFP-IMP *β* also detected a strong YFP fluorescence signal in
589 nucleus (Fig. S7). In contrast, co-expression of controls cYFP-SD and nYFP,
590 cYFP-Sw-5b and nYFP, cYFP and nYFP-IMP α1, cYFP and nYFP-IMP α2 or cYFP
591 and nYFP-IMP *β* did not show fluorescence signal in *N. benthamiana* leaf cells (Fig.
592 S7).

593

594 **Silencing *importin α1*, *α2* and *β* expression abolished Sw-5b nucleus**
595 **accumulation and host resistance to TSWV systemic infection**

596 To determine the functions of importin α1, α2 and β in Sw-5b nucleus localization, we

597 silenced *importin α1, α2, β, α1* and *α2,* and *α1* and *α2* and *β* expressions, respectively,
598 in *N. benthamiana* leaves using a tobacco rattle virus (TRV)-based virus-induced gene
599 silencing (VIGS) vector, and then transiently expressed YFP-Sw-5b in these plants.
600 Analyses of these plants through RT-PCR using gene specific primers showed that
601 silencing of these *importin* genes in *N. benthamiana* leaves were successful (Fig.
602 S8a). However, silencing individual *importin* gene or both *importin α1* and *α2* was
603 not enough to block the nucleus accumulation of YFP-Sw-5b (Fig. 8a). In contrast,
604 after *importin α1*, *α2* and *β* were all silenced through VIGS, the nucleus accumulation
605 of YFP-Sw-5b was inhibited (Fig. 8a, the middle image in the bottom panel).

606 To investigate the effects of nuclear import defected Sw-5b on host immunity to
607 TSWV systemic infection, we silenced these *importin* genes in the Sw-5b transgenic
608 *N. benthamiana* plants as described above, and then inoculated them with TSWV. The
609 results showed that the plants silenced for *importin α1*, *α2*, and *β* gene, individually,
610 did not show TSWV systemic infection (Fig. 8b and Fig. S8b). In addition, the
611 transgenic plants silenced for both *importin α1* and *α2* genes also did not show
612 TSWV systemic infection (Fig. 8b and Fig. S8b). In contrast, after silencing *importin*
613 *α1*, *α2* and *β* together, the plants developed clear TSWV symptoms in systemic
614 leaves followed by HR (Fig. 8b, white arrow and Fig. S8b), indicating that the nucleus
615 accumulation of Sw-5b is indispensable for the induction of host immunity against
616 TSWV systemic infection.

617

618 **Discussion**

619 In this report, we provide evidence to show that the cytoplasm-accumulated and the
620 nucleus-accumulated Sw-5b, a tomato immune receptor, play different roles in
621 inducing host defense against TSWV infection in plant. The cytoplasmic Sw-5b
622 functions to induce a strong cell death response to inhibit TSWV replication. This
623 host response is, however, insufficient to block virus intercellular and long-distance
624 movement. The nuclear-localized Sw-5b triggers a host defense that weakly inhibit
625 viral replication but strongly inhibit tospovirus intercellular and systemic movement.
626 These findings suggest that tomato Sw-5b NLR induces different types of defense
627 responses by cytoplasm and nucleus partitioning to combat virus at different infection
628 steps. Furthermore, the cytoplasmic and the nuclear Sw-5b act synergistically to
629 confer a strong host immunity to TSWV infection in plant. We also demonstrated that
630 the extra SD domain functioned as a critical intracellular translocation modulator,
631 allowing Sw-5b receptor to translocate from cytoplasm to nucleus to trigger the
632 immunity. The Sw-5b NB-LRR controls its cytoplasm localization. Unlike Rx CC
633 domain, Sw-5b CC domain is not sufficient to translocate NB-LRR into nucleus.
634 Strikingly, the SD is crucial for Sw-5b to translocate from cytoplasm for nucleus. This
635 SD-mediated receptor translocation is dependent on importins α and β.

636 Successful virus infection in plant requires several steps including viral replication
637 in the initially infected cells followed by cell-to-cell and long-distance movement
638 (Heinlein, 2015; Wang, 2015). After entering into plant cells, virus first encode
639 multiple proteins needed for its replication. Once the initial replication is established,
640 virus will encode specific protein(s), known as movement proteins (MPs), to traffic

641 viral genome or virions into adjacent cells through plasmodesmata in cell walls, and
642 then long-distantly into other parts of the plant to cause a systemic infection (Rao,
643 2002; Lucas, 2006; Taliansky *et al.*, 2008). To date, multiple plant NLRs, conferring
644 host resistance against plant viruses have been identified (Soosaar *et al.*, 2005; Meier
645 *et al.*, 2019), but how these plant NLRs induce host resistance against virus infection
646 remain largely unknown.

647 In this study, we have determined that the forced cytoplasm accumulation of
648 Sw-5b can induce a stronger cell death than that caused by the accumulation of Sw-5b
649 in both cytoplasm and nucleus. While, the cell death induced by the forced nucleus
650 accumulation of Sw-5b was significantly weakened. We then analyzed
651 Sw-5b-mediated immunity against TSWV replication using a TSWV mini-replicon
652 system and a movement defective NSm mutant. Our results showed that the forced
653 cytoplasm accumulation of Sw-5b can induce a strong host defense against virus
654 replication in cells. This finding implies that cytoplasm is one of the main source of
655 defense signaling against TSWV replication. The defense signaling generated in
656 nucleus can only induce a weak defense against TSWV replication. Therefore, the
657 nuclear localized Sw-5b is only partially responsible for the induction of host defense
658 against TSWV replication. It is also possible that this nuclear localized
659 Sw-5b-induced weak host response is caused by a trace of NLS-YFP-Sw-5b
660 maintained in the cytoplasm that maybe below the detection limit of Confocal
661 Microscope. It has been shown to accumulate in both cytoplasm and nucleus, and the
662 forced cytoplasm accumulation of Barley MLA10 enhance cell death signaling (Bai *et*

663 *al.*, 2012). We speculate that, for both MLA10 and Sw-5b, the cytoplasm
664 accumulation is crucial for the initiation and/or amplification of the cell death
665 signaling. The CC and the TIR domain of several plant NLRs have been shown to
666 trigger cell death (Swiderski *et al.*, 2009; Krasileva *et al.*, 2010; Bernoux *et al.*, 2011;
667 Collier *et al.*, 2011; Maekawa *et al.*, 2011; Bai *et al.*, 2012; Chen *et al.*, 2017; Wang
668 *et al.*, 2020). Analyses of the three dimensional structures of Arabidopsis ZAR1
669 resistosome have also shown that its CC domain can form pentamer structures that
670 was able to target into host cell membranes, leading to ion leakage and cell death
671 (Wang *et al.*, 2019a; Wang *et al.*, 2019b). We speculate that cell death likely cause the
672 toxicity on viral replicase or other proteins associated with virus replication in cells.

673 Plant virus encodes specific movement protein(s) to traffic viral genome between
674 cells and then leaves to cause systemic infection (Rao, 2002; Lucas, 2006; Taliansky
675 *et al.*, 2008). We reported previously that TSWV NSm alone can move between plant
676 cells (Feng *et al.*, 2016). In this study, we investigated the effect of the
677 Sw-5b-mediated host defense on TSWV intercellular movement. Through this study,
678 we have determined that after the recognition of NSm, Sw-5b receptor induced a
679 strong reaction to block NSm intercellular trafficking. Previous reports have some
680 indications on the role of plant NLRs in viral movement. Nevertheless it has no direct
681 evidence showing that plant NLRs induce resistance against viral movement. Deom
682 and colleagues had shown that the 9.4-kDa fluorescein isothiocyanate-labeled dextran
683 was unable to move between cells in the transgenic tobacco *N* leaves expressing
684 tobacco mosaic virus (TMV) movement protein at 24°C, an HR-permissive

685 temperature (Deom *et al.*, 1991). However, that study did not involve a TMV Avr
686 protein. In a different report, TMV-GFP showed a limited cell-to-cell movement in
687 leaves of tobacco cv. Sumsan NN at 33°C, an HR-nonpermissive temperature (Canto
688 & Palukaitis, 2002). Li and colleagues found that after treatment of SMV-inoculated
689 Jidou 7 resistant plants with a callose synthase inhibitor, the plants showed enlarged
690 HR lesions (Li *et al.*, 2012). The soybean *Rsv3* induced extreme resistance. However,
691 after this extremely resistant soybean line was treated with a callose synthase inhibitor,
692 the plants developed HR lesions upon SMV-G5H inoculation (Seo *et al.*, 2014). These
693 reports indicate that plant NLRs likely involves the defense against viral movement.
694 Here we provide the direct evidence that Sw-5b NLR can induce a strong defense
695 response to impede NSm intercellular trafficking. More importantly, we have
696 determined that the induction of host immunity to TSWV intercellular movement
697 requires the accumulation of Sw-5b in nucleus. Although the cytoplasmic Sw-5b can
698 induce a strong cell death response, it cannot prevent TSWV NSm cell-to-cell
699 movement. Consequently, we propose that nucleus is a key compartment to generate
700 defense signaling to block TSWV cell-to-cell movement.

701 In this study, although the NES-YFP-Sw-5b transgenic *N. benthamiana* plants
702 showed an HR, they were unable to stop TSWV systemic infection. We also showed
703 that Sw-5b YFP-NB-ARC-LRR (112 kDa) accumulates in cytoplasm exclusively (Fig.
704 7b), however, transgenic *N. benthamiana* plants expressing YFP-NB-ARC-LRR show
705 strong systemic HR trailing caused by TSWV infection. Based on these findings, we
706 conclude that HR cell death alone is not sufficient to block TSWV long-distance

707 movement. In our study, the NLS-YFP-Sw-5b transgenic plants were resistant to
708 TSWV systemic infection. After silencing the expressions of *importin α1*, *α2* and *β*
709 simultaneously to inhibit the nucleus accumulation of Sw-5b, however, the resistance
710 to TSWV systemic infection was abolished. These findings indicate that the
711 Sw-5b-mediated resistance signaling against viral systemic infection is generated in
712 nucleus. Some plant NLRs are known to interact with specific transcription factors in
713 nucleus upon recognition of pathogen effectors (Cui *et al.*, 2015; Kapos *et al.*, 2019).
714 The immune regulator EDS1 has also been shown to accumulate in nucleus to
715 reprogram RNA transcription (Garcia *et al.*, 2010; Heidrich *et al.*, 2011; Cui *et al.*,
716 2015; Lapin *et al.*, 2020). How Sw-5b regulates host immunity in nucleus requires
717 further investigations.

718 Several plant immune receptors and immune regulators, including, e.g. potato Rx
719 (Slootweg *et al.*, 2010; Tameling *et al.*, 2010), tobacco N (Burch-Smith *et al.*, 2007;
720 Caplan, JL *et al.*, 2008), barley MLA10 (Shen *et al.*, 2007), Arabidopsis
721 RRS1-R/RPS4, and snc1 (Deslandes *et al.*, 2003; Wirthmueller *et al.*, 2007; Cheng *et*
722 *al.*, 2009), as well as Arabidopsis NPR1 (Katagiri & Tsuda, 2010), and EDS1 (Lapin
723 *et al.*, 2020) have been found to be nucleocytoplasmic. For some of them, nuclear
724 accumulation of NLRs are required for the induction of plant immunity to pathogen
725 attacks. Moreover, the MLA10-YFP-NES fusion was found to induce a strong cell
726 death response, but not a strong host resistance to powdery mildew fungus infection.
727 In contrast, the MLA10-YFP-NLS fusion inhibited its activity to induce a cell death
728 response, but caused a host immunity to this pathogen (Bai *et al.*, 2012). In many

729 plant-pathogen interactions, cell death responses can be uncoupled from disease
730 resistance (Bendahmane *et al.*, 1999; Gassmann, 2005; Coll *et al.*, 2010; Heidrich *et*
731 *al.*, 2011). This separation raises questions about how host resistance prevents
732 pathogen invasion and what are the roles of cell death during pathogen infection. It is
733 unclear whether the MLA10-YFP-NES-induced cell death has some inhibitory effects
734 on powdery mildew fungus infection. In this study, we determined that cytoplasm-
735 and nuclear-accumulation of Sw-5b have different functions. The
736 cytoplasm-accumulated Sw-5b induces a strong defense against virus replication,
737 whereas the nuclear-accumulated Sw-5b induced an inhibition of virus cell-to-cell and
738 long distance movement. Both cytoplasmic and nuclear Sw-5b are needed to confer a
739 synergistic and full defense against tospovirus infection.

740 We have also determined that Sw-5b NB-ARC-LRR and SD domains are
741 important to regulate the proper subcellular localization of Sw-5b and the proper
742 nucleoplasmic distribution of Sw-5b is needed to elicit full immune responses to
743 inhibit different TSWV infection steps. Sw-5b NB-ARC-LRR controls its cytoplasm
744 localization. The CC domain of the Sw-5b is not sufficient to target the receptor into
745 nuclear. Importantly, the extended SD of Sw-5b is absolutely required for the nucleus
746 translocation. Because non-canonical domains are frequently found in other NLRs
747 and are quite diversified, our findings have broad implications to investigate the
748 potential new functions of non-canonical domains that integrated in the plant NLRs to
749 regulate the plant immunity against pathogen invasions.

750 Through co-IP, Mass Spectrometry and BiFC analysis, we found that the extended

751 SD domain and Sw-5b interacted with host importin machineries to translocate the
752 Sw-5b receptor from cytoplasm into nucleus to mediate local and systemic resistance
753 to tospovirus. Recent studies have shown that nuclearporin MOS3, MOS6 and nuclear
754 pore complex component MOS7/Nup88 proteins played important roles in regulating
755 Arabidopsis innate immunity (Palma *et al.*, 2005; Zhang & Li, 2005; Cheng *et al.*,
756 2009). We found that when *importin α1*, *importin α2* and *importin β* gene were all
757 silenced through VIGS, the nucleus targeting of Sw-5b were completely blocked, and
758 consequently, the Sw-5b-mediated systemic immunity to tospovirus infection was
759 compromised. Importin α and β are known to form a nucleus import complex.
760 Binding with importin β could activate importin α to form a binding surface for NLS
761 proteins (Stewart, 2007). Hence, disruption of either importin α or importin β would
762 block the nucleus import of NLS proteins. Because silencing *importin α* or
763 *importin β* gene expression through VIGS did not disrupt the nuclear targeting of
764 Sw-5b, we speculate that a non-canonical nuclear import pathway may take part in
765 importing Sw-5b into nucleus.

766 Based on the above results, we have created a working model for the Sw-5b
767 NLR-induced host resistance against TSWV replication, and intercellular and
768 long-distance movement in plant (Fig. 9). Upon recognition of NSm in cytoplasm,
769 Sw-5b switched from an autoinhibited state to an activated state. The activated Sw-5b
770 accumulated in cytoplasm and also translocate into nucleus via importins α and β .
771 The cytoplasm-accumulated and the nucleus-accumulated Sw-5b play different roles
772 in inducing host immunity against TSWV infection. The cytoplasmic Sw-5b functions

773 to induce a cell death response to inhibit TSWV replication, while the nuclear Sw-5b
774 functions to induce a weak host defense against TSWV replication, but a strong
775 defense against TSWV cell-to-cell and long-distance movement. The concerted
776 defense signaling generated in the cytoplasm and nucleus resulted in a strong host
777 resistance to tospovirus infection.
778
779
780 **Acknowledgments**
781 This work was supported by the National Natural Science Foundation of China
782 (31630062, 31925032 and 31870143), the Fundamental Research Funds for the
783 Central Universities (JCQY201904 and KYXK202012), Youth Science and
784 Technology Innovation Program to XT.
785
786 **Author contributions**
787 HC XQ, XC and XT, designed the research; HC, XQ and XC, TY, MF, JC, RC, HH,
788 YZ, YM, DS, YX, MZ performed the experiments; HC, XSD and XT interpreted the
789 result and wrote the paper.
790
791 **ORCID**
792 Hongyu Chen, 0000-0001-8142-0653
793 Yi Xu, 0000-0002-1913-4530
794 Min Zhu, 0000-0002-9354-4300

Xiaorong Tao, 0000-0003-1259-366X

Competing interests

The authors declare that nocompeting interests exist.

Data availability

All data produced in this study are presented in this manuscript or as the supporting files

References

Axtell MJ, Staskawicz BJ. 2003. Initiation of RPS2-specified disease resistance in Arabidopsis is coupled to the AvrRpt2-directed elimination of RIN4. *Cell* **112**(3): 369-377.

Bai S, Liu J, Chang C, Zhang L, Maekawa T, Wang Q, Xiao W, Liu Y, Chai J, Takken FL, Schulze-Lefert P, Shen QH. 2012. Structure-function analysis of barley NLR immune receptor MLA10 reveals its cell compartment specific activity in cell death and disease resistance. *PLoS Pathog* **8**(6): e1002752.

Bendahmane A, Kanyuka K, Baulcombe DC. 1999. The Rx gene from potato controls separate virus resistance and cell death responses. *Plant Cell* **11**(5): 781-792.

Bernoux M, Ve T, Williams S, Warren C, Hatters D, Valkov E, Zhang X, Ellis JG, Kobe B, Dodds PN. 2011. Structural and functional analysis of a plant resistance protein TIR domain reveals interfaces for self-association, signaling, and autoregulation. *Cell Host Microbe* **9**(3): 200-211.

Brommonschenkel SH, Frary A, Frary A, Tanksley SD. 2000. The broad-spectrum tospovirus resistance gene Sw-5 of tomato is a homolog of the root-knot nematode resistance gene Mi. *Mol Plant Microbe Interact* **13**(10): 1130-1138.

Burch-Smith TM, Schiff M, Caplan JL, Tsao J, Czymmek K, Dinesh-Kumar SP. 2007. A novel role for the TIR domain in association with pathogen-derived elicitors. *PLoS Biol* **5**(3): e68.

Canto T, Palukaitis P. 2002. Novel N gene-associated, temperature-independent resistance to the movement of tobacco mosaic virus vectors neutralized by a cucumber mosaic virus RNA1 transgene. *J Virol* **76**(24): 12908-12916.

Caplan J, Padmanabhan M, Dinesh-Kumar SP. 2008. Plant NB-LRR Immune Receptors: From Recognition to Transcriptional Reprogramming. *Cell Host Microbe* **3**(3): 126-135.

827 **Caplan JL, Mamillapalli P, Burch-Smith TM, Czymmek K, Dinesh-Kumar SP. 2008.**
828 Chloroplastic protein NRIP1 mediates innate immune receptor recognition of a viral effector.
829 *Cell* **132**(3): 449-462.
830 **Cesari S, Bernoux M, Moncuquet P, Kroj T, Dodds PN. 2014.** A novel conserved mechanism for
831 plant NLR protein pairs: the "integrated decoy" hypothesis. *Front Plant Sci* **5**: 606.
832 **Cesari S, Moore J, Chen C, Webb D, Periyannan S, Mago R, Bernoux M, Lagudah ES, Dodds**
833 **PN. 2016.** Cytosolic activation of cell death and stem rust resistance by cereal MLA-family
834 CC-NLR proteins. *Proc Natl Acad Sci U S A* **113**(36): 10204-10209.
835 **Cesari S, Thilliez G, Ribot C, Chalvon V, Michel C, Jauneau A, Rivas S, Alaux L, Kanzaki H,**
836 **Okuyama Y, Morel JB, Fournier E, Tharreau D, Terauchi R, Kroj T. 2013.** The rice
837 resistance protein pair RGA4/RGA5 recognizes the Magnaporthe oryzae effectors AVR-Pia
838 and AVR1-CO39 by direct binding. *Plant Cell* **25**(4): 1463-1481.
839 **Chen T, Liu D, Niu X, Wang J, Qian L, Han L, Liu N, Zhao J, Hong Y, Liu Y. 2017.** Antiviral
840 Resistance Protein Tm-2(2) Functions on the Plasma Membrane. *Plant Physiol* **173**(4):
841 2399-2410.
842 **Chen X, Zhu M, Jiang L, Zhao W, Li J, Wu J, Li C, Bai B, Lu G, Chen H, Moffett P, Tao X. 2016.**
843 A multilayered regulatory mechanism for the autoinhibition and activation of a plant
844 CC-NB-LRR resistance protein with an extra N-terminal domain. *New Phytol* **212**(1):
845 161-175.
846 **Cheng YT, Germain H, Wiermer M, Bi D, Xu F, Garcia AV, Wirthmueller L, Despres C, Parker**
847 **JE, Zhang Y, Li X. 2009.** Nuclear pore complex component MOS7/Nup88 is required for
848 innate immunity and nuclear accumulation of defense regulators in Arabidopsis. *Plant Cell*
849 **21**(8): 2503-2516.
850 **Coll NS, Vercammen D, Smidler A, Clover C, Van Breusegem F, Dangl JL, Epple P. 2010.**
851 Arabidopsis type I metacaspases control cell death. *Science* **330**(6009): 1393-1397.
852 **Collier SM, Hamel LP, Moffett P. 2011.** Cell death mediated by the N-terminal domains of a unique
853 and highly conserved class of NB-LRR protein. *Mol Plant Microbe Interact* **24**(8): 918-931.
854 **Collier SM, Moffett P. 2009.** NB-LRRs work a "bait and switch" on pathogens. *Trends Plant Sci*
855 **14**(10): 521-529.
856 **Cui H, Tsuda K, Parker JE. 2015.** Effector-triggered immunity: from pathogen perception to robust
857 defense. *Annu Rev Plant Biol* **66**: 487-511.
858 **Das B, Sengupta S, Prasad M, Ghose TK. 2014.** Genetic diversity of the conserved motifs of six
859 bacterial leaf blight resistance genes in a set of rice landraces. *BMC Genet* **15**: 82.
860 **De Oliveira AS, Koolhaas I, Boiteux LS, Caldararu OF, Petrescu AJ, Oliveira Resende R,**
861 **Kormelink R. 2016.** Cell death triggering and effector recognition by Sw-5 SD-CNL proteins
862 from resistant and susceptible tomato isolines to Tomato spotted wilt virus. *Mol Plant Pathol*
863 **17**(9): 1442-1454.
864 **Deom CM, Wolf S, Holt CA, Lucas WJ, Beachy RN. 1991.** Altered function of the tobacco mosaic
865 virus movement protein in a hypersensitive host. *Virology* **180**(1): 251-256.
866 **Deslandes L, Olivier J, Peeters N, Feng DX, Khounlotham M, Boucher C, Somssich I, Genin S,**
867 **Marco Y. 2003.** Physical interaction between RRS1-R, a protein conferring resistance to
868 bacterial wilt, and PopP2, a type III effector targeted to the plant nucleus. *Proc Natl Acad Sci*
869 *U S A* **100**(13): 8024-8029.
870 **Dodds PN, Rathjen JP. 2010.** Plant immunity: towards an integrated view of plant-pathogen

871 interactions. *Nat Rev Genet* **11**(8): 539-548.
872 **Ea VDB, Jones JD. 1998.** Plant disease-resistance proteins and the gene-for-gene concept. *Trends in*
873 *Biochemical Sciences* **23**(12): 454-456(453).
874 **Engelhardt S, Boevink PC, Armstrong MR, Ramos MB, Hein I, Birch PR. 2012.** Relocalization of
875 late blight resistance protein R3a to endosomal compartments is associated with effector
876 recognition and required for the immune response. *Plant Cell* **24**(12): 5142-5158.
877 **Ernst K, Kumar A, Kriseleit D, Kloos DU, Phillips MS, Ganal MW. 2002.** The broad-spectrum
878 potato cyst nematode resistance gene (Hero) from tomato is the only member of a large gene
879 family of NBS-LRR genes with an unusual amino acid repeat in the LRR region. *Plant J* **31**(2):
880 127-136.
881 **Feng M, Cheng R, Chen M, Guo R, Li L, Feng Z, Wu J, Xie L, Hong J, Zhang Z, Kormelink R,**
882 **Tao X. 2020.** Rescue of tomato spotted wilt virus entirely from complementary DNA clones.
883 *Proc Natl Acad Sci U S A* **117**(2): 1181-1190.
884 **Feng Z, Xue F, Xu M, Chen X, Zhao W, Garcia-Murria MJ, Mingarro I, Liu Y, Huang Y, Jiang**
885 **L, Zhu M, Tao X. 2016.** The ER-Membrane Transport System Is Critical for Intercellular
886 Trafficking of the NSm Movement Protein and Tomato Spotted Wilt Tospovirus. *PLoS*
887 *Pathog* **12**(2): e1005443.
888 **Gao Z, Chung EH, Eitas TK, Dangl JL. 2011.** Plant intracellular innate immune receptor Resistance
889 to Pseudomonas syringae pv. maculicola 1 (RPM1) is activated at, and functions on, the
890 plasma membrane. *Proc Natl Acad Sci U S A* **108**(18): 7619-7624.
891 **Garcia AV, Blanvillain-Baufume S, Huibers RP, Wiermer M, Li G, Gobbato E, Rietz S, Parker**
892 **JE. 2010.** Balanced nuclear and cytoplasmic activities of EDS1 are required for a complete
893 plant innate immune response. *PLoS Pathog* **6**: e1000970.
894 **Gassmann W. 2005.** Natural variation in the Arabidopsis response to the avirulence gene hopPsyA
895 uncouples the hypersensitive response from disease resistance. *Mol Plant Microbe Interact*
896 **18**(10): 1054-1060.
897 **Germain H, Seguin A. 2011.** Innate immunity: has poplar made its BED? *New Phytol* **189**(3):
898 678-687.
899 **Hallwass M, de Oliveira AS, de Campos Dianese E, Lohuis D, Boiteux LS, Inoue-Nagata AK,**
900 **Resende RO, Kormelink R. 2014.** The Tomato spotted wilt virus cell-to-cell movement
901 protein (NSM) triggers a hypersensitive response in Sw-5-containing resistant tomato lines
902 and in Nicotiana benthamiana transformed with the functional Sw-5b resistance gene copy.
903 *Mol Plant Pathol* **15**(9): 871-880.
904 **Heidrich K, Wirthmueller L, Tasset C, Pouzet C, Deslandes L, Parker JE. 2011.** Arabidopsis
905 EDS1 connects pathogen effector recognition to cell compartment-specific immune responses.
906 *Science* **334**(6061): 1401-1404.
907 **Heinlein M. 2015.** Plant virus replication and movement. *Virology* **479-480**: 657-671.
908 **Horsefield S, Burdett H, Zhang X, Manik MK, Shi Y, Chen J, Qi T, Gilley J, Lai JS, Rank MX,**
909 **Casey LW, Gu W, Ericsson DJ, Foley G, Hughes RO, Bosanac T, von Itzstein M,**
910 **Rathjen JP, Nanson JD, Boden M, Dry IB, Williams SJ, Staskawicz BJ, Coleman MP,**
911 **Ve T, Dodds PN, Kobe B. 2019.** NAD(+) cleavage activity by animal and plant TIR domains
912 in cell death pathways. *Science* **365**(6455): 793-799.
913 **Inoue H, Hayashi N, Matsushita A, Xinqiong L, Nakayama A, Sugano S, Jiang CJ, Takatsuji H.**
914 **2013.** Blast resistance of CC-NB-LRR protein Pb1 is mediated by WRKY45 through

915 protein-protein interaction. *Proc Natl Acad Sci U S A* **110**(23): 9577-9582.
916 **Jones JD, Vance RE, Dangl JL. 2016.** Intracellular innate immune surveillance devices in plants and
917 animals. *Science* **354**(6316).
918 **Jubic LM, Saile S, Furzer OJ, El Kasmi F, Dangl JL. 2019.** Help wanted: helper NLRs and plant
919 immune responses. *Curr Opin Plant Biol* **50**: 82-94.
920 **Kanneganti TD, Bai X, Tsai CW, Win J, Meulia T, Goodin M, Kamoun S, Hogenhout SA. 2007.**
921 A functional genetic assay for nuclear trafficking in plants. *Plant J* **50**(1): 149-158.
922 **Kanzaki H, Yoshida K, Saitoh H, Fujisaki K, Hirabuchi A, Alaux L, Fournier E, Tharreau D,**
923 **Terauchi R. 2012.** Arms race co-evolution of Magnaporthe oryzae AVR-Pik and rice Pik
924 genes driven by their physical interactions. *Plant J* **72**(6): 894-907.
925 **Kapos P, Devendrakumar KT, Li X. 2019.** Plant NLRs: From discovery to application. *Plant Sci* **279**:
926 3-18.
927 **Katagiri F, Tsuda K. 2010.** Understanding the plant immune system. *Mol Plant Microbe Interact*
928 **23**(12): 1531-1536.
929 **Kawano Y, Fujiwara T, Yao A, Housen Y, Hayashi K, Shimamoto K. 2014.**
930 Palmitoylation-dependent membrane localization of the rice resistance protein pit is critical
931 for the activation of the small GTPase OsRac1. *J Biol Chem* **289**(27): 19079-19088.
932 **Kong L, Qiu X, Kang J, Wang Y, Chen H, Huang J, Qiu M, Zhao Y, Kong G, Ma Z, Wang Y, Ye**
933 **W, Dong S, Ma W, Wang Y. 2017.** A Phytophthora Effector Manipulates Host Histone
934 Acetylation and Reprograms Defense Gene Expression to Promote Infection. *Curr Biol* **27**(7):
935 981-991.
936 **Kormelink R, Garcia ML, Goodin M, Sasaya T, Haenni AL. 2011.** Negative-strand RNA viruses:
937 the plant-infecting counterparts. *Virus Res* **162**(1-2): 184-202.
938 **Kormelink R, Storms M, Van Lent J, Peters D, Goldbach R. 1994.** Expression and subcellular
939 location of the NSM protein of tomato spotted wilt virus (TSWV), a putative viral movement
940 protein. *Virology* **200**(1): 56-65.
941 **Kourelis J, van der Hoorn RAL. 2018.** Defended to the Nines: 25 Years of Resistance Gene Cloning
942 Identifies Nine Mechanisms for R Protein Function. *Plant Cell* **30**(2): 285-299.
943 **Krasileva KV, Dahlbeck D, Staskawicz BJ. 2010.** Activation of an Arabidopsis resistance protein is
944 specified by the in planta association of its leucine-rich repeat domain with the cognate
945 oomycete effector. *Plant Cell* **22**(7): 2444-2458.
946 **Kroj T, Chanclud E, Michel-Romiti C, Grand X, Morel JB. 2016.** Integration of decoy domains
947 derived from protein targets of pathogen effectors into plant immune receptors is widespread.
948 *New Phytol* **210**(2): 618-626.
949 **Lanford RE, Butel JS. 1984.** Construction and characterization of an SV40 mutant defective in
950 nuclear transport of T antigen. *Cell* **37**(3): 801-813.
951 **Lapin D, Bhandari DD, Parker JE. 2020.** Origins and Immunity Networking Functions of EDS1
952 Family Proteins. *Annu Rev Phytopathol* **58**: 253-276.
953 **Le Roux C, Huet G, Jauneau A, Camborde L, Tremousaygue D, Kraut A, Zhou B, Levaillant M,**
954 **Adachi H, Yoshioka H, Raffaele S, Berthome R, Coute Y, Parker JE, Deslandes L. 2015.**
955 A receptor pair with an integrated decoy converts pathogen disabling of transcription factors
956 to immunity. *Cell* **161**(5): 1074-1088.
957 **Leastro MO, Pallas V, Resende RO, Sanchez-Navarro JA. 2017.** The functional analysis of distinct
958 tospovirus movement proteins (NSM) reveals different capabilities in tubule formation,

959 cell-to-cell and systemic virus movement among the tospovirus species. *Virus Res* **227**: 57-68.
960 **Li J, Huang H, Zhu M, Huang S, Zhang W, Dinesh-Kumar SP, Tao X. 2019.** A Plant Immune
961 Receptor Adopts a Two-Step Recognition Mechanism to Enhance Viral Effector Perception.
962 *Mol Plant* **12**(2): 248-262.
963 **Li W, Lewandowski DJ, Hilf ME, Adkins S. 2009.** Identification of domains of the Tomato spotted
964 wilt virus NSm protein involved in tubule formation, movement and symptomatology.
965 *Virology* **390**(1): 110-121.
966 **Li W, Zhao Y, Liu C, Yao G, Wu S, Hou C, Zhang M, Wang D. 2012.** Callose deposition at
967 plasmodesmata is a critical factor in restricting the cell-to-cell movement of Soybean mosaic
968 virus. *Plant Cell Rep* **31**(5): 905-916.
969 **Li X, Kapos P, Zhang Y. 2015.** NLRs in plants. *Curr Opin Immunol* **32**: 114-121.
970 **Lopez C, Aramburu J, Galipienso L, Soler S, Nuez F, Rubio L. 2011.** Evolutionary analysis of
971 tomato Sw-5 resistance-breaking isolates of Tomato spotted wilt virus. *J Gen Virol* **92**(Pt 1):
972 210-215.
973 **Lucas WJ. 2006.** Plant viral movement proteins: agents for cell-to-cell trafficking of viral genomes.
974 *Virology* **344**(1): 169-184.
975 **Lukasik-Shreepaathy E, Slootweg E, Richter H, Goverse A, Cornelissen BJ, Takken FL. 2012.**
976 Dual regulatory roles of the extended N terminus for activation of the tomato MI-1.2
977 resistance protein. *Mol Plant Microbe Interact* **25**(8): 1045-1057.
978 **Ma S, Lapin D, Liu L, Sun Y, Song W, Zhang X, Logemann E, Yu D, Wang J, Jirschitzka J, Han**
979 **Z, Schulze-Lefert P, Parker JE, Chai J. 2020.** Direct pathogen-induced assembly of an
980 NLR immune receptor complex to form a holoenzyme. *Science* **370**(6521).
981 **Ma Y, Guo H, Hu L, Martinez PP, Moschou PN, Cevik V, Ding P, Duxbury Z, Sarris PF, Jones**
982 **JDG. 2018.** Distinct modes of derepression of an Arabidopsis immune receptor complex by
983 two different bacterial effectors. *Proc Natl Acad Sci U S A* **115**(41): 10218-10227.
984 **Ma Z, Song T, Zhu L, Ye W, Wang Y, Shao Y, Dong S, Zhang Z, Dou D, Zheng X, Tyler BM,**
985 **Wang Y. 2015.** A Phytophthora sojae Glycoside Hydrolase 12 Protein Is a Major Virulence
986 Factor during Soybean Infection and Is Recognized as a PAMP. *Plant Cell* **27**(7): 2057-2072.
987 **Ma Z, Zhu L, Song T, Wang Y, Zhang Q, Xia Y, Qiu M, Lin Y, Li H, Kong L, Fang Y, Ye W,**
988 **Wang Y, Dong S, Zheng X, Tyler BM, Wang Y. 2017.** A paralogous decoy protects
989 Phytophthora sojae apoplastic effector PsXEG1 from a host inhibitor. *Science* **355**(6326):
990 710-714.
991 **Maekawa T, Cheng W, Spiridon LN, Toller A, Lukasik E, Saijo Y, Liu P, Shen QH, Micluta MA,**
992 **Somssich IE, Takken FLW, Petrescu AJ, Chai J, Schulze-Lefert P. 2011.** Coiled-coil
993 domain-dependent homodimerization of intracellular barley immune receptors defines a
994 minimal functional module for triggering cell death. *Cell Host Microbe* **9**(3): 187-199.
995 **Meier N, Hatch C, Nagalakshmi U, Dinesh-Kumar SP. 2019.** Perspectives on intracellular
996 perception of plant viruses. *Mol Plant Pathol* **20**(9): 1185-1190.
997 **Meyers BC, Kozik A, Griego A, Kuang H, Michelmore RW. 2003.** Genome-wide analysis of
998 NBS-LRR-encoding genes in Arabidopsis. *Plant Cell* **15**(4): 809-834.
999 **Milligan SB, Bodeau J, Yaghoobi J, Kaloshian I, Zabel P, Williamson VM. 1998.** The root knot
1000 nematode resistance gene Mi from tomato is a member of the leucine zipper, nucleotide
1001 binding, leucine-rich repeat family of plant genes. *Plant Cell* **10**(8): 1307-1319.
1002 **Mittler R, Herr EH, Orvar BL, van Camp W, Willekens H, Inze D, Ellis BE. 1999.** Transgenic

1003 tobacco plants with reduced capability to detoxify reactive oxygen intermediates are
1004 hyperresponsive to pathogen infection. *Proc Natl Acad Sci U S A* **96**(24): 14165-14170.
1005 **Oliver JE, Whitfield AE. 2016.** The Genus Tospovirus: Emerging Bunyaviruses that Threaten Food
1006 Security. *Annu Rev Virol* **3**(1): 101-124.
1007 **Padmanabhan MS, Ma S, Burch-Smith TM, Czymmek K, Huijser P, Dinesh-Kumar SP. 2013.**
1008 Novel positive regulatory role for the SPL6 transcription factor in the N TIR-NB-LRR
1009 receptor-mediated plant innate immunity. *PLoS Pathog* **9**(3): e1003235.
1010 **Palma K, Zhang Y, Li X. 2005.** An importin alpha homolog, MOS6, plays an important role in plant
1011 innate immunity. *Curr Biol* **15**(12): 1129-1135.
1012 **Peiro A, Canizares MC, Rubio L, Lopez C, Moriones E, Aramburu J, Sanchez-Navarro J. 2014.**
1013 The movement protein (NSm) of Tomato spotted wilt virus is the avirulence determinant in
1014 the tomato Sw-5 gene-based resistance. *Mol Plant Pathol* **15**(8): 802-813.
1015 **Qi D, DeYoung BJ, Innes RW. 2012.** Structure-function analysis of the coiled-coil and leucine-rich
1016 repeat domains of the RPS5 disease resistance protein. *Plant Physiol* **158**(4): 1819-1832.
1017 **Qi D, Innes RW. 2013.** Recent Advances in Plant NLR Structure, Function, Localization, and
1018 Signaling. *Front Immunol* **4**: 348.
1019 **Rao ALNC, Y. G，Khan, J. A，Dijkstra, J. 2002.** Molecular biology of plant virus movement.
1020 *Plant Viruses As Molecular Pathogens*.
1021 **Sarris PF, Cevik V, Dagdas G, Jones JD, Krasileva KV. 2016.** Comparative analysis of plant
1022 immune receptor architectures uncovers host proteins likely targeted by pathogens. *BMC Biol*
1023 **14**: 8.
1024 **Sarris PF, Duxbury Z, Huh SU, Ma Y, Segonzac C, Sklenar J, Derbyshire P, Cevik V, Rallapalli**
1025 **G, Saucet SB, Wirthmueller L, Menke FL, Sohn KH, Jones JD. 2015.** A Plant Immune
1026 Receptor Detects Pathogen Effectors that Target WRKY Transcription Factors. *Cell* **161**(5):
1027 1089-1100.
1028 **Scholthof KB, Adkins S, Czosnek H, Palukaitis P, Jacquot E, Hohn T, Hohn B, Saunders K,**
1029 **Candresse T, Ahlquist P, Hemenway C, Foster GD. 2011.** Top 10 plant viruses in
1030 molecular plant pathology. *Mol Plant Pathol* **12**(9): 938-954.
1031 **Seo JK, Kwon SJ, Cho WK, Choi HS, Kim KH. 2014.** Type 2C protein phosphatase is a key
1032 regulator of antiviral extreme resistance limiting virus spread. *Sci Rep* **4**: 5905.
1033 **Seong K, Seo E, Witek K, Li M, Staskawicz B. 2020.** Evolution of NLR resistance genes with
1034 noncanonical N-terminal domains in wild tomato species. *New Phytol* **227**(5): 1530-1543.
1035 **Shen QH, Saijo Y, Mauch S, Biskup C, Bieri S, Keller B, Seki H, Ulker B, Somssich IE,**
1036 **Schulze-Lefert P. 2007.** Nuclear activity of MLA immune receptors links isolate-specific and
1037 basal disease-resistance responses. *Science* **315**(5815): 1098-1103.
1038 **Slootweg E, Roosien J, Spiridon LN, Petrescu AJ, Tameling W, Joosten M, Pomp R, van Schaik**
1039 **C, Dees R, Borst JW, Smant G, Schots A, Bakker J, Goverse A. 2010.** Nucleocytoplasmic
1040 distribution is required for activation of resistance by the potato NB-LRR receptor Rx1 and is
1041 balanced by its functional domains. *Plant Cell* **22**(12): 4195-4215.
1042 **Soosaar JL, Burch-Smith TM, Dinesh-Kumar SP. 2005.** Mechanisms of plant resistance to viruses.
1043 *Nat Rev Microbiol* **3**(10): 789-798.
1044 **Spassova M I PTW, Folkertsma R T, et al. 2001.** The tomato gene Sw-5 is a member of the coiled
1045 coil, nucleotide binding, leucine-rich repeat class of plant resistance genes and confers
1046 resistance to TSWV in tobacco. *Molecular Breeding.* **7(2)**: 151.

1047 **Stewart M. 2007.** Molecular mechanism of the nuclear protein import cycle. *Nat Rev Mol Cell Biol*
1048 **8**(3): 195-208.
1049 **Swiderski MR, Birker D, Jones JD. 2009.** The TIR domain of TIR-NB-LRR resistance proteins is a
1050 signaling domain involved in cell death induction. *Mol Plant Microbe Interact* **22**(2):
1051 157-165.
1052 **Takemoto D, Rafiqi M, Hurley U, Lawrence GJ, Bernoux M, Hardham AR, Ellis JG, Dodds PN,**
1053 **Jones DA. 2012.** N-terminal motifs in some plant disease resistance proteins function in
1054 membrane attachment and contribute to disease resistance. *Mol Plant Microbe Interact* **25**(3):
1055 379-392.
1056 **Takken FLW, Goverse A. 2012.** How to build a pathogen detector: structural basis of NB-LRR
1057 function. *Current Opinion in Plant Biology* **15**(4): 375-384.
1058 **Taliansky M, Torrance L, Kalinina NO. 2008.** Role of plant virus movement proteins. *Methods Mol*
1059 *Biol* **451**: 33-54.
1060 **Tameling WI, Nooijen C, Ludwig N, Boter M, Slootweg E, Goverse A, Shirasu K, Joosten MH.**
1061 **2010.** RanGAP2 mediates nucleocytoplasmic partitioning of the NB-LRR immune receptor
1062 Rx in the Solanaceae, thereby dictating Rx function. *Plant Cell* **22**(12): 4176-4194.
1063 **Tasset C, Bernoux M, Jauneau A, Pouzet C, Briere C, Kieffer-Jacquinod S, Rivas S, Marco Y,**
1064 **Deslandes L. 2010.** Autoacetylation of the Ralstonia solanacearum effector PopP2 targets a
1065 lysine residue essential for RRS1-R-mediated immunity in Arabidopsis. *PLoS Pathog* **6**(11):
1066 e1001202.
1067 **Turina M, Kormelink R, Resende RO. 2016.** Resistance to Tospoviruses in Vegetable Crops:
1068 Epidemiological and Molecular Aspects. *Annu Rev Phytopathol* **54**: 347-371.
1069 **van der Vossen EA, Gros J, Sikkema A, Muskens M, Wouters D, Wolters P, Pereira A, Allefs S.**
1070 **2005.** The Rpi-blb2 gene from Solanum bulbocastanum is an Mi-1 gene homolog conferring
1071 broad-spectrum late blight resistance in potato. *Plant J* **44**(2): 208-222.
1072 **van Wersch S, Li X. 2019.** Stronger When Together: Clustering of Plant NLR Disease resistance
1073 Genes. *Trends Plant Sci* **24**(8): 688-699.
1074 **van Wersch S, Tian, L., Hoy, R., Li, X. . 2020.** Plant NLRs: The whistleblowers of
1075 plant immunity. *Plant Commun*: doi: https://doi.org/10.1016/j.xplc.2019.100016.
1076 **Vos P, Simons G, Jesse T, Wijbrandi J, Heinen L, Hogers R, Frijters A, Groenendijk J,**
1077 **Diergaarde P, Reijans M, Fierens-Onstenk J, de Both M, Peleman J, Liharska T,**
1078 **Hontelez J, Zabeau M. 1998.** The tomato Mi-1 gene confers resistance to both root-knot
1079 nematodes and potato aphids. *Nat Biotechnol* **16**(13): 1365-1369.
1080 **Vossen JH, van Arkel G, Bergervoet M, Jo KR, Jacobsen E, Visser RG. 2016.** The Solanum
1081 demissum R8 late blight resistance gene is an Sw-5 homologue that has been deployed
1082 worldwide in late blight resistant varieties. *Theor Appl Genet* **129**(9): 1785-1796.
1083 **Wan L, Essuman K, Anderson RG, Sasaki Y, Monteiro F, Chung EH, Osborne Nishimura E,**
1084 **DiAntonio A, Milbrandt J, Dangl JL, Nishimura MT. 2019.** TIR domains of plant immune
1085 receptors are NAD(+)-cleaving enzymes that promote cell death. *Science* **365**(6455): 799-803.
1086 **Wang A. 2015.** Dissecting the molecular network of virus-plant interactions: the complex roles of host
1087 factors. *Annu Rev Phytopathol* **53**: 45-66.
1088 **Wang J, Chen T, Han M, Qian L, Li J, Wu M, Han T, Cao J, Nagalakshmi U, Rathjen JP, Hong**
1089 **Y, Liu Y. 2020.** Plant NLR immune receptor Tm-22 activation requires NB-ARC
1090 domain-mediated self-association of CC domain. *PLoS Pathog* **16**(4): e1008475.

1091 **Wang J, Hu M, Wang J, Qi J, Han Z, Wang G, Qi Y, Wang HW, Zhou JM, Chai J. 2019a.**
1092 Reconstitution and structure of a plant NLR resistosome conferring immunity. *Science*
1093 **364**(6435).
1094 **Wang J, Wang J, Hu M, Wu S, Qi J, Wang G, Han Z, Qi Y, Gao N, Wang HW, Zhou JM, Chai J.**
1095 **2019b.** Ligand-triggered allosteric ADP release primes a plant NLR complex. *Science*
1096 **364**(6435).
1097 **Wen W, Meinkoth JL, Tsien RY, Taylor SS. 1995.** Identification of a signal for rapid export of
1098 proteins from the nucleus. *Cell* **82**(3): 463-473.
1099 **Wirthmueller L, Zhang Y, Jones JD, Parker JE. 2007.** Nuclear accumulation of the Arabidopsis
1100 immune receptor RPS4 is necessary for triggering EDS1-dependent defense. *Curr Biol* **17**(23):
1101 2023-2029.
1102 **Zhang Y, Li X. 2005.** A putative nucleoporin 96 Is required for both basal defense and constitutive
1103 resistance responses mediated by suppressor of npr1-1,constitutive 1. *Plant Cell* **17**(4):
1104 1306-1316.
1105 **Zhao W, Jiang L, Feng Z, Chen X, Huang Y, Xue F, Huang C, Liu Y, Li F, Liu Y, Tao X. 2016.**
1106 Plasmodesmata targeting and intercellular trafficking of Tomato spotted wilt tospovirus
1107 movement protein NSm is independent of its function in HR induction. *J Gen Virol* **97**(8):
1108 1990-1997.
1109 **Zhu M, Jiang L, Bai B, Zhao W, Chen X, Li J, Liu Y, Chen Z, Wang B, Wang C, Wu Q, Shen Q,**
1110 **Dinesh-Kumar SP, Tao X. 2017.** The Intracellular Immune Receptor Sw-5b Confers
1111 Broad-Spectrum Resistance to Tospoviruses through Recognition of a Conserved 21-Amino
1112 Acid Viral Effector Epitope. *Plant Cell* **29**(9): 2214-2232.
1113 **Zhu M, van Grinsven IL, Kormelink R, Tao X. 2019.** Paving the Way to Tospovirus Infection:
1114 Multilined Interplays with Plant Innate Immunity. *Annu Rev Phytopathol* **57**: 41-62.

1115

1116

1117

1118

1119 **FIGURE LEGENDS**

1120 **Fig. 1.** Subcellular localization of Sw-5b in *Nicotiana benthamiana* and tomato leaf
1121 cells. (a) Schematic diagrams of Sw-5b. (b) Subcellular localizations of free YFP
1122 (left), YFP-Sw-5b (middle) and autoactive YFP-Sw-5b^{D857V} mutant (right) in *N.*
1123 *benthamiana* leaf cells at 24 hours post agro-infiltration (hpi). (c) Subcellular
1124 localization of free YFP (left), YFP-Sw-5b (middle) and autoactive YFP-Sw-5b^{D857V}
1125 mutant (right) in tomato leaf cells at 24 hpi. N nucleus, and C cytoplasm inside the
1126 cell are indicated. Bar = 10 μm. (d) Nucleocytoplasmic partitioning analysis of
1127 YFP-Sw-5b and autoactive YFP-Sw-5b^{D857V}. Total lysate (T) from p2300S empty
1128 vector (EV), YFP-Sw-5b or YFP-Sw-5b^{D857V} expressing leaves were fractionated into
1129 cytoplasm and nucleus, and analyzed by immunoblots using antibodies against YFP.
1130 The actin and histone were used as a cytoplasm marker and nucleus marker,
1131 respectively, in the fractionation analysis. Ponceau S staining was also used as
1132 cytoplasm marker.

1133

1134 **Fig. 2.** Effect of Sw-5b subcellular localization pattern on HR induction. (a) Confocal
1135 images of *N. benthamiana* leaf cells transiently expressing NES-YFP-Sw-5b,
1136 nes-YFP-Sw-5b, NLS-YFP-Sw-5b or nls-YFP-Sw-5b fusion. The images were taken
1137 at 24–36 hpi. N nucleus and C cytoplasm (c). Bar = 10 μm. (b) Induction of HR in *N.*
1138 *benthamiana* leaf tissues co-expressing NSm and one of the five Sw-5b fusion
1139 proteins. The infiltrated *N. benthamiana* leaf was photographed at 3 dpi (left image).
1140 Induction of HR in the infiltrated tissues were visualized using a trypan blue staining

1141 method (right image). (c) Immunoblot analysis of NES-YFP-Sw-5b, nes-YFP-Sw-5b,
1142 NLS-YFP-Sw-5b, and nls-YFP-Sw-5b expressions in the infiltrated *N. benthamiana*
1143 leaf tissues. These fusion proteins were enriched using the GFP-Trap beads prior to
1144 SDS-PAGE, and the blot was probed using an YFP specific antibody. Ponceau-S
1145 staining was used to estimate sample loadings. (d) Time course analysis of ion
1146 leakage in Nicotiana benthamiana leaves co-expressing NSm with one of the five
1147 Sw-5b fusion proteins. Measurements were performed at 4 h intervals starting from
1148 24 to 48 hpi. Error bars (SEs) were calculated using the results from three biological
1149 replicates per treatment collected at each time point.
1150
1151 **Fig. 3.** The effect of cytoplasm- and nucleus-targeted Sw-5b on viral replication. (a)
1152 Schematic representation of binary constructs to express TSWV $SR_{(-)eGFP}$
1153 mini-genome replicon, TSWV L RNA segment containing an optimized RdRp and
1154 $NSm^{H93A\&H94A}$ mutant that defected in viral movement. Minus sign (-) and 5′ to 3′
1155 designation represent the negative (genomic)-strand of tospovirus RNA. 35S: a
1156 double 35S promoter; HH: hammerhead ribozyme; RZ: hepatitis delta virus (HDV)
1157 ribozyme; NOS: nopaline synthase terminator; 35S Ter: a 35S transcription terminator.
1158 (b) Accumulation of eGFP fluorescence in *N. benthamiana* leaves co-expressing
1159 p2300S empty vector (EV), Sw-5b, NES-Sw-5b, nes-Sw-5b, NLS-Sw-5b, or
1160 nls-Sw-5b with TSWV $SR_{(-)eGFP}$, L, and $NSm^{H93A\&H94A}$ at 4 days post infiltration (dpi)
1161 viewed with a fluorescence microscope. Bar represents 400 μm. (c) Immunoblot
1162 analysis of expression of eGFP proteins in leaves shown in panel (b) using specific

1163 antibodies against YFP. Ponceau S staining of rubisco large subunit is shown for
1164 protein loading control.
1165
1166 **Fig. 4.** Effect of subcellular localization of Sw-5b on cell-to-cell movement of NSm
1167 in leaf epidermis of *N. benthamiana.* (a) Schematic diagram of the binary construct to
1168 co-express mCherry-HDEL and NSm-GFP. (b) Cell-to-cell movement analysis of
1169 NSm-GFP in *N. benthamiana* leaves co-expressing p2300S empty vector (EV), Sw-5b,
1170 NES-Sw-5b, NLS-Sw-5b, or nls-Sw-5b with the construct harboring both
1171 mCherry-HDEL and NSm-GFP. *Agrobacterium* containing the construct to co-express
1172 mCherry-HDEL and NSm-GFP was diluted 500 times for expression in a single
1173 epidermal cell. All other *Agrobacterium* were infiltrated at the concentration of OD_{600}
1174 = 0.2. Bar, 50 μm.
1175
1176 **Fig. 5.** Analysis of cytoplasm- and nucleus-targeted Sw-5b-mediated host immunity
1177 to TSWV systemic infection. (a) TSWV systemic infection in transgenic *N.*
1178 *benthamiana* plants expressing NES-YFP-Sw-5b, nes-YFP-Sw-5b, NLS-YFP-Sw-5b,
1179 nls-YFP-Sw-5b, YFP-Sw-5b or p2300S empty vector (EV) driven by 35S promoter.
1180 TSWV-inoculated plants were photographed at 15 dpi. White arrow indicates the
1181 systemic leaves showing HR trailing. White arrowhead indicates the systemic leaves
1182 showing mosaic. (b) Immunoblot analysis of NES-YFP-Sw-5b, nes-YFP-Sw-5b,
1183 NLS-YFP-Sw-5b, nls-YFP-Sw-5b and YFP-Sw-5b expressions in different transgenic
1184 *N. benthamiana* plants. EV plants transformed with an empty vector and were used as

1185 a negative control. (c) RT-PCR analysis of TSWV accumulation in the systemic
1186 leaves of different transgenic *N. benthamiana* plants at 15 dpi.
1187
1188 **Fig. 6.** Joint effects of cytoplasm- and nucleus-targeted Sw-5b on defenses against
1189 tospovirus infection in *Nicotiana benthamiana* leaves. (a) Schematic representation of
1190 binary constructs to express TSWV $SR_{(+)eGFP}$-$M_{(-)op}$ and TSWV L RNA segment
1191 containing an optimized RdRp. 35S: a double 35S promoter; HH: hammerhead
1192 ribozyme; RZ: hepatitis delta virus (HDV) ribozyme; NOS: nopaline synthase
1193 terminator. (b) Accumulation of eGFP fluorescence in *N. benthamiana* leaves
1194 co-expressing p2300S empty vector (EV), Sw-5b, NES-Sw-5b, NLS-Sw-5b, or
1195 NES-Sw-5b+NLS-Sw-5b with TSWV $SR_{(+)eGFP}$-$M_{(-)op}$ at 4 days post infiltration (dpi)
1196 viewed with a fluorescence microscope. Bar represents 400 μm. (c) Immunoblot
1197 analysis of expression of eGFP proteins in leaves shown in panel (b) using specific
1198 antibodies against YFP. Ponceau S staining of rubisco large subunit is shown for
1199 protein loading control. (d) Quantification of eGFP proteins in leaves shown in panel
1200 (c).
1201
1202 **Fig. 7.** Functional analysis and subcellular localization patterns of individual or
1203 combined Sw-5b domains. (a) Schematic diagrams showing a full length Sw-5b or
1204 Sw-5b domains fused with YFP. (b) Confocal images of *N. benthamiana* leaf
1205 epidermal cells expressing various YFP fusions. Images of the cells were taken at 24
1206 hpi. N nucleus, Nu nucleolus, and C cytoplasm. Bar = 10 μm. (c) TSWV-inoculated

1207 transgenic *N. benthamiana* plants expressing these various YFP fusions and
1208 photographed at 15 dpi.
1209
1210 **Fig. 8.** Roles of *importins* α and β in YFP-Sw-5b nucleus targeting and
1211 Sw-5b-mediated immunity to TSWV systemic infection. (a) Transient expression of
1212 YFP-Sw-5b in *N. benthamiana* leaf epidermal cells silenced for *importin*
1213 $\alpha 1$ (IMP α1 KD), *importin* $\alpha 2$ (IMP α2 KD), *importin* $\alpha 1$ and $\alpha 2$ (IMP α1 & α2 KD),
1214 *importin* β (IMP β KD) or *importin* $\alpha 1$ and $\alpha 2$ and β (IMP α1 & α2 & β KD) through
1215 VIGS. Images of the cells were captured using a confocal microscope at 26 hpi. N
1216 nucleus, C cytoplasm. Bar = 10 μm. (b) YFP-Sw-5b transgenic *N. benthamiana* plants
1217 were silenced for *importin* $\alpha 1$, *importin* $\alpha 2$, *importin* $\alpha 1$ and $\alpha 2$, *importin* β or
1218 *importin* $\alpha 1$ and $\alpha 2$ and β expression through VIGS followed by inoculation with
1219 TSWV. TSWV-inoculated YFP-Sw-5b transgenic *N. benthamiana* plants were
1220 photographed at 15 dpi. White arrowhead indicates HR trailing in systemic leaves.
1221
1222 **Fig. 9.** A working model for Sw-5b. Sw-5b furcates disease resistances by proper
1223 nucleocytoplasmic partition to block different infection steps of tomato spotted wilt
1224 tospovirus. Sw-5b switched from the autoinhibited state to an activated state upon
1225 recognition of NSm in the cytoplasm. Cytoplasm portion of Sw-5b induce cell death
1226 and defense that inhibit viral replication. The activated Sw-5b also translocated into
1227 nucleus via *importins* α and β. Nucleus-localized Sw-5b induces a defense that block
1228 viral cell-to-cell and long-distance movement. Cytoplasm- and nucleus-localized

1229 Sw-5b have additively effects on defense to inhibit viral replication, intercellular and

1230 long-distance movement during tospovirus infection.

1231

1232 **Supporting Information**

1233 **Short legends**

1234 **Fig. S1** Sw-5b recognizes TSWV NSm in cytoplasm.

1235 **Fig. S2** Analysis of virus replication monitoring system using a TSWV-based
1236 mini-genome replicon and a movement defective NSm mutant.

1237 **Fig. S3** Effects of nes-Sw-5b and nls-Sw-5b on NSm-GFP cell-to-cell movement and
1238 effects of Sw-5b and EV on NSm^{T120N}-GFP cell-to-cell movement.

1239 **Fig. S4** Effects of cytoplasmic and nuclear Sw-5b on host immunity to TSWV
1240 systemic infection.

1241 **Fig. S5** Cytoplasmic and nuclear Sw-5b activity on TSWV-GFP cell-to-cell
1242 movement in *N. benthamiana* leaves.

1243 **Fig. S6** An immunoblot showing the accumulations of various YFP-tagged proteins
1244 expressed in different transgenic *N. benthamiana* plants and RT-PCR analysis of
1245 TSWV accumulation in the systemic leaves.

1246 **Fig. S7** Bimolecular fluorescence complementation (BiFC) assay of cYFP-SD,
1247 cYFP-Sw-5b and nYFP-Importin α1 (nYFP-IMP α1), nYFP-Importin α2 (nYFP-IMP
1248 α2), nYFP-Importin β (nYFP-IMP β) interaction in *N. benthamiana* leaf epidermal
1249 cells.

1250 **Fig. S8** RT-PCR analyses of *importin a1*, *a2* and *b* expressions in the assayed plants
1251 and their effects on TSWV systemic infection.

1252 **Table S1.** List of primers used in this study.

1253 **Table S2.** Response of six different types of transgenic *Nicotiana benthamina* plants

1254 driven by 35S promoter to TSWV infection.

1255 **Table S3.** Response of six different types of transgenic *Nicotiana benthamina* plants

1256 driven by Sw-5b native promoter to TSWV infection.

1257 **Table S4.** Response of six different types of transgenic *Nicotiana benthamina* plants

1258 to TSWV infection.

1259 **Table S5.** Mass spectrum data of YFP-SD

1260 **Table S6.** Mass spectrum data of YFP-Sw-5b

1261

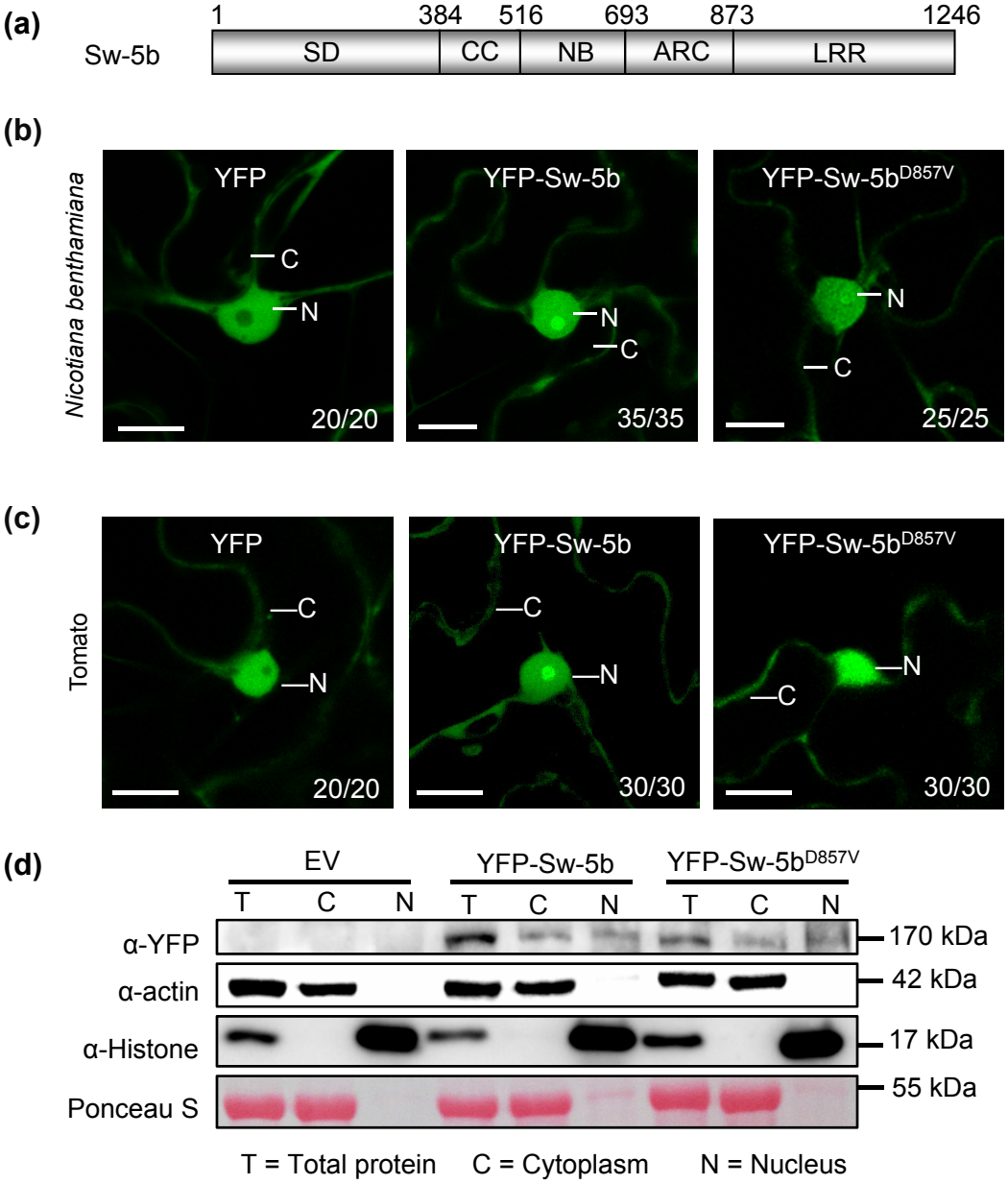

Fig. 1. Subcellular localization of Sw-5b in *Nicotiana benthamiana* and tomato leaf cells. (a) Schematic diagram of Sw-5b. (b) Subcellular localizations of free YFP (left), YFP-Sw-5b (middle) and autoactive YFP-Sw-5b^{D857V} mutant (right) in *N. benthamiana* leaf cells at 24 hours post agro-infiltration (hpi). (c) Subcellular localization of free YFP (left), YFP-Sw-5b (middle) and autoactive YFP-Sw-5b^{D857V} mutant (right) in tomato leaf cells at 24 hpi. N nucleus, and C cytoplasm inside the cell are indicated. Bar = 10 μm. (d) Nucleocytoplasmic partitioning analysis of YFP-Sw-5b and autoactive YFP-Sw-5b^{D857V}. Total lysate (T) from p2300S empty vector (EV), YFP-Sw-5b or YFP-Sw-5b^{D857V} expressing leaves were fractionated into cytoplasm and nucleus, and analyzed by immunoblots using antibodies against YFP. The actin and histone were used as a cytoplasm marker and nucleus marker, respectively, in the fractionation analysis. Ponceau S staining was also used as cytoplasm marker.

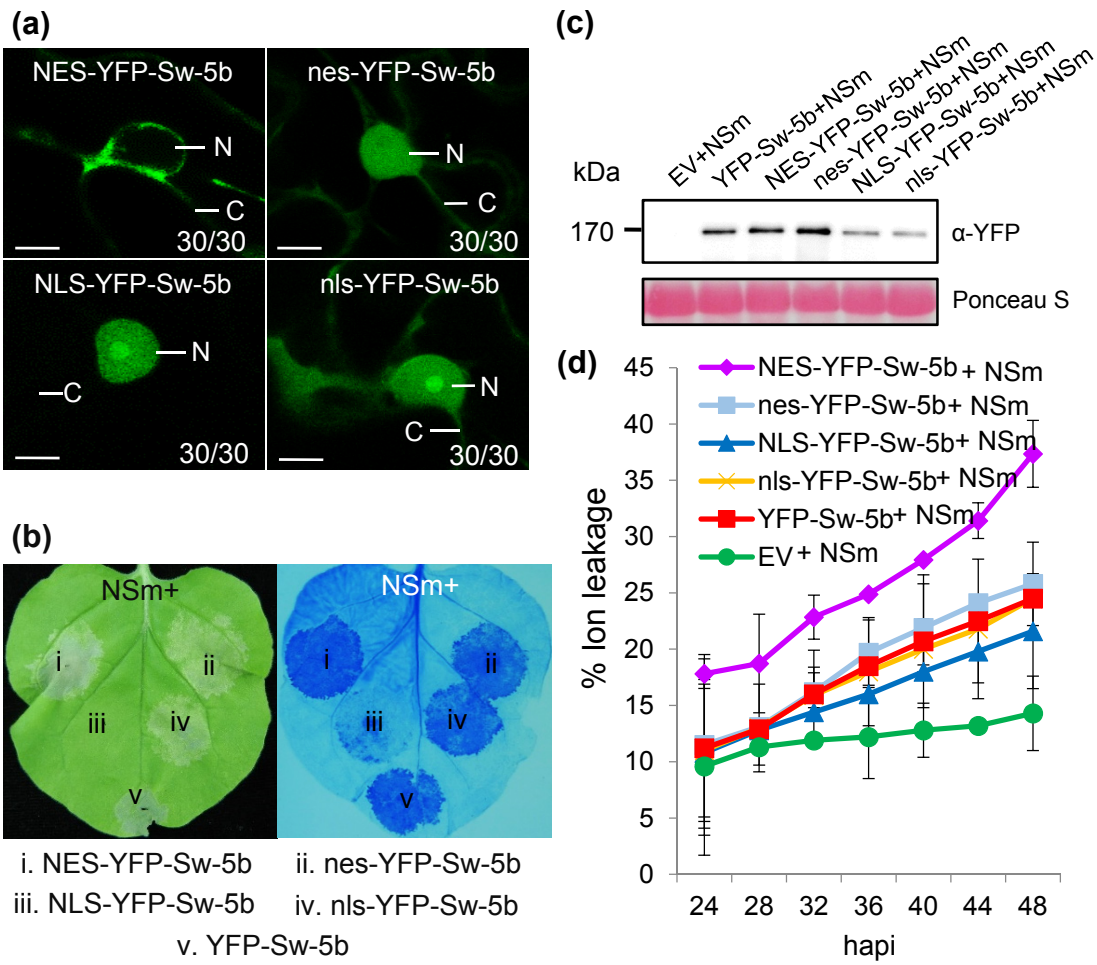

Fig. 2. Effect of Sw-5b subcellular localization pattern on HR induction. (a) Confocal images of *N. benthamiana* leaf cells transiently expressing NES-YFP-Sw-5b, nes-YFP-Sw-5b, NLS-YFP-Sw-5b or nls-YFP-Sw-5b fusion. The images were taken at 24–36 hpi. N nucleus and C cytoplasm (c). Bar = 10 µm. (b) Induction of HR in *N. benthamiana* leaf tissues co-expressing NSm and one of the five Sw-5b fusion proteins. The infiltrated *N. benthamiana* leaf was photographed at 3 dpi (left image). Induction of HR in the infiltrated tissues were visualized using a trypan blue staining method (right image). (c) Immunoblot analysis of NES-YFP-Sw-5b, nes-YFP-Sw-5b, NLS-YFP-Sw-5b, and nls-YFP-Sw-5b expressions in the infiltrated *N. benthamiana* leaf tissues. These fusion proteins were enriched using the GFP-Trap beads prior to SDS-PAGE, and the blot was probed using an YFP specific antibody. Ponceau-S staining was used to estimate sample loadings. (d) Time course analysis of ion leakage in Nicotiana benthamiana leaves co-expressing NSm with one of the five Sw-5b fusion proteins. Measurements were performed at 4 h intervals starting from 24 to 48 hpi. Error bars (SEs) were calculated using the results from three biological replicates per treatment collected at each time point.

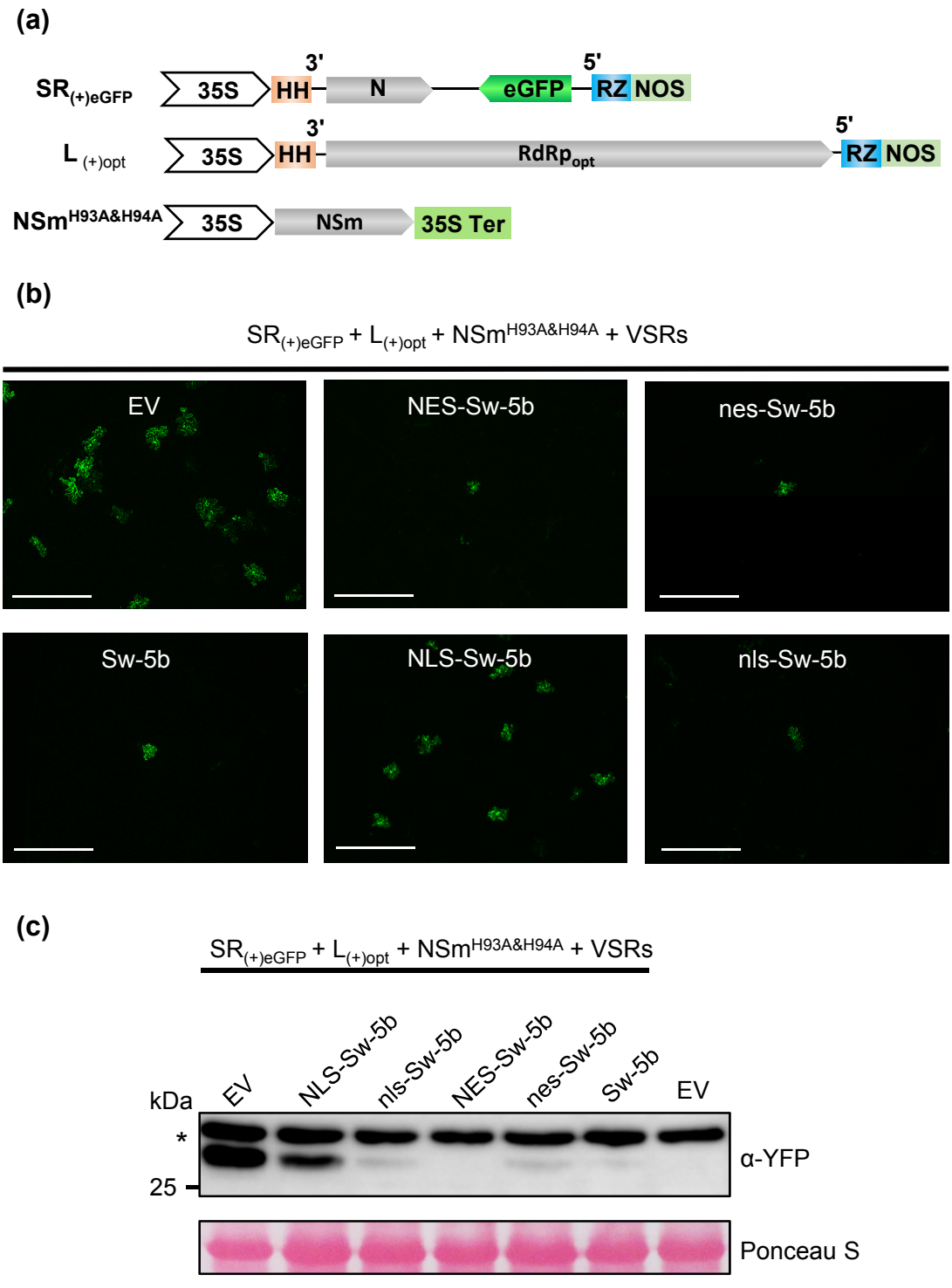
(a)
SR(+)eGFP
35S
HH
3'
N
eGFP
5'
RZ
NOS
L (+)opt
35S
HH
3'
RdRpopt
5'
RZ
NOS
NSmH93A&H94A
35S
NSm
35S Ter
(b)
SR(+)eGFP + L(+)opt + NSmH93A&H94A + VSRs
EV
NES-Sw-5b
nes-Sw-5b
Sw-5b
NLS-Sw-5b
nls-Sw-5b
(c)
SR(+)eGFP + L(+)opt + NSmH93A&H94A + VSRs
kDa
EV
NLS-Sw-5b
nls-Sw-5b
NES-Sw-5b
nes-Sw-5b
Sw-5b
EV
*
25
α-YFP
Ponceau S

Fig. 3. The effect of cytoplasm- and nucleus-targeted Sw-5b on viral replication. (a) Schematic representation of binary constructs to express TSWV $SR_{(-)eGFP}$ mini-genome replicon, TSWV L RNA segment containing an optimized RdRp and $NSm^{H93A\&H94A}$ mutant that defected in viral movement. Minus sign (-) and 5′ to 3′ designation represent the negative (genomic)-strand of tospovirus RNA. 35S: a double 35S promoter; HH: hammerhead ribozyme; RZ: hepatitis delta virus (HDV) ribozyme; NOS: nopaline synthase terminator; 35S Ter: a 35S transcription terminator. (b) Accumulation of eGFP fluorescence in *N. benthamiana* leaves co-expressing p2300S empty vector (EV), Sw-5b, NES-Sw-5b, nes-Sw-5b, NLS-Sw-5b, or nls-Sw-5b with TSWV $SR_{(-)eGFP}$, L, and $NSm^{H93A\&H94A}$ at 4 days post infiltration (dpi) viewed with a fluorescence microscope. Bar represents 400 μm. (c) Immunoblot analysis of expression of eGFP proteins in leaves shown in panel (b) using specific antibodies against YFP. Ponceau S staining of rubisco large subunit is shown for protein loading control.

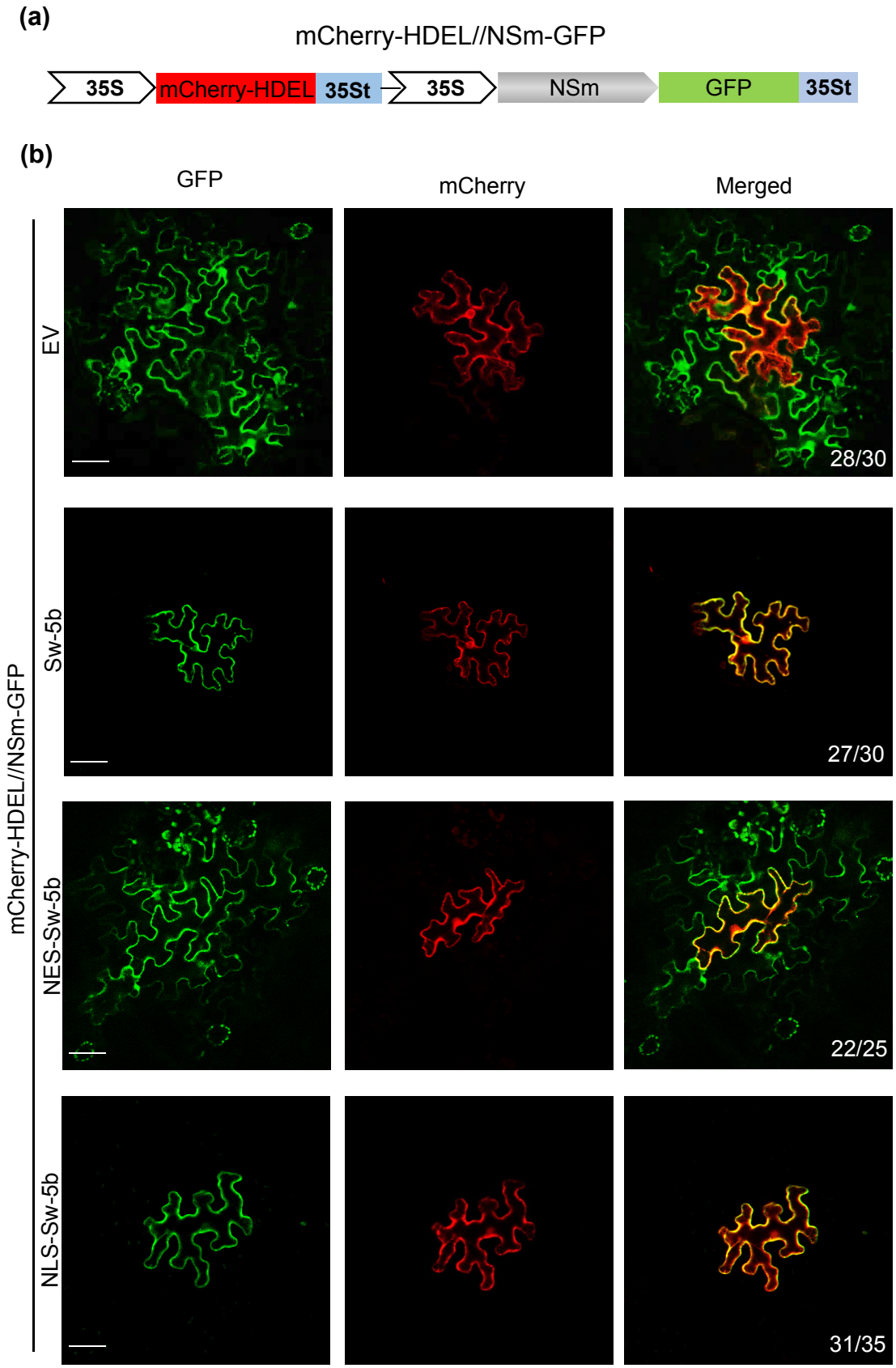
(a)
mCherry-HDEL//NSm-GFP
35S
mCherry-HDEL
35St
35S
NSm
GFP
35St
(b)
GFP
mCherry
Merged
mCherry-HDEL//NSm-GFP
EV
Sw-5b
NES-Sw-5b
NLS-Sw-5b
28/30
27/30
22/25
31/35

Fig. 4. Effect of subcellular localization of Sw-5b on cell-to-cell movement of NSm in leaf epidermis of *N. benthamiana.* (a) Schematic diagram of the binary construct to co-express mCherry-HDEL and NSm-GFP. (b) Cell-to-cell movement analysis of NSm-GFP in *N. benthamiana* leaves co-expressing p2300S empty vector (EV), Sw-5b, NES-Sw-5b, NLS-Sw-5b, or nls-Sw-5b with the construct harboring both mCherry-HDEL and NSm-GFP. *Agrobacterium* containing the construct to co-express mCherry-HDEL and NSm-GFP was diluted 500 times for expression in a single epidermal cell. All other *Agrobacterium* were infiltrated at the concentration of OD_{600} = 0.2. Bar = 50 μm.

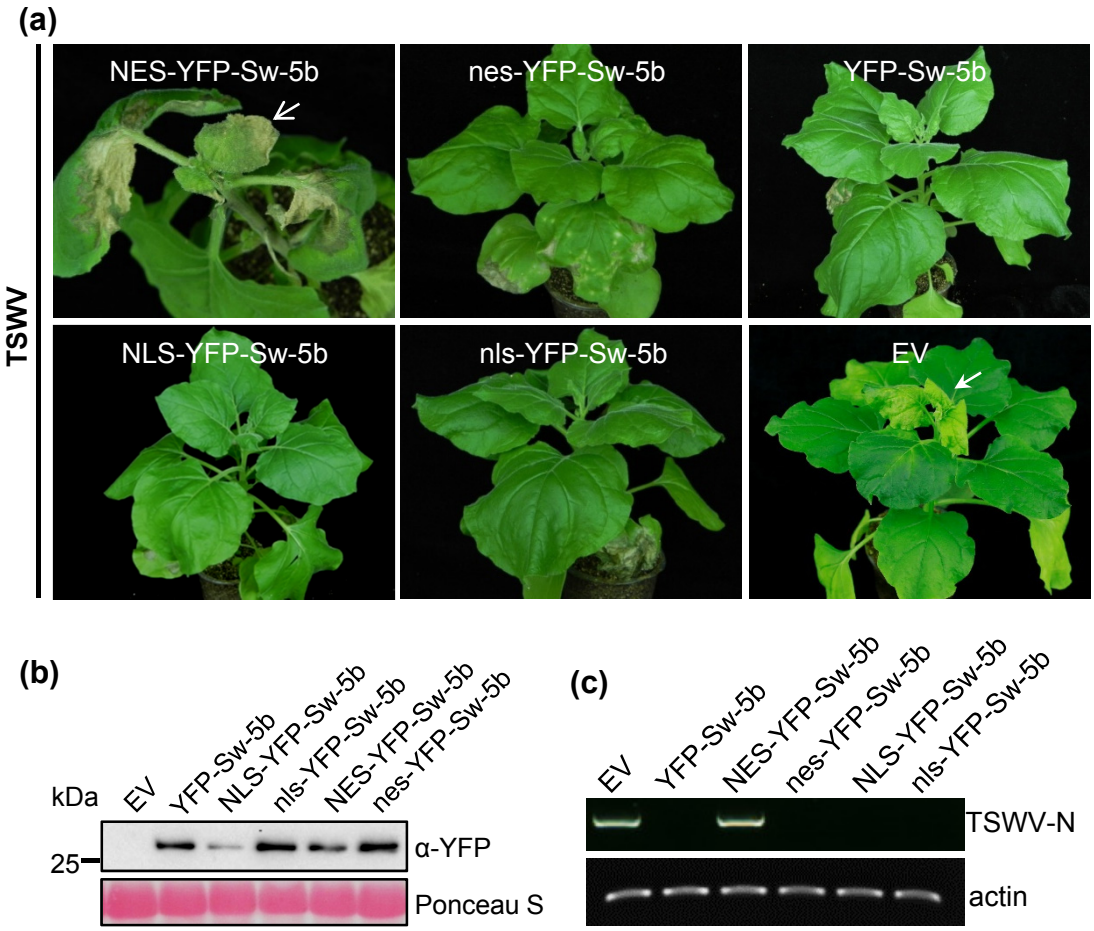

Fig. 5. Analysis of cytoplasm- and nucleus-targeted Sw-5b-mediated host immunity to TSWV systemic infection. (a) TSWV systemic infection in transgenic *N. benthamiana* plants expressing NES-YFP-Sw-5b, nes-YFP-Sw-5b, NLS-YFP-Sw-5b, nls-YFP-Sw-5b, YFP-Sw-5b or p2300S empty vector (EV) driven by 35S promoter. TSWV-inoculated plants were photographed at 15 dpi. White arrow indicates the systemic leaves showing HR trailing. White arrowhead indicates the systemic leaves showing mosaic. (b) Immunoblot analysis of NES-YFP-Sw-5b, nes-YFP-Sw-5b, NLS-YFP-Sw-5b, nls-YFP-Sw-5b and YFP-Sw-5b expressions in different transgenic *N. benthamiana* plants. EV plants transformed with an empty vector and were used as a negative control. (c) RT-PCR analysis of TSWV accumulation in the systemic leaves of different transgenic *N. benthamiana* plants at 15 dpi.

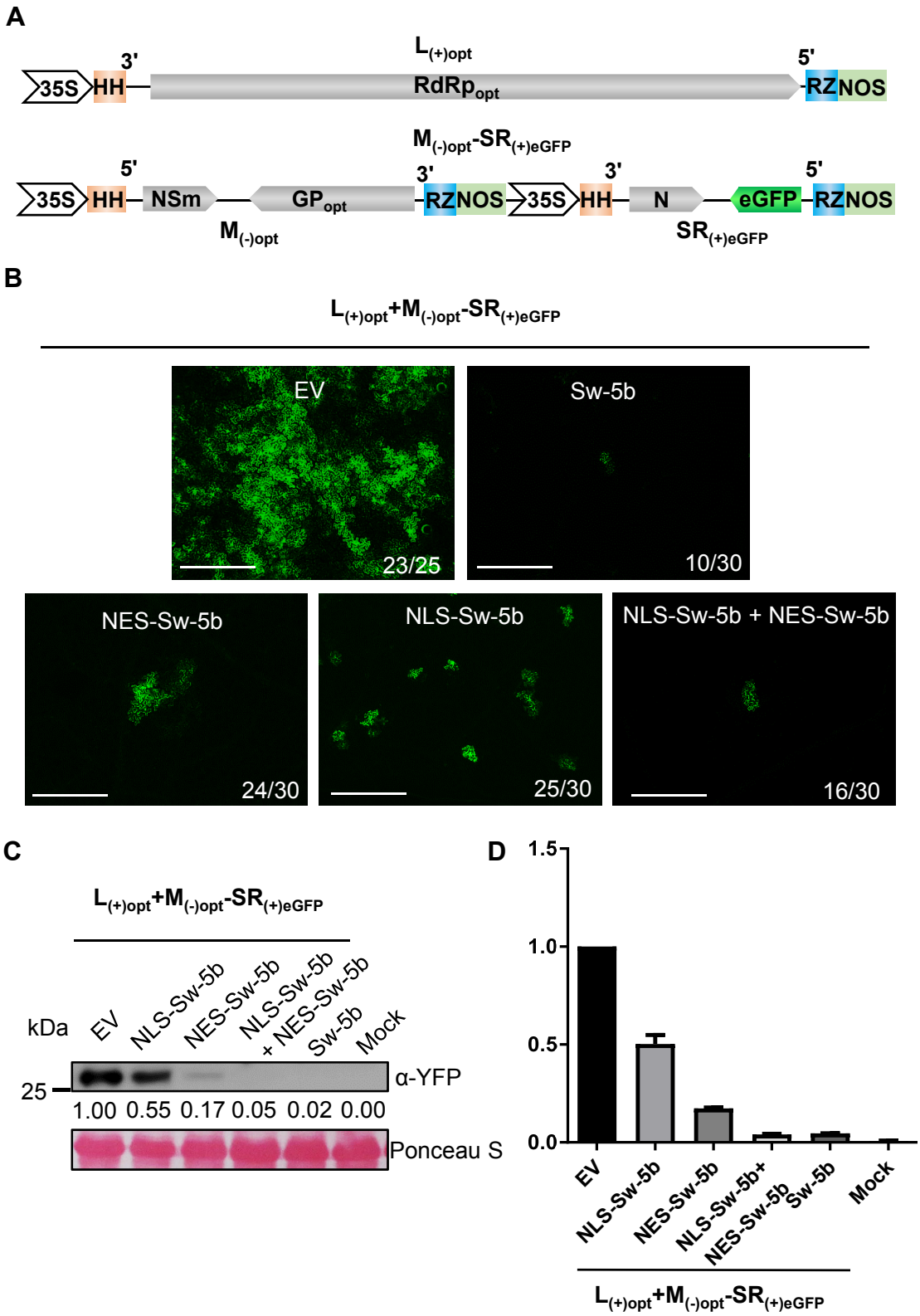
A
L(+)opt
3'
5'
35S
HH
RdRpopt
RZNOS
M(-)opt-SR(+)eGFP
5'
3'
3'
5'
35S
HH
NSm
GPopt
RZNOS
35S
HH
N
eGFP
RZNOS
M(-)opt
SR(+)eGFP
B
L(+)opt+M(-)opt-SR(+)eGFP
EV
23/25
Sw-5b
10/30
NES-Sw-5b
24/30
NLS-Sw-5b
25/30
NLS-Sw-5b + NES-Sw-5b
16/30
C
L(+)opt+M(-)opt-SR(+)eGFP
kDa
EV
NLS-Sw-5b
NES-Sw-5b
NLS-Sw-5b + NES-Sw-5b
Sw-5b
Mock
25
α-YFP
1.00 0.55 0.17 0.05 0.02 0.00
Ponceau S
D
1.5
1.0
0.5
0.0
EV
NLS-Sw-5b
NES-Sw-5b
NLS-Sw-5b+ NES-Sw-5b
Sw-5b
Mock
L(+)opt+M(-)opt-SR(+)eGFP

Fig. 6. Joint effects of cytoplasm- and nucleus-targeted Sw-5b on defenses against tospovirus infection in *Nicotiana benthamiana* leaves. (a) Schematic representation of binary constructs to express TSWV $SR_{(+)eGFP}$-$M_{(-)op}$ and TSWV L RNA segment containing an optimized RdRp. 35S: a double 35S promoter; HH: hammerhead ribozyme; RZ: hepatitis delta virus (HDV) ribozyme; NOS: nopaline synthase terminator. (b) Accumulation of eGFP fluorescence in *N. benthamiana* leaves co-expressing p2300S empty vector (EV), Sw-5b, NES-Sw-5b, NLS-Sw-5b, or NES-Sw-5b+NLS-Sw-5b with TSWV $SR_{(+)eGFP}$-$M_{(-)op}$ at 4 days post infiltration (dpi) viewed with a fluorescence microscope. Bar represents 400 μm. (c) Immunoblot analysis of expression of eGFP proteins in leaves shown in panel (b) using specific antibodies against YFP. Ponceau S staining of rubisco large subunit is shown for protein loading control. (d) Quantification of eGFP proteins in leaves shown in panel (c).

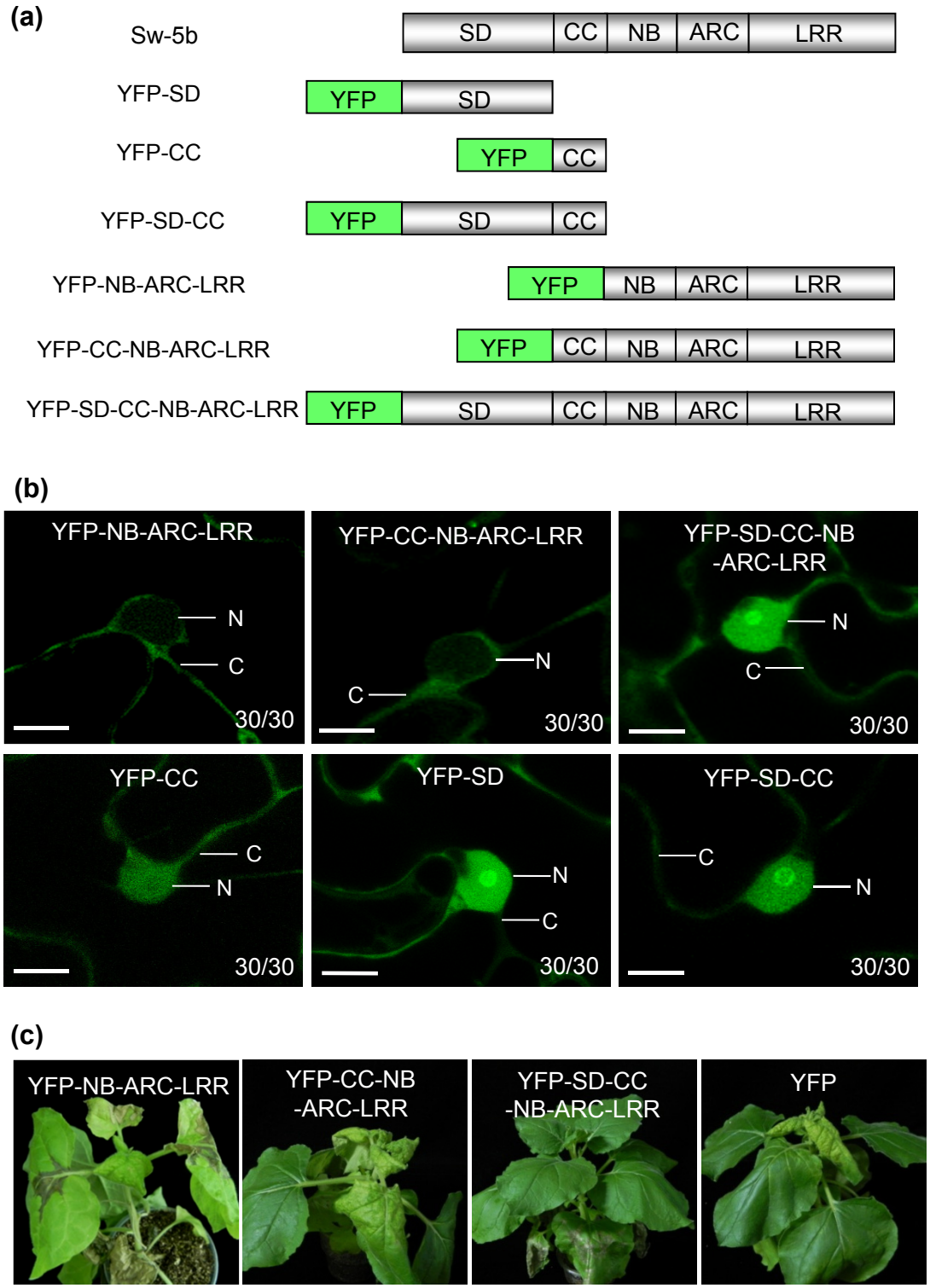

Fig. 7. Functional analysis and subcellular localization patterns of individual or combined Sw-5b domains. (a) Schematic diagram showing a full length Sw-5b or Sw-5b domains fused with YFP. (b) Confocal images of *N. benthamiana* leaf epidermal cells expressing various YFP fusions. Images of the cells were taken at 24 hpi. N nucleus, and C cytoplasm. Bar = 10 μm. (c) TSWV-inoculated transgenic *N. benthamiana* plants expressing these various YFP fusions and photographed at 15 dpi.

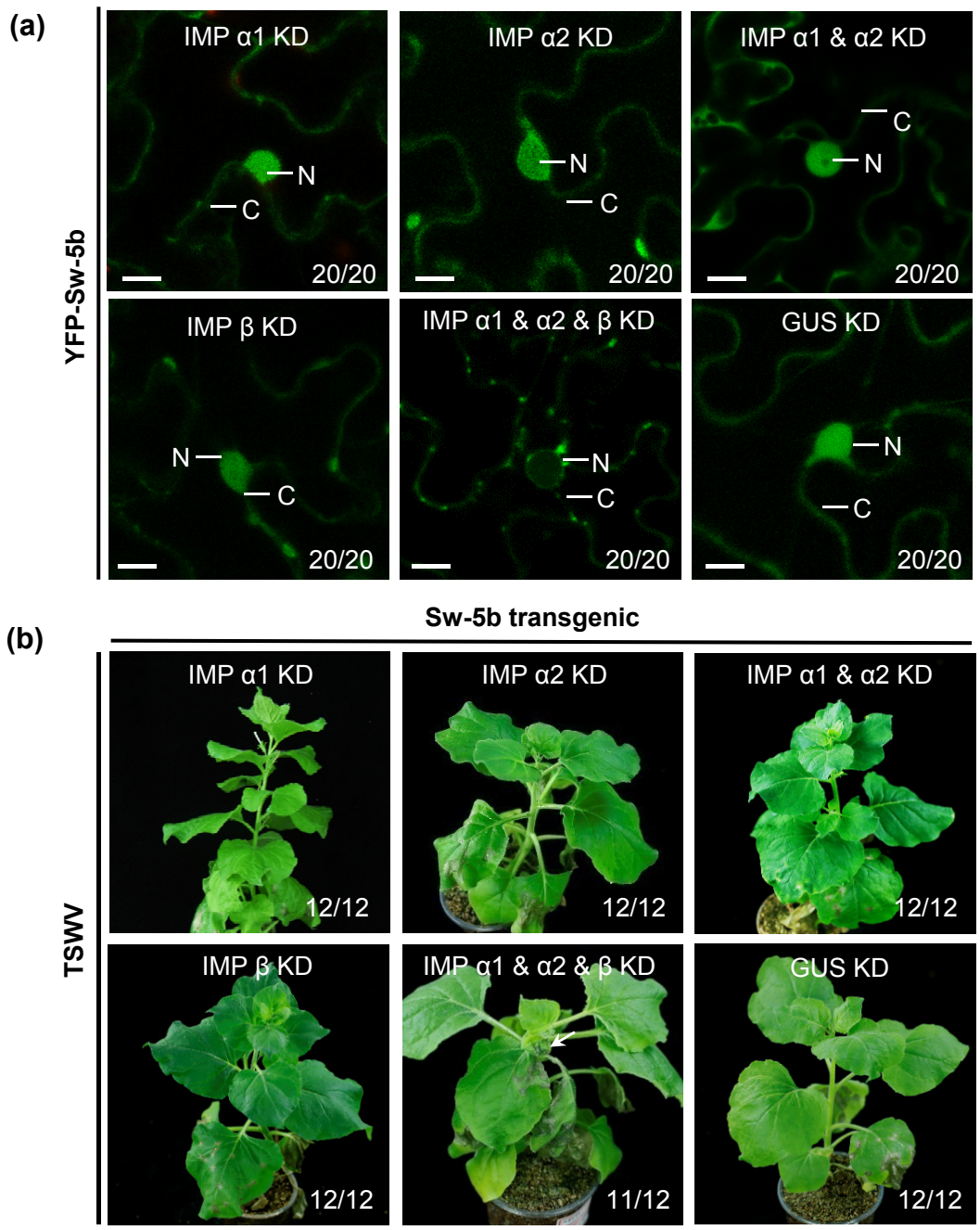

Fig. 8. Roles of *importins α* and *β* in YFP-Sw-5b nucleus targeting and Sw-5b-mediated immunity to TSWV systemic infection. (a) Transient expression of YFP-Sw-5b in *N. benthamiana* leaf epidermal cells silenced for *importin α1* (IMP α1 KD), *importinα2* (IMP α2 KD), *importin* α*1* and α*2* (IMP α1 & α2 KD), *importin β* (IMP β KD) or *importin* α*1* and *β2* and *β* (IMP α1 & α2 & β KD) through VIGS. Images of the cells were captured using a confocal microscope at 26 hpi. N nucleus, C cytoplasm. Bar = 10 mm. (b) YFP-Sw-5b transgenic *N. benthamiana* plants were silenced for *importin a1, importin* α*2*, *importin* α*1* and α*2*, *importin β* or *importin* α*1* and α*2* and *β* expression through VIGS followed by inoculation with TSWV. TSWV-inoculated YFP-Sw-5b transgenic *N. benthamiana* plants were photographed at 15 dpi. White arrowhead indicates HR trailing in systemic leaves.

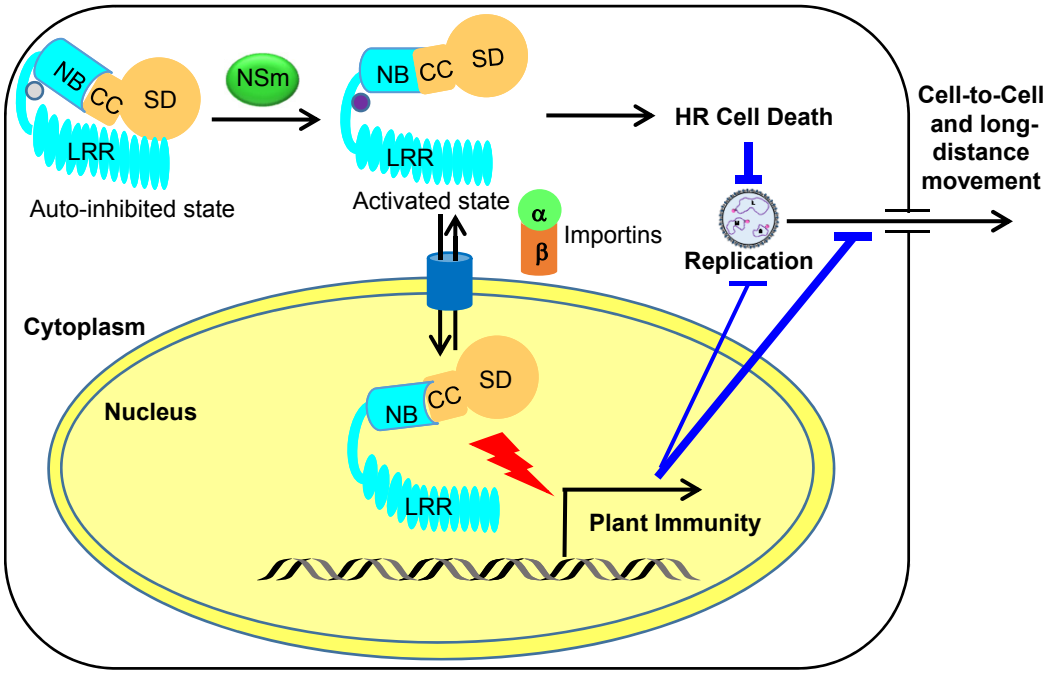

Fig. 9. A working model for Sw-5b. Sw-5b furcates disease resistances by proper nucleocytoplasmic partition to block different infection steps of tomato spotted wilt tospovirus. Sw-5b switched from the autoinhibited state to an activated state upon recognition of NSm in the cytoplasm. Cytoplasm portion of Sw-5b induce cell death and defense that inhibit viral replication. The activated Sw-5b also translocated into nucleus via *importins a* and *b* . Nucleus-localized Sw-5b induces a defense that block viral cell-to-cell and long-distance movement. Cytoplasm- and nucleus-localized Sw-5b have additively effects on defense to inhibit viral replication, intercellular and long-distance movement during tospovirus infection.

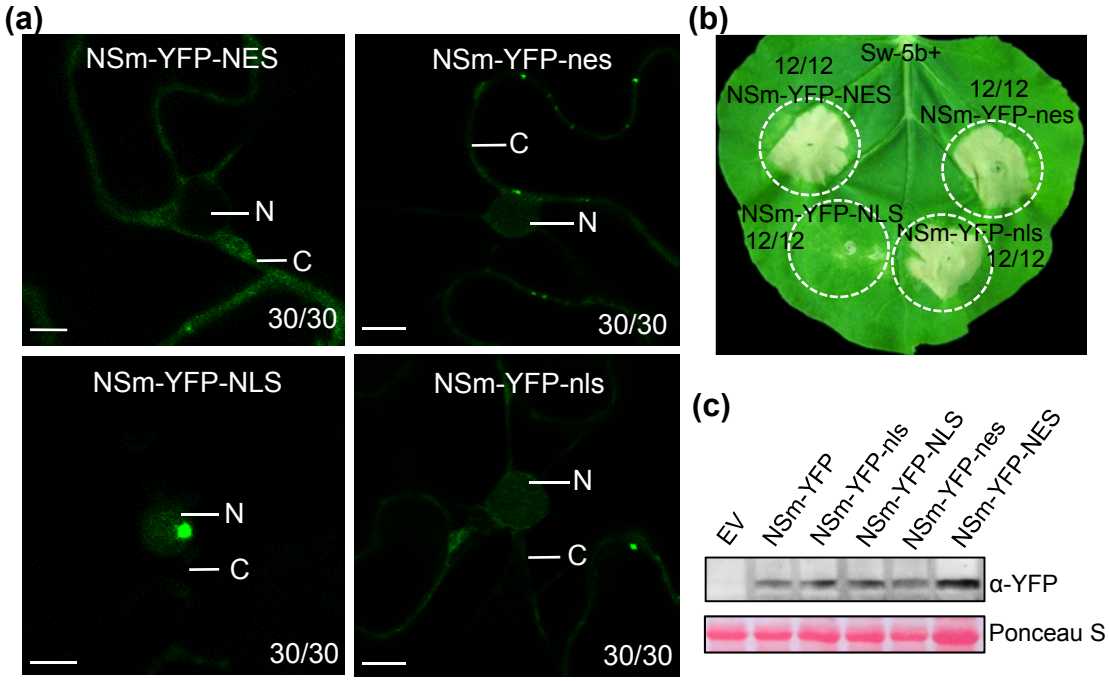

Fig. S1 Sw-5b recognizes TSWV NSm in cytoplasm. (a) Transient expressions of NSm-YFP-NES, NSm-YFP-nes, NSm-YFP-NLS, and NSm-YFP-nls, respectively, in *N. benthamiana* leaves through agro-infiltration. Epidermal cells expressing various fusion proteins were imaged under a confocal microscope at 24 hpai. The numbers in each image indicate the number of cells showing this subcellular localization pattern and the total number of cells examined per treatment. N, nucleus; C, cytoplasm. Bar = 10 μm. (b) Various fusion proteins described in (a) were, individually, co-expressed with Sw-5b in *N. benthamiana* leaves. A representative leaf was photographed at 5 dpai. (c) Western blot analysis of various NSm fusion protein expressions in the assayed *N. benthamiana* leaves using a YFP specific antibody. Leaf areas co-expressing Sw-5b and EV were used as negative controls. The Ponceau S stained Rubisco large subunit gel was used to show sample loadings.

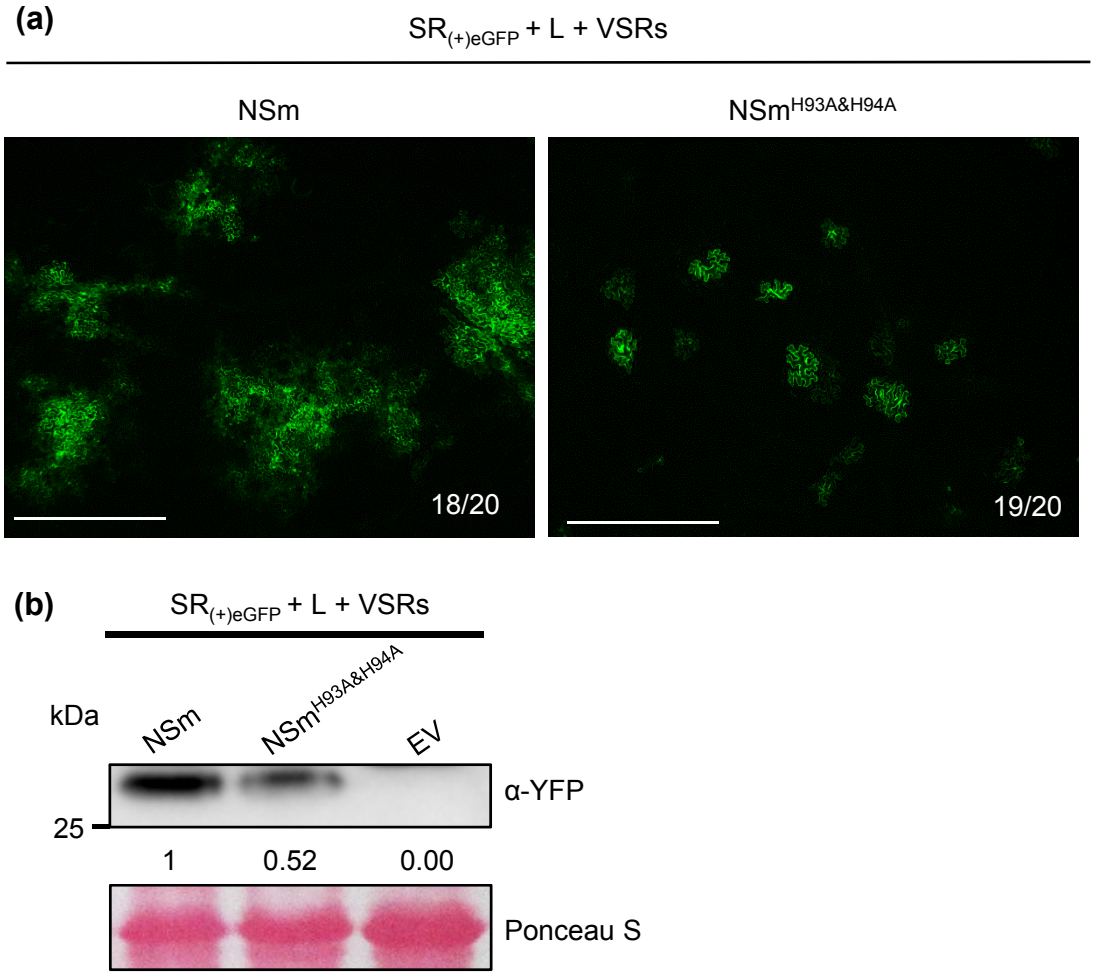

Fig. S2 Analysis of virus replication monitoring system using a TSWV-based mini-genome replicon and a movement defective NSm mutant. (a) $SR_{(+)eGFP}$, $L_{(+)opt}$, VSRs and NSm or $NSm^{H93A\&H94A}$ mutant were transiently co-expressed in *N. benthamiana* leaves through agro-infiltration. The infiltrated leaves were examined and imaged under a confocal microscope at 4 dpai. The numbers in each image indicate the number of cells showing similar expression pattern and the total number of cells examined per treatment. Bar = 400 μm. (b) Western blot analysis of eGFP accumulation in assayed leaves using a YFP specific antibody. Leaves co-expressing $SR_{(+)eGFP}$, $L_{(+)opt}$, VSRs and EV were used as negative controls. The Ponceau S stained Rubisco large subunit gel was used to show sample loadings.

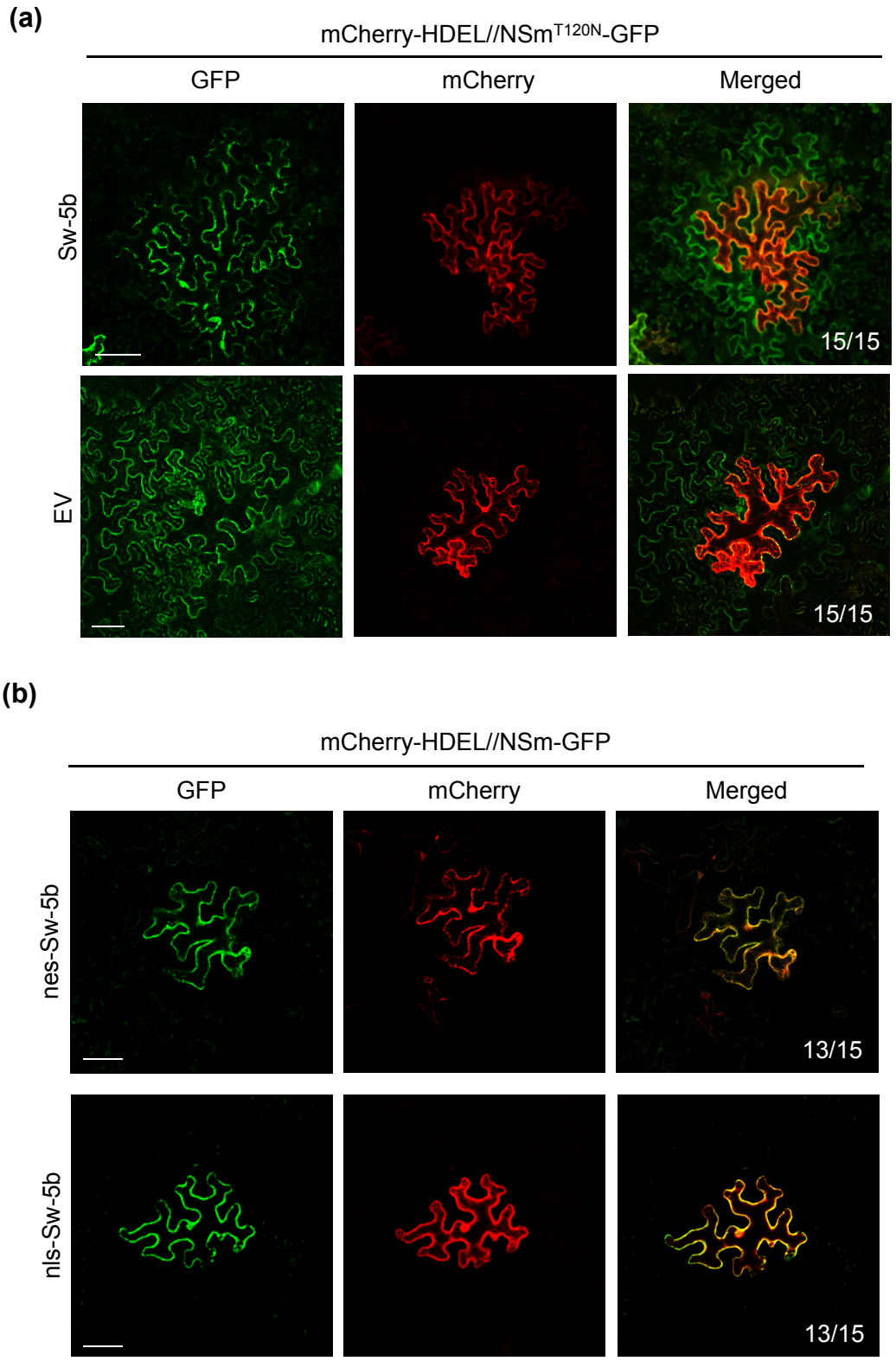
(a)
mCherry-HDEL//NSm^{T120N}-GFP
GFP
mCherry
Merged
Sw-5b
EV
15/15
15/15
(b)
mCherry-HDEL//NSm-GFP
GFP
mCherry
Merged
nes-Sw-5b
nls-Sw-5b
13/15
13/15

Fig. S3 Effects of nes-Sw-5b and nls-Sw-5b on NSm-GFP cell-to-cell movement and effects of Sw-5b and EV on NSm^{T120N}-GFP cell-to-cell movement. (a) Sw-5b and EV were, respectively, co-expressed with mCherry-HDEL//NSm^{T120N}-GFP in *N. benthamiana* leaves through agro-infiltration. (b) nes-Sw-5b and nls-Sw-5b were, respectively, co-expressed with mCherry-HDEL//NSm-GFP in *N. benthamiana* leaves through agro-infiltration. The Agrobacterium culture carrying pmCherry-HDEL//NSm-GFP or pmCherry-HDEL//NSm^{T120N}-GFP was first adjusted to OD_{600} = 0.2 and then further diluted 500 times prior to use. All other Agrobacterium cultures were adjusted to OD_{600} = 0.2 prior to use. The numbers in each image indicate the number of cells showing similar expression pattern and the total number of cells examined per treatment. Bar = 50 μm.

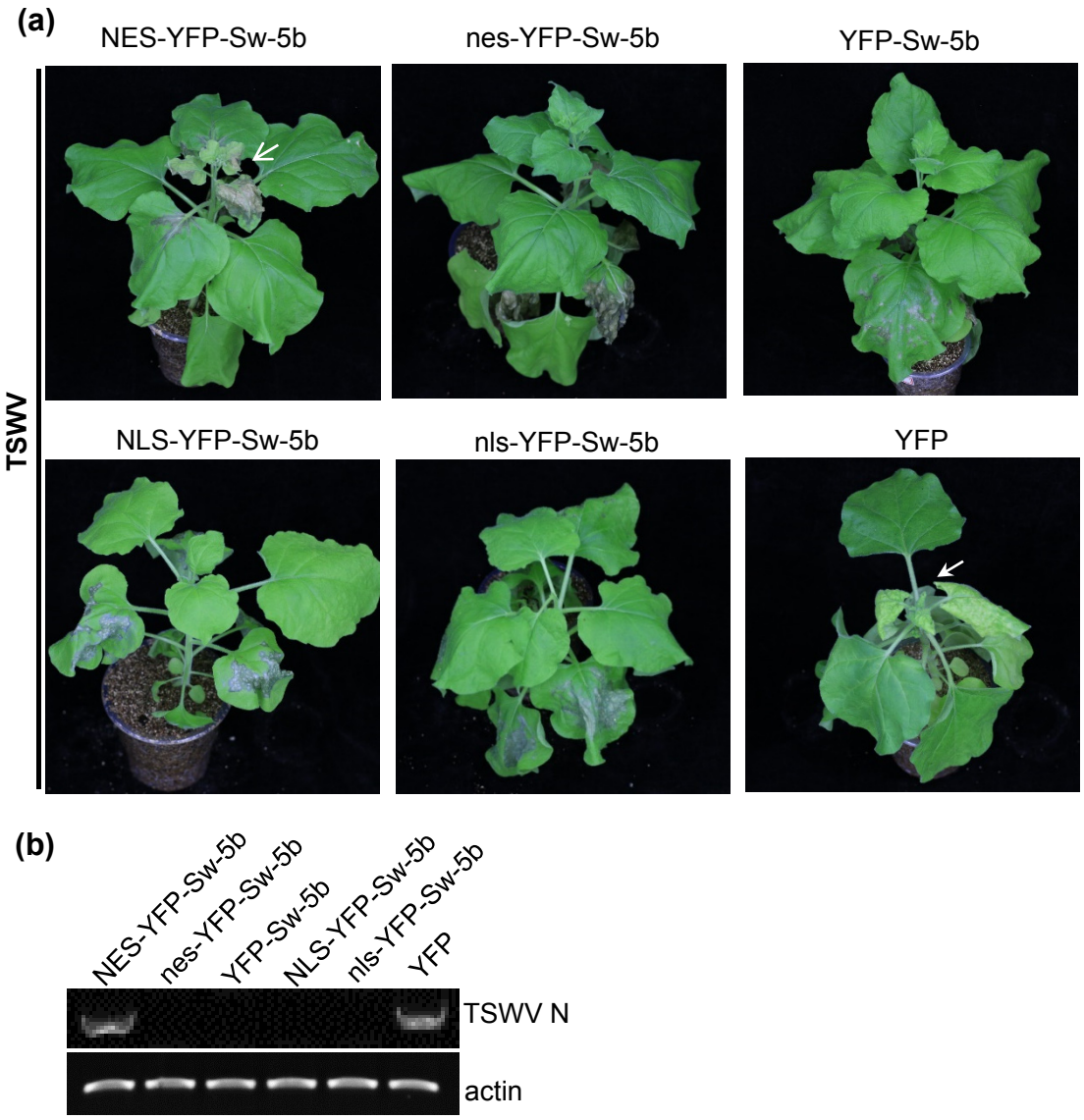

Fig. S4 Effects of cytoplasmic and nuclear Sw-5b on host immunity to TSWV systemic infection. (a) Transgenic *N. benthamiana* lines expressing NES-YFP-Sw-5b, nes-YFP-Sw-5b, NLS-YFP-Sw-5b, nls-YFP-Sw-5b or YFP-Sw-5b, driven by the Sw-5b promoter, were used in this study. The EV transgenic plants were used as controls. The transgenic plants were inoculated with TSWV and photographed at 15 dpi. White arrow indicate the systemic leaves showing HR trailing. White arrowhead indicates the systemic leaves showing mosaic symptoms. (b) RT-PCR detection of TSWV infection in the systemic leaves of the assayed *N. benthamiana* plants at 15 dpi.

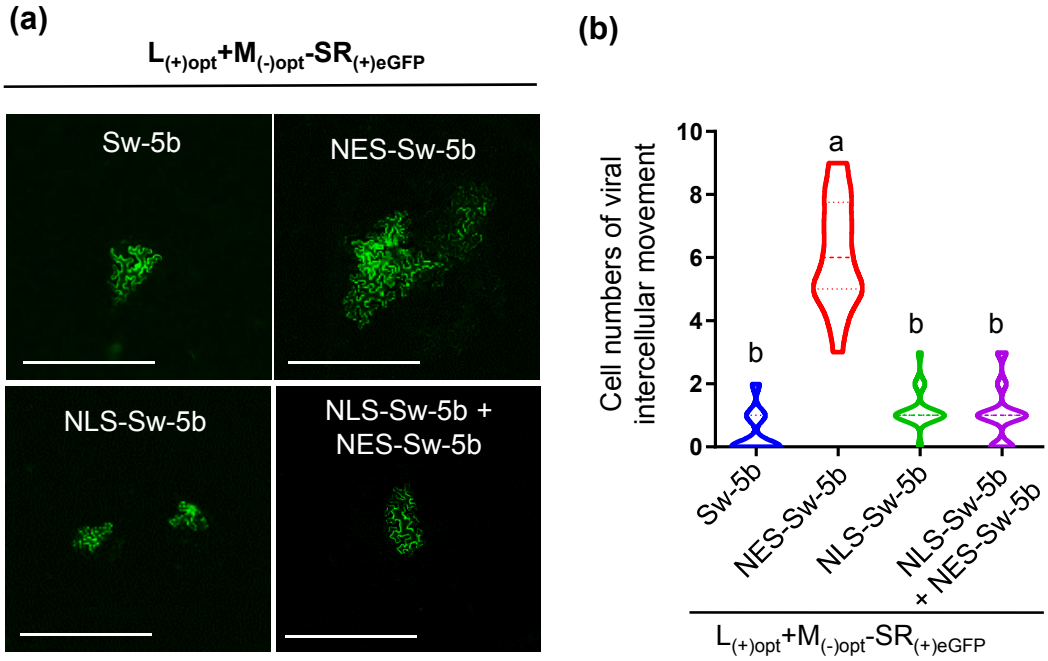

Fig. S5 Cytoplasmic and nuclear Sw-5b activity on TSWV-GFP cell-to-cell movement in *N. benthamiana* leaves. (a) $pL_{(+)opt}$ and $pSR_{(+)eGFP}$-$M_{(-)opt}$ were co-inoculated with TSWV-GFP into *Nicotiana benthamiana* leaves through agro-infiltration. The inoculated leaves were examined and imaged under a confocal microscope at 4 dpai. Bar = 400 μm. (b) Statistic analysis of TSWV-GFP cell-to-cell movement in the assayed *N. benthamiana* leaves from Figure 7B. A total of 9 assayed leaves were used for each treatment.

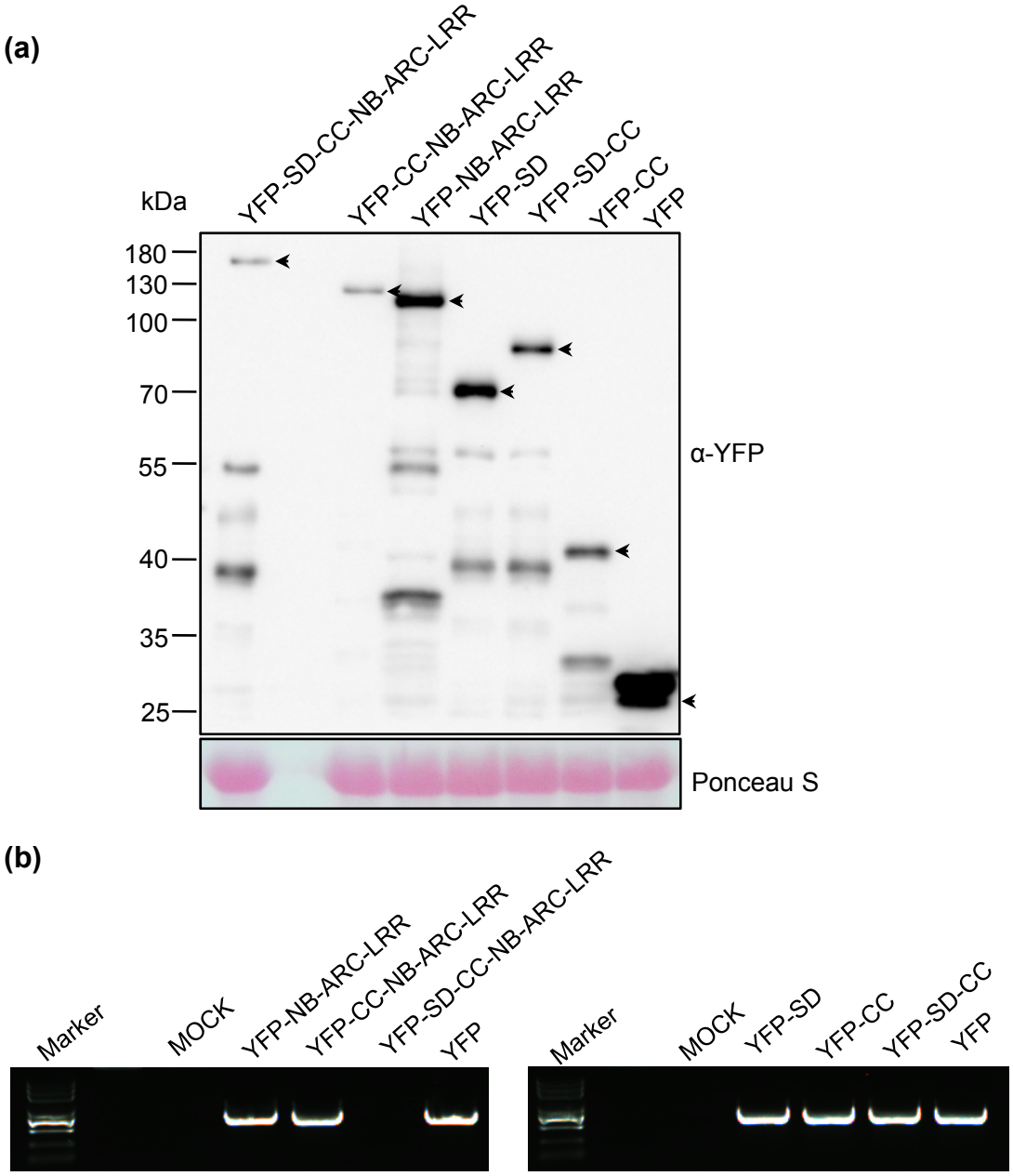

Fig. S6 An immunoblot showing the accumulations of various YFP-tagged proteins expressed in different transgenic *N. benthamiana* plants and RT-PCR analysis of TSWV accumulation in the systemic leaves. (a) The fusion proteins were detected using an YFP specific antibody. Arrows indicate the positions of the expressed fusion proteins. Ponceau S stained Rubisco large subunits were used to estimate sample loadings. (b) RT-PCR analysis of TSWV accumulation in the systemic leaves of different transgenic *N. benthamiana* plants at 15 dpi.

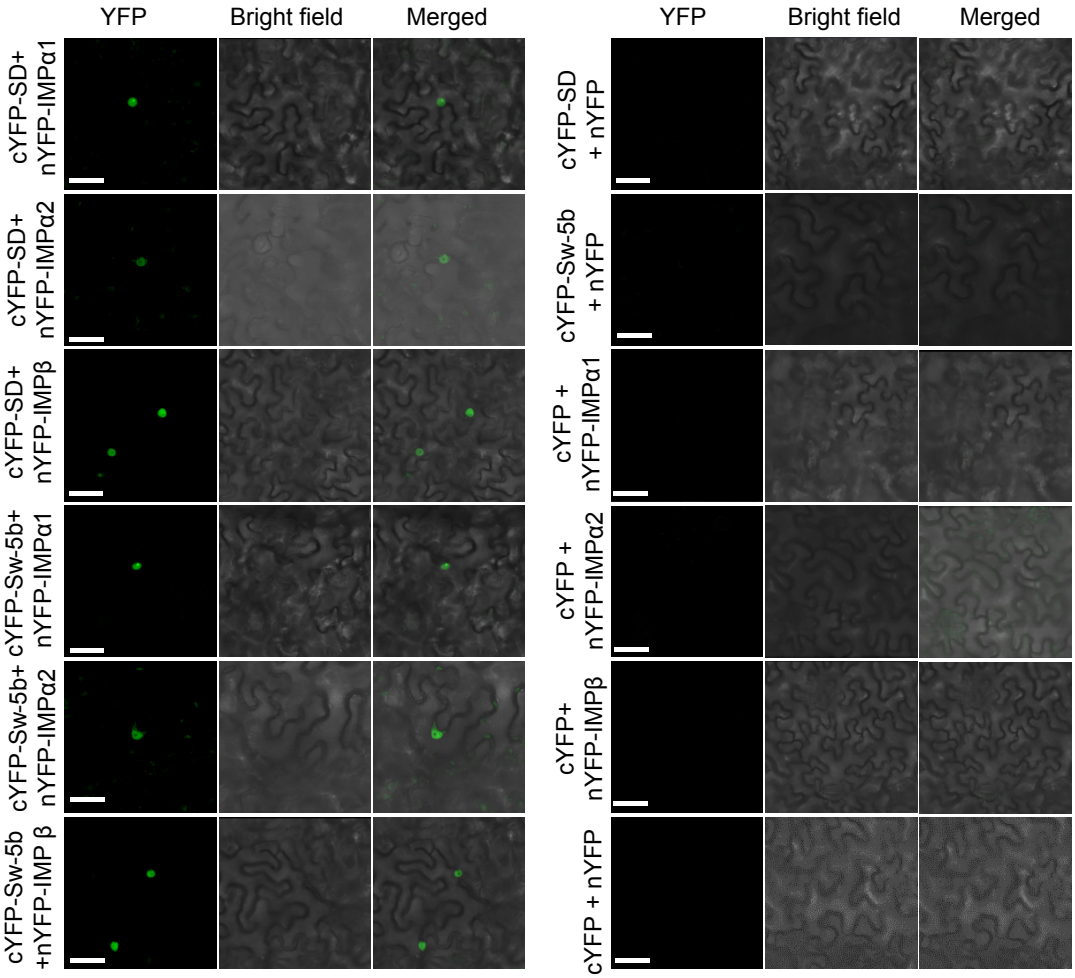

Fig. S7 Bimolecular fluorescence complementation (BiFC) assay of cYFP-SD, cYFP-Sw-5b and nYFP-Importin α1 (nYFP-IMP α1), nYFP-Importin α2 (nYFP-IMP α2), nYFP-Importin β (nYFP-IMP β) interaction in N. benthamiana leaf epidermal cells. Confocal images were taken at 26 hour post agro-infiltration. Leaf epidermal cells co-expressing cYFP-SD and nYFP, cYFP-Sw-5b and nYFP or cYFP and nYFP-IMP α1, nYFP-IMP α2, nYFP-IMP β were used as controls. Bar = 50 μm.

(a)

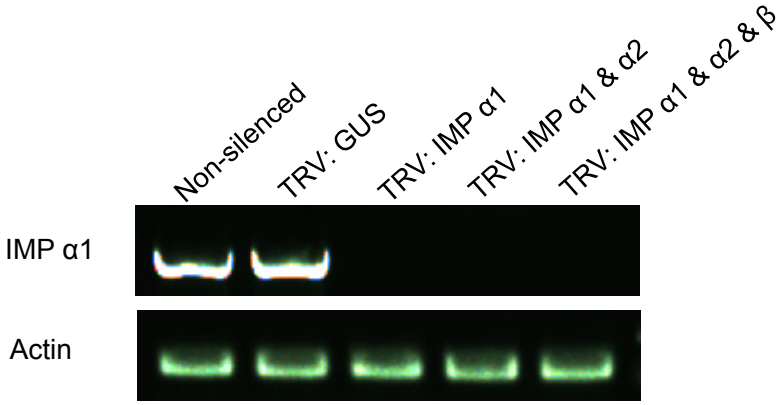
Non-silenced
TRV: GUS
TRV: IMP α1
TRV: IMP α1 & α2
TRV: IMP α1 & α2 & β
IMP α1
Actin

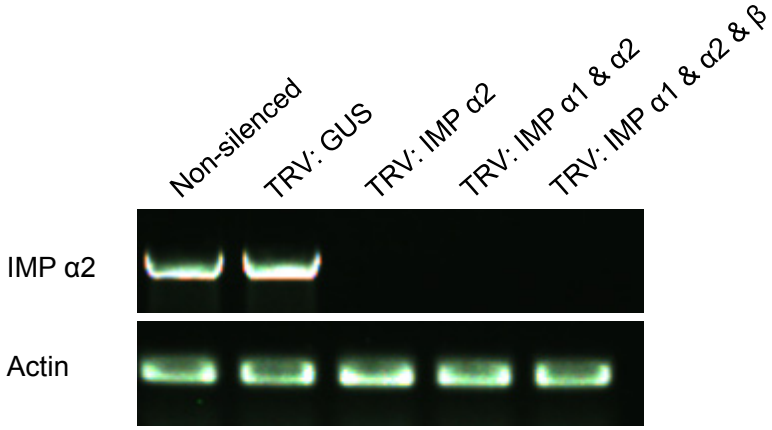
Non-silenced
TRV: GUS
TRV: IMP α2
TRV: IMP α1 & α2
TRV: IMP α1 & α2 & β
IMP α2
Actin

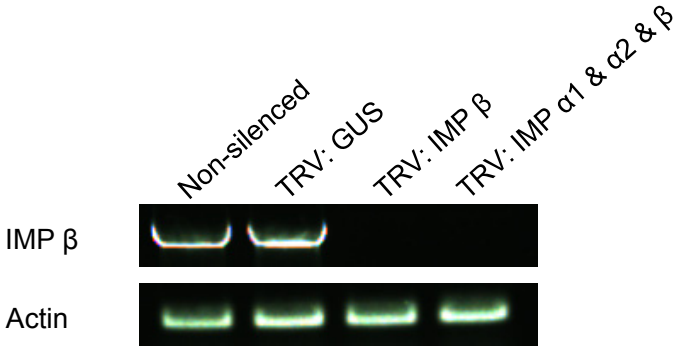
Non-silenced
TRV: GUS
TRV: IMP β
TRV: IMP α1 & α2 & β
IMP β
Actin

(b)

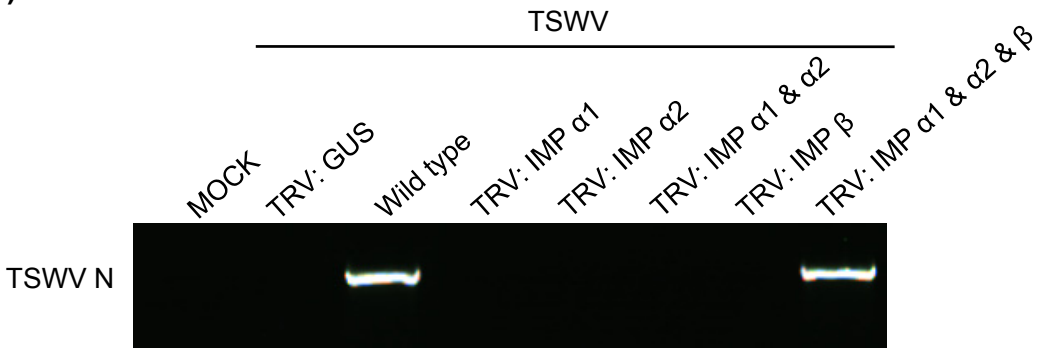
TSWV
MOCK
TRV: GUS
Wild type
TRV: IMP α1
TRV: IMP α2
TRV: IMP α1 & α2
TRV: IMP β
TRV: IMP α1 & α2 & β
TSWV N

Fig. S8 RT-PCR analyses of *importin* α*1*, α*2* and *β* expressions in the assayed plants and their effects on TSWV systemic infection. (a) Expressions of *importin* α*1,* α*2*, and *β* in Sw-5b transgenic *N. benthamiana* plants were silenced individually or together using a TRV-based VIGS vector. The gene silencing results were determined through semi-quantitative RT-PCR using gene specific primers. PCR products obtained after 25 cycles of PCR reaction were visualized in 1% agrose gel through electrophoresis. (b) RT-PCR detection of TSWV systemic infection in the assayed plants. The resulting PCR products were visualized in 1% agrose gel through electrophoresis.